

Contractor Final Report for the Period: October 1, 2016 through April 30, 2018
Project/Contract Title: **REE Identification and Characterization of Coal and Coal By-products Containing
High Rare Earth Element Concentrations**

Paul Ziemkiewicz, PhD, PI Director, WV Water Research Institute
West Virginia University

West Virginia University Research Corporation
886 Chestnut Ridge Road, PO Box 6845
Morgantown, WV 26506-6845
Phone Number: 304-293-6958
Email: pziemkie@wvu.edu

Xingbo Liu, PhD, Co-PI
Statler College of Engineering
Department of Mechanical and Aerospace Engineering
West Virginia University

Aaron Noble, PhD, Co-PI College of Engineering
Mining and Minerals Engineering
Virginia Tech

SUBMITTED BY:

Paul Ziemkiewicz

Principal Investigator

Phone Number: 304-293-6858

Email: pziemkie@wvu.edu

SUBMITTED UNDER DOE/NETL CONTRACT NO. DE-FE-0026444

CONTRACTOR'S DUNS ID: 191510239

CONTRACT PERFORMANCE PERIOD: 10/1/2016 through 4/30/2018

SUBMITTED TO:

U.S. Department of Energy National Energy Technology Laboratory
Charles Miller

23 July 2018

Table of Contents

LIST OF TABLES.....	1
LIST OF FIGURES.....	2
EXECUTIVE SUMMARY	4
INTRODUCTION.....	4
METHODS	6
SAMPLING SITES	6
SAMPLING METHODOLOGY	8
I. AMD sampling.....	8
II. AMD sludge sampling	9
III. Step-by-step sampling procedure.....	9
IV. Sample Analysis and Characterization.....	10
V. Resource Dimensions: REEs in Raw AMD and AMD Sludge	12
VI. Leaching Tests.....	12
Methods and Approach.....	12
DATA MANAGEMENT.....	17
ENVIRONMENTAL HEALTH AND SAFETY.....	17
RESULTS.....	17
CHEMICAL COMPOSITION OF AMD AND AMD SLUDGE	18
I. Statistical Analysis of the Data.....	18
CAPACITY OF AMD TO SUPPLY REE IN THE CAPP AND NAPP COAL BASINS	29
I. Stored REE resource	29
II. Annual REE production.....	32
III. Acid Leaching Trials.....	36
V. Data Modeling and Analysis	46
VI. Discussion and Implications.....	52
VII. XRD analysis of sludge samples	53
REFERENCES.....	55
APPENDIX A. XRD SPECTRA	57
SECTION A1: XRD SPECTRA OF DRIED SLUDGE SAMPLES COLLECTED DURING FIRST PASS SAMPLING.....	57
SECTION A2: XRD SPECTRA OF DRIED SLUDGE SAMPLES COLLECTED DURING SECOND PASS SAMPLING.....	76
APPENDIX B: IDENTIFIED PATTERNS LIST OF CORRESPONDING SLUDGE SAMPLES.....	95
APPENDIX C: SAMPLE SITE INFORMATION	109
APPENDIX D: SAMPLE RESULTS (FROM EDX).....	124
APPENDIX E: TABLE OF ABBREVIATIONS	137

List of Tables

Table 1. Sampling plan for northern (NAPP) and central (CAPP) Appalachian coal basin sites.....	7
Table 2. Sampled sites according to coal basin.....	7
Table 3. Number of chemical determinations included in this study	8
Table 4. Sample site data entry form.....	10
Table 5. Analytical parameters, methods, analytical laboratories and method detection limits (MDL) used in this study.....	11

Table 6. Leach characterization test parameters.....	15
Table 7. Test series descriptions.	17
Table 8. Summary of population sizes (n), means and confidence intervals (CI): two tailed tests and α , the probability of a type 1 error = 0.05.	19
Table 9. Ratios of confidence interval (CI) to mean for data presented in Table 8.	20
Table 10. AMD and sludge REE content in central (CAPP) and northern (NAPP) Appalachian coal basins. Additional parameters include U, Th, Co and sludge moisture content. T, L and HREE refer to total, light (green shading) and heavy (purple shading) REE. Critical REEs are highlighted in red.	23
Table 11. The proportion of individual REE in untreated AMD and AMD sludge in the CAPP and NAPP coal basins. T, L and HREE refer to total, light (green shading) and heavy (purple shading) REE. Critical REEs are highlighted in red.	24
Table 12. REE in both CAPP and NAPP basins ranked according to proportion of TREE.	25
Table 13. Conventional AMD treatment increased REE concentration from aqueous phase (AMD) to solid phase (sludge) at rates specific to each element and was nominally affected by coal basin.	27
Table 14. Results of sludge cell sampling, 76 sites in CAPP and NAPP. DW = dry weight basis; CV = contained value; SL = sludge.	30
Table 15. Summary of basinal REEs content and value in the sludge resource.....	32
Table 16. Two estimates of AMD production in the northern and central Appalachian coal basins (L/sec).	33
Table 17. Sludge density was determined hygrometrically and was found to vary within narrow limits. Confidence intervals represent the range in which 95% of the population's samples are likely to occur. They were determined using the student's t statistic and the parameters listed in the table.	33
Table 18. Basis for determining REE basket price and contained value. Oxide prices (MREO) were used to estimate resource value.	33
Table 19. Parameters and values used for REE reserve and value estimation. DW=Dry weight.	34
Table 20. Estimated annual NAPP and CAPP REE production from AMD.....	34

List of Figures

Figure 1. Classification of REE used in this study.	5
Figure 2. Leach test apparatus. The apparatus includes a multi-position stirrer hot plate and sealed sampling ports.....	14
Figure 3. The relationship between the pH of raw AMD and the concentration of TREE in the aqueous phase.....	21
Figure 4. The relationship between the pH of raw AMD and the concentration of TREE in the resulting AMD treatment sludge.	22
Figure 5 The proportion of individual REE in untreated AMD.	26
Figure 6. The proportion of individual REE in AMD sludge.....	26
Figure 7. Concentration factor indicates the change in concentration from aqueous (AMD) to solid (sludge) phase because of AMD treatment. The results are determined on a mass basis. The data include CAPP and NAPP coal basins. Green=LREE, Purple=HREE. TREE represents the overall concentration factor.	28
Figure 8. Predicted sludge TREE. The model uses the field parameters pH and EC to estimate the TREE concentration in AMD sludge. SL = sludge.....	35
Figure 9. Average assay for all sludge samples, as determined by handheld XRF.....	36
Figure 10. Maximum elemental concentration determined from full population of sludge samples (n=150).....	37
Figure 11. Maximum elemental concentration determined from full population of sludge samples	

(n=140).....	38
Figure 12. Average assay for sludge samples, itemized by primary species classification group.....	39
Figure 13. Sludge moisture data categorized by major elemental species. The vertical lines indicate data ranges while the boxes represent the upper and lower quartiles around the median value (horizontal lines across each box).	40
Figure 14. Acid consumption test results for test series #1 - test repeatability.	40
Figure 15. Acid consumption test results for test series #2 – solids concentration. The x axis represents measured pH.....	41
Figure 16. Acid consumption test results for test series #3 - acid comparison.	42
Figure 17. Acid consumption test results for test series #4 - intra-site variation.....	43
Figure 18. Acid consumption test results for test series #5 - site-to-site variation.	44
Figure 19. Acid consumption test results for test series #5 - site-to-site variation, classified by major elemental species.	45
Figure 20. Example of best and worst data fits.....	46
Figure 21. Examples of extreme values (and the resultant curves) for each of the three fitting parameters.....	47
Figure 22. Distribution of model fitting parameters determined from test series #4 - intra-site variation.	48
Figure 23. Distribution of model fitting parameters determined from test series #5 – site to site variation, categorized by primary elemental species.	49
Figure 24. Cross-Plots showing the three fitting parameters (pH Max, alpha and d50) plotted against Fe, Ca, Si and Al assay values.....	50
Figure 25. Parody plot showing measured starting pH versus pH _{Max} model parameter.	51
Figure 26. Distribution of output pH values categorized by primary elemental species. Output pH was predicted using Equation 2 at an arbitrary acid dose of 0.1 g/g (left panel) and 0.5 g/g (right panel). All other fitting parameters were derived from the raw data for each sludge sample.....	53
Figure 27. Characteristic results from drying method test; a.u. = arbitrary units.	54

Executive Summary

Previous work by the research team at West Virginia University (WVU) found that precipitates resulting from regulatorily mandated treatment of acid mine drainage (AMD) effluents are enriched in rare earth elements (REEs). The objectives of this study included a regional characterization and valuation of this potential resource.

Beginning in December 2016, sampling was conducted at 140 AMD treatment sites in Maryland, Ohio, Pennsylvania and West Virginia. Both untreated, or raw AMD and the solid precipitates, or AMD sludge, were collected at each site resulting in 185 raw AMD and 629 AMD sludge samples. Those samples were analyzed for REE content, major ions and key physical parameters.

This final report summarizes the results of the first comprehensive characterization of the potential for AMD to supply feedstock to a domestic REE industry.

Key findings:

- The dominant factor controlling the Total REE (TREE) concentration in raw AMD is the pH of the raw water.
- REE content of untreated AMD: TREE concentrations in untreated AMD averaged 233.5 µg/L (ppb) across the Central Appalachian Basin (CAPP) and 304.2 µg/L across the Northern Appalachian Basin (NAPP). The average of both basins is 286.9 µg/L.
- REE content of AMD sludge: TREE concentration in AMD sludge averaged 666.4 g/t (ppm) in the CAPP and 750.6 g/t in the NAPP.
- The average sludge concentration across both basins was 631.1 g/t.
- The actinides Thorium (Th) and Uranium (U) comprised less than 2% of TREE content in AMD sludge.
- Cobalt (Co) concentrations in both CAPP and NAPP sludges were similar and were approximately equal to TREE concentration.
- Estimated annual REE production: 808 tons with a contained value of \$192 million/year.
- REE in storage cells at sampled mines: 395 tons with a contained value of \$87.5 million. This includes the results of this and a previous study.
- Acid consumption during sludge dissolution was found to be one of the most significant factors determining the economics of REE recovery.
- Sludge sites with high levels of unreacted lime consumed the most acid while those with high iron hydroxide concentrations consumed the least.
- Leaching AMD sludge with nitric, hydrochloric and sulfuric acids all resulted in near complete dissolution of the matrix. However, nitric acid had the least tendency for anomalously high or low readings and was selected for further parametric testing.
- Acid addition to sludge and subsequent pH changes indicated an initial buffering with lime followed by a steep decline as metal hydroxides dissolved.

Introduction

AMD is a longstanding environmental problem and has been studied extensively since the 1960s. While the process of AMD formation, control and treatment technologies are well understood¹, its potential to supply critical materials, specifically REEs has been studied only recently. AMD is produced in vast quantities at both abandoned and current coal mining and preparation facilities. Coal producers are required to treat AMD to meet permitted water quality standards. Current AMD treatment is focused

on meeting the pollution discharge limits imposed by the Clean Water Act: 33 U.S.C. §1251 et seq. (1972) for regulated, compliant water ². AMD treatment consists of acid neutralization, mechanical or chemical oxidation and the settling of metal precipitates. Treatment systems remove metal contaminants as flocculated precipitates (flocs), which are then separated from discharge-quality water by either mechanical or gravitational settling methods³. Known as AMD treatment precipitates or sludge, these metal flocs are enriched in REEs. Our earlier studies demonstrated that treatment of low pH AMD (< pH 5.5) produces a sludge with exceptionally high REE concentrations, often an order of magnitude greater than the surrounding rock strata.

AMD results from the oxidation of pyrite, a mineral common to the Appalachian region’s coal measures^{4 5 6 7}. Pyrite oxidation generates sulfuric acid ⁸ which leaches REEs from associated rock. During AMD treatment, REEs precipitate with the primary regulated metal ions of iron (Fe), aluminum (Al) and manganese (Mn) hydroxides.

AMD treatment systems are tailored to specific discharges and are designed to minimize capital and operating costs while meeting regulatory discharge standards. The resultant precipitates consist largely of Al, Fe and Mn oxy-hydroxides plus gypsum and carbonates. Iron is the dominant metal in strongly acidic AMD. Initially Fe occurs in its reduced (Fe²⁺) state, oxidation to Fe³⁺ and precipitation as Fe(OH)₃ is nearly complete at pH 3.5 while Al³⁺ and Mn²⁺ hydroxides precipitate at pH values of 4.0 and 9.0, respectively. Prior results² show that REEs precipitate along a pH gradient nearly identical to Fe³⁺ supporting the thesis REEs co-precipitate with the other metal cations. These metal hydroxide precipitates are collected in settling basins while treated water is decanted to surface discharge. Initially-formed AMD sludge is about 99% water. The solid fraction settles over time and depending on the treatment and storage process, may reach solids concentrations of 20 to 30%.

This project instituted a regional sampling effort that included an initial survey of sludge REE concentrations at a wide variety of AMD treatment sites. The results were used to identify sites with a high potential for REE recovery. A subset of this original population was selected for a second phase of intensive sampling to better determine variability within sites. Analytical methods follow and include REE concentrations and other important site and treatment factors. Consistent with the USDOE/NETL nomenclature, **Figure 1** summarizes the classification of REEs according to light, heavy and critical elements. This nomenclature will be used throughout the report.

Rare Earth Elements																			
		Light		Critical															
		Heavy		*Unstable															
H																	He		
Li	Be											B	C	N	O	F	Ne		
Na	Mg											Al	Si	P	S	Cl	Ar		
K	Ca	Sc	Ti	V	Cr	Mn	Fe	Co	Ni	Cu	Zn	Ga	Ge	As	Se	Br	Kr		
Rb	Sr	Y	Zr	Nb	Mo	Tc	Ru	Rh	Pd	Ag	Cd	In	Sn	Sb	Te	I	Xe		
Cs	Ba	La	Hf	Ta	W	Re	Os	Ir	Pt	Au	Hg	Tl	Pb	Bi	Po	At	Rn		
Fr	Ra	Ac																	
			Ce	Pr	Nd	Pm*	Sm	Eu	Gd	Tb	Dy	Ho	Er	Tm	Yb	Lu			
			Th	Pa	U	Np	Pt	Am	Cm	Bk	Cf	Es	Fm	Md	No	Lr			

Figure 1. Classification of REE used in this study.

Methods

Sampling Sites

The Appalachian coal basin is characterized by closely spaced, relatively thin seams (three to six feet) and while surface mines typically extract coal from multiple seams on discrete benches, the resulting spoil and refuse is nearly always a mixture of multiple seams, their partings and overburdens. Many underground mines collect AMD from overlying deep mines; thus, an AMD discharge may represent single or multiple coal units. In characterizing the geologic source at a given site, we attempt to identify the dominant seam or seams.

AMD treatment systems may treat large e.g., up to 5,000 gpm (gallons/minute) single discharges pumped from underground mine complexes, multiple, small (< 100 gpm), or even ephemeral discharges from surface mines. Many of the latter respond rapidly to precipitation and recharge events. A given mine property will normally have multiple AMD discharge points. While operators consolidate discharges to improve treatment efficiency, multiple treatment sites within a given mine are the norm. Many AMD treatment units will dispatch effluent to multiple sludge cells either in series or in parallel to optimize metal floc precipitation and dehydration. We define a treatment site according to a discrete AMD source and its individual sludge cells. Both AMD discharges and sludge cells were sampled.

Sampling was conducted in two campaigns. The initial sampling consisted of a regional survey of 140 AMD discharges. It formed the basis for our estimates of the REE resource available in surface sludge cells and the annual production rate (flux) based on AMD generation regardless if the sludge was deposited in surface cells, buried in surface mining operations or injected into deep mine voids. A subsequent, intensive sampling campaign focused on potentially attractive sites based on either the surface sludge resource or annual flux. These sites were sampled to a maximum of ten (10) sludge samples per site. Thus, between one and 10 samples were collected and analyzed. Statistical analysis was conducted on those sites with multiple samples. A sample location table is provided in Appendix C.

The nature of AMD formation and treatment reduces the sampling error of a given site's sludge. For example, AMD chemistry represents the integration of reactions that occur at small scales, such as the pore water surrounding pyritic versus non-pyritic rock grains and localized oxidizing versus reducing environments. This integration occurs over the scale of mines ranging from hundreds of acres to 20 square miles or more in the case of large, underground mine complexes. AMD sludge further integrates variations in discharge chemistry by aggregating metal loads over periods of months or years in sludge storage cells. Therefore, expected REE concentrations in sludge from a given source would vary within narrow bounds.

As a result, the maximum sample size in the proposed study was 10 per sludge source over at least two sampling dates, allowing sampling of a nominal 75 AMD treatment sites summarized in **Table 1**. It is important to note some of the cooperating companies permitted access only under the terms of a non-disclosure agreement. Thus, as a rule, we identify those sites by site code and provide locations on a state and county basis. Detailed site information, as appropriate, including latitude/longitude coordinates are included in NETL's EDX database (summarized in Appendix D).

Table 1. Sampling plan for northern (NAPP) and central (CAPP) Appalachian coal basin sites.

Coal basin	# sites	Sampling events/year	# samples/site	Total # samples
CAPP	15	2	5	150
NAPP	60	2	5	600
Total	75			750

To focus sampling on the most promising sites, operators were surveyed prior to developing the final sampling plan according to the site selection criteria listed below. Site selection then focused on AMD discharges with the following operational criteria:

1. *Untreated AMD pH*: pH values less than 5 are associated with the highest TREE concentrations
2. *AMD treatment system*: Caustic and anhydrous ammonia would be favored over hydrated lime systems as the sludge would be less diluted with gypsum and lime;
3. *Discharge volume*: Volume will be used to estimate TREE production;
4. *Site access*: Physical access as well as operator approval for sampling as well as later development; and
5. *Sludge management*: As it affects subsequent availability for recovery/transportation.

We also collected untreated AMD samples at each treatment facility to assess the raw water chemistry and identify correlations between raw water parameters and sludge REE content. **Table 2** summarizes the actual number of sites and samples analyzed during the preliminary and intensive sampling campaigns. **Table 3** summarizes the chemical determinations included in this study.

Table 2. Sampled sites according to coal basin.

Coal basin	Treatment sites		Number of samples	
	AMD	Sludge	AMD	Sludge
CAPP	32	42	55	144
NAPP	107	112	130	485
Subtotal	139	154	185	629
total		293		814

Table 3. Number of chemical determinations included in this study.

REE	Number of analyses	Other	Number of analyses
Sc	798	U	508
Y	811	Th	494
La	805		
Ce	812	Co	523
Pr	795	pH	139
Nd	803		
Sm	801	Major ions	
Eu	789	Al	615
Gd	803	Ca	648
Tb	789	Fe	651
Dy	800	Mg	644
Ho	799	Mn	642
Er	800	Na	538
Tm	741	Si	651
Yb	802	Cl	274
Lu	747	SO4	536
subtotal	12,695		6,863
total			19,558

Sampling Methodology

I. AMD sampling

Standard AMD sampling protocols were implemented to provide a representative grab sample of each discharge. Samples were collected at the center of the pipe or channel, avoiding contact or proximity to the banks, pipe or conduit walls, or other sources of subsurface emanation or contamination. Field measurements of pH, specific conductance, dissolved oxygen and water temperature were obtained at the time of grab sample collection utilizing available instrumentation. Instruments were decontaminated after each measurement and thoroughly exposed to the new target media, allowed to stabilize for one minute before recording reading.

The instruments typically available and calibration schedule are:

- pH – Oakton pH Testr3+; unit calibrated to pH 4.01 and 7.0 daily, end-of-day.
- Dissolved oxygen (DO) – Hach HQ-30d; unit calibration performed daily, end-of-day.
- Electrical conductivity (EC) – Hanna HI98311/12; unit calibration performed daily, end-of-day.

In cases where the discharge was less than 100 gpm, the flow rate was determined using a five gallon [20 liter (L)] graduated bucket and stopwatch. Three measurements were conducted and averaged. Stream cross-section and width were measured with an engineer rule in decimal feet and velocity was measured using flow meters according to the operating manuals provided by the manufacturer.

The flow instruments included:

- Marsh McBirney Flo-Mate 2000 for all streams deeper than 0.2 feet.

- Global Water Flow Probe FP-111 for all streams.

Surface impoundments vary in size, shape and waste content and may stratify according to sludge composition and water content. The number of samples, the type of sample(s) and the sample location(s) were based on accessibility and safety. Commonly used equipment to collect samples from surface impoundments were clean, unused polyethylene containers. All equipment was compatible with the waste and cleaned to prevent any cross-contamination of the sample.

II. AMD sludge sampling

Waste samples were collected using a clean, decontaminated, stainless steel scoop to within three centimeters (cm) of the top of a one gallon wide-mouth polyethylene container.

Sludge samples were not chemically-preserved to eliminate the potential for inadvertent chemical reaction between the sample and preservative. After the samples were collected and containerized, the outsides of the containers were cleaned with water, paper towels and/or oil wipes to remove any spilled sample from the exterior of the containers. Sample containers were identified with tags and sealed for custody purposes as soon as possible. After the sample container had been tagged and sealed, each container was placed in a separate plastic bag and secured with electrical tape before being placed in a cooler.

III. Step-by-step sampling procedure

1. Sampling personnel were equipped with adequate personal protective equipment (PPE) such as boots, hard hat (if active site), safety glasses and nitrile gloves.
2. Site data were recorded and the identification form (**Table 4**) was completed.
3. A clean, unused 0.5 L polyethylene container (pre-preserved with 1M HNO₃) and intact lid was opened and filled with AMD from the pipe, stream, or pool by pointing the opening upstream and submerging the container, without loss of the nitric acid preservative.
4. A clean, unused four-liter polyethylene container with intact lid was opened and filled with AMD sludge using a stainless-steel scoop.
5. Care was taken to avoid introducing surface contaminants, vegetation, insects and other materials. The containers were filled with minimal headspace (less than one cm for an AMD sample and less than three cm for sludge samples).
6. The containers were tightly capped and placed in a cooler without ice. The samples were delivered to the West Virginia Water Research Institute (WVWRI) laboratory for logging and preparation for transport to the commercial laboratory under chain-of-custody.
7. Maximum holding time for REE is 180 days. It was never exceeded.
8. Post sampling, PPE were cleaned and nitrile gloves and other disposable sampling supplies were disposed of appropriately. Scoops and other field instruments were cleaned for re-use.

Table 4. Sample site data entry form.

Sample date:	
Sampled by:	
County:	
State:	
Coal basin:	
Coal seam:	
Source type:	
Site identification number (ID):	
Site operator:	
AMD treatment process:	
AMD treatment chemical:	
AMD treatment system discharge (gpm):	
Field Parameters:	
Raw pH	
Raw electric conductivity ($\mu\text{S}/\text{cm}$)	
Treated pH	
Treated electric conductivity ($\mu\text{S}/\text{cm}$)	
Sludge management system:	
Onsite sludge storage volume:	

IV. Sample Analysis and Characterization

Sludge Preparation and Analysis

REEs and major ion concentrations were determined on both aqueous and solid (sludge) samples. **Table 5** summarizes analytical parameters and the laboratory selected to undertake the analytical work. In addition, sludge moisture content was determined at the analytical laboratory so that sludge concentrations could be expressed on a dry weight basis.

In addition, most of the sampling sites and the respective operators were familiar to the researchers. These operators assisted in identifying candidate sites and finalizing the sampling program. Familiarity with property operators and access to the sites was essential to gain site access albeit frequently under the conditions of a non-disclosure agreement which restricted public identification of specific sites and operators. Analytical services were provided by three laboratories: SGS Canada Ltd. (sludge samples). Test America, Inc. (aqueous REE samples) and the National Research Center for Coal and Energy (NRCCE) Analytical Lab at West Virginia University (WVU; aqueous samples - major ions). Details are included in **Table 5**.

Table 5. Analytical parameters, methods, analytical laboratories and method detection limits (MDL) used in this study.

	Aqueous (Test America)		Solids (SGS Canada)	
	method	MDL µg/L	method	MDL g/t
Sc	6060A	0.14	GS_IMS28V	3.0
Y	6060A	0.028	GS_IMS28V	3.0
La	6060A	0.026	GS_IMS28V	3.0
Ce	6060A	0.026	GS_IMS28V	3.0
Pr	6060A	0.022	GS_IMS28V	0.5
Nd	6060A	0.03	GS_IMS28V	5.0
Sm	6060A	0.03	GS_IMS28V	0.5
Eu	6060A	0.022	GS_IMS28V	0.3
Gd	6060A	0.028	GS_IMS28V	0.5
Tb	6060A	0.02	GS_IMS28V	0.5
Dy	6060A	0.022	GS_IMS28V	0.5
Ho	6060A	0.024	GS_IMS28V	0.3
Er	6060A	0.03	GS_IMS28V	0.5
Tm	6060A	0.024	GS_IMS28V	0.3
Yb	6060A	0.026	GS_IMS28V	0.5
Lu	6060A	0.022	GS_IMS28V	0.5

	Major ions Aqueous (WVU Lab)		Major ions Solids (SGS Canada)	
Al	200.7	0.021	GS_IMS28V	0.5
Ca	200.7	0.01	GS_IMS28V	0.5
Cl	200.7	0.035	GS_IMS28V	0.5
Fe	200.7	0.013	GS_IMS28V	0.5

AMD sludge samples (minimum one gallon each) and a one gallon AMD source water sample were collected at each site. The latter were stored at 4°C until transported to the WVWRI lab for processing. Appropriate preservation and refrigeration methods, hold times and chain-of-custody procedures were strictly followed. Aqueous samples were preserved with 2% HNO₃ acid to pH 2.0.

AMD sludge is essentially precipitated metal hydroxide floc. Other than weak agglomerative effects, particle size is very small, uniform in size and density obviating the benefit of float/sink separation. Rather than a float/sink test, we used acid leaching as a primary separation mechanism to identify leachable versus non-leachable fractions.

X-ray diffraction (XRD) analysis was also conducted on many of the sludge samples collected to date. In many cases, XRD has yielded almost no crystal structures indicating that the metal hydroxides were highly hydrated, amorphous solids resulting in apparently uniform composition.

REE aqueous concentrations were determined using inductively coupled plasma-mass spectrometry (ICP-MS). AMD sludge samples were initially digested by sodium peroxide (Na₂O₂) fusion and re-

dissolution in hydrochloric acid. This method appears to be comparable with the United States Environmental Protection Agency's (USEPA's) total digestion method 3052 (microwave digestion) for total REEs. Resulting aqueous analysis was then undertaken using ICP-MS. Major ions such as Fe and Al in aqueous phase were determined by inductively coupled plasma optical emission spectrometry (ICP-OES).

V. Resource Dimensions: REEs in Raw AMD and AMD Sludge

Two key parameters were used to evaluate the economic value of the AMD-based REE resource: basket price and contained price. Both parameters are widely used in the mineral extraction industry. Basket price is the proportion of an individual REE's contribution to the combined value of REEs in sludge.

Dimensioned as \$/kg TREE on a dry-weight basis, basket price is essentially the weighted value of a sludge sample. Contained value is the value of REEs in a ton of sludge on a dry-weight basis and is dimensioned as \$/ton sludge dry weight. REE prices are quoted on an oxide and metal basis, the latter assumes refining to individual elements as pure metal products. Unsure of the costs to take our product from oxide to pure metal, a conservative approach is taken by assigning oxide values to our product.

The AMD based REE resources within the Appalachian Basin include raw AMD and AMD sludge. The on-site, stored REE resource amount (existing and accessible sludge) was estimated through field surveys and satellite imagery. Raw AMD production is subject to strong temporal variations in both quality and quantity. REE concentrations were characterized in the NAPP and CAPP basins and values were assigned to estimate regional AMD production. Two approaches were used to estimate sludge quality: 1) basket price based on regional sludge and AMD quality; and 2) basket price based on individual site calculations.

VI. Leaching Tests

Methods and Approach

Leaching tests (also denoted as acid titration or acid consumption tests) were conducted on sludge samples to identify the amount of acid (mass of acid per unit dry weight sludge) needed to reach various target pH values. Data from these tests provide an indirect measure of overall process amenability and cost, since most REE extraction processes will begin with an acid leaching stage. Each test was conducted using a standardized protocol and several "test series" were conducted to fully evaluate the influence of specific independent variables. The raw results were analyzed using standard statistical approaches and a non-linear empirical model was fitted to the experimental data to provide another approach to the analysis. The results thus provide quantitative metrics used to assess a sludge sample's amenability to acid leaching.

After acquiring the field samples and recovering sub-samples for REE analysis, each one-gallon sample bucket was delivered to the appropriate university laboratory for acid leaching tests as well as other characterizations, including sludge moisture content and major metal content via XRF. To determine the sludge moisture content, approximately 10 grams of wet sludge were sampled from the bucket and weighed using an analytical balance. The sample was then dried overnight in a laboratory oven at 80° C and after full desiccation, the sample was then re-weighed. The moisture content was then determined by the weight difference before and after desiccation. Following the moisture analysis, the dried

samples were then analyzed for major metal content using a Niton XL2 handheld XRF analyzer. Each sludge specimen was first ground by hand using a mortar and pestle and then closely packed into an XRF cup using a single cotton ball. The XRF scan used the "Mining Cu/Zn" mode with a 60 second overall scan time. Elements included in the analysis were: Ba, Sb, Sn, Mo, Nb, Zr, Sr, Rb, Bi, As, Pb, W, Zn, Cu, Ni, Co, Fe, Mn, Cr, V, Ti, Ca, K, Al, P, Si, Cl, S and Mg; however, the major elements prioritized in this study included: Fe, Ca, Al, Si, Mn and S. These two characterization tests, sludge moisture and XRF, provide context and explanation for the raw leaching test data. For example, the sludge moisture content can be used to normalize acid addition to a dry mass basis. Likewise, the XRF data can be used to categorize the results based on the primary metal species present in the sludge.

The acid leaching tests followed a strict experimental protocol, whereby the mixing intensity, acid type, acid concentration, leaching temperature and leaching time were all held constant. During the tests, acid was incrementally added with the cumulative acid dose being the independent variable, while pH was measured as the primary experimental response. All leach tests were performed in a standard test apparatus like the one shown in **Figure 2**. The apparatus includes a multi-position stirrer hot plate and specialized glassware that includes ports for sampling and pH measurement. A reflux condenser was initially added to the test apparatus to ensure that acid evaporation did not distort the acid consumption measurements; however, visual observations during the preliminary trials showed that no acid was condensing during the tests. This result is not unexpected, since all tests were performed at ambient temperature. As a result, the reflux condenser was later removed and not used for most of the test series. The laboratory pH meter was calibrated daily using three pH buffer solutions, namely pH 7, 4 and 2.

A standardized test protocol was employed to ensure consistency and reproducibility between test runs. Each test was completed by a trained experimental technician/graduate student working under the supervision of a project PI or co-PI. All steps were conducted under an approved chemical hygiene plan (CHP). Key safety elements included a laboratory fume hood and sufficient personal protective equipment, including but not limited to acid-resistant gloves, safety glasses or goggles, a suitable lab coat, closed-toed shoes and other equipment as needed.

Diluted acid solutions were generated by mixing stock acid and deionized water at a ratio needed to create the desired acid concentration for testing, typically 3 mol/L. The acids utilized in the leaching tests included hydrochloric (37%), nitric (70%) and sulfuric (95%). All reagents were provided by standard laboratory chemical vendors, including Sigma Aldrich (St. Louis, MO), Fisher Scientific (Hampton, NH) and others. Diluted solutions were stored for the duration of the project, which did not exceed 18 months.

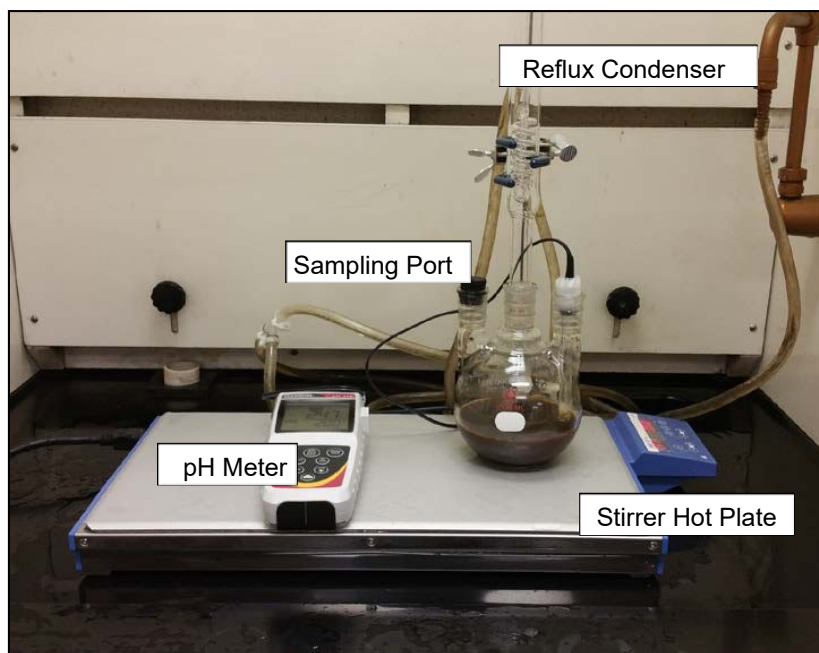


Figure 2. Leach test apparatus. The apparatus includes a multi-position stirrer hot plate and sealed sampling ports.

During the test sequence, approximately 100 grams of wet sludge were first recovered from the desired one-gallon sample container. This material was placed into the leaching vessel and weighed to determine the wet sludge mass. Next, 100 mL of distilled water were mixed into the leaching vessel and the apparatus was then mounted on the magnetic stirrer plate. The stirrer rate was set to 300 RPM and the solution was fully mixed for two minutes. After mixing, the initial pH (i.e. with no acid addition) was recorded. Acid was then added following an exponential sequence starting with 1 mL and doubling with each subsequent acid addition (i.e. 2 mL, 4 mL, 8 mL, 16 mL, etc.). After each acid addition, the solution was mixed for 5 minutes and the pH was then recorded after the reaction was complete. Acid addition continued until the steady state pH reached a value less than 0.5, which typically required six to nine acid addition steps depending on the specific test specimen. After reaching the target pH point, the test was stopped and the acid waste was disposed following the guidelines of the CHP. The raw data was then logged using a standard test database sheet in Microsoft Excel. Each test was repeated at least three times using representative splits from the same bucket. Data from the three replicate runs were averaged to produce a single result representative of the bucket sample.

The standard experimental parameters for the acid leaching tests are given in **Table 6**. Preliminary tests and prior knowledge have confirmed that these values are suitable for the given experimental procedure.

Table 6. Leach characterization test parameters.

Parameter	Unit	Value
Acid Type	--	Nitric , Sulfuric and Hydrochloric
Acid Concentration	Mol/L	3
Acid Addition Increments	mL	1, 2, 4, 8, 16, 32, 64 and 128
Time Increment between Additions	Min.	5
Final Leach pH	--	< 0.5
Leach Temperature	--	Ambient
Solid to liquid ratio (wet solids)	--	0.5:1, 1:1 , 1.5:1
Sludge mass	Grams	50, 100 , 150
Stirrer Speed	RPM	300
Replicate Trials	--	3 to 10
Note: Bold entries indicate standard values. Others evaluated as part of experimental design.		

The raw experimental data was pre-processed by first normalizing the acid addition (measured in mL) to the mass of acid per unit dry weight sludge (given in g/g). This normalization is given by equation 1:

(1)

$$d = \frac{V_a w C}{M_w (1 - u)} \left[\frac{1}{1000} \right]$$

where d is the normalized acid dose (in g/g), V_a is the cumulative volume of acid added (in mL), w is the molecular weight of the acid (in g/mol), C is the acid concentration (in mol/L), M_w is the wet mass of the sludge recorded before the test and u is the sludge moisture content. The conversion factor [1/1000] provides the conversion from mL to L needed in the numerator.

After normalization, the data is presented as measured pH versus normalized acid dose on a semi-log x plot. This approach thus creates a unique acid consumption curve for each sludge sample. To facilitate a quantitative statistical evaluation of the data, a non-linear empirical model was derived to simplify each curve to a finite number of fitting parameters. Several two and three factor models were evaluated; however, the model found to provide the best balance between fitting accuracy and fitting robustness is given by equation 2:

(2)

$$pH(d) = pH_{Max} - \left(\frac{1}{1 + \exp\left(a \left(1 - \log\left\{\frac{d}{d_{50}}\right\}\right)\right)} \right) pH_{Max}$$

where $pH(d)$ is the measured pH at a given acid dose, d [in g/g]. pH_{max} , α and d_{50} are fitting parameters for the empirical equation.

This specific model was selected over competing models because the fitting parameters directly refer to geometric intricacies of the acid consumption curve. Specifically, pH_{Max} is the y-axis position of the high asymptote, or approximately the starting pH of the sludge in an aqueous solution. α is related to the slope of the curve at the inflection point. High α values indicate a fast transition from high pH to low pH while lower α values indicate a shallower slope. Lastly, d_{50} is related to the x-axis position of the inflection point. Low d_{50} values refer to a lower pH which can be achieved at smaller acid dosages, while higher d_{50} values indicate a higher dosage is needed to produce low pH values.

The experimental efforts were organized into five primary test series (and one preliminary series) to progressively validate the test method and evaluate several sources of variation in the experimental results. **Table 7** summarizes the objectives and samples used in each test series.

Table 7. Test series descriptions.

Series ID	Series Name	Number of Test Runs	Samples Evaluated	Objective
0	Preliminary Tests	3	SL-1-10 SL-3-1	Validate experimental protocols.
1	Test Repeatability	10	SL-3-1	Evaluate variability of the test results on a single sample.
2	Solids Concentration	3	SL-21-5	Validate the applicability of dry mass normalization approach.
3	Acid Comparison	9	SL-40-1 SL-51-1 SL-67-1	Evaluate the difference between nitric, sulfuric and hydrochloric acid.
4	Intra-Site Variation	38	SL-40-1 SL-67-1 SL-51-1 SL-66-1	Assess the variability of the test results on samples taken from multiple locations at the same site.
5	Site-to-Site Variation	153	All (x153)	Assess one sample from each site.

Data Management

The final research data collected and created during the proposed work is meant to be of a public nature and for widespread dissemination. Data was provided to the DOE-NETL in required format for sample characterization information to be compatible or easily transferable to their Energy Data eXchange (EDX) public database.

Field and laboratory notebooks were maintained for field data and analytical results. All observations, analyses/results, etc., were recorded in the notebooks and transferred to electronic files providing easy access. Notebooks were also scanned and stored electronically. Per institutional policies, data and metadata will be retained for a minimum of three years after the final report is accepted by NETL. Electronic data will be preserved in backups, conducted on a regular basis, in the form of DVDs and WVU's network storage. Backups are performed on a nightly basis and allows access to previous versions of files to guard against data corruption. The workstation network was protected by centrally managed network firewalls and a centrally monitored anti-virus protection system that notifies WVU's Office of Information Technology of any potential threats. These archives were stored in multiple places as detailed above.

Environmental Health and Safety

The health and environmental effects from the release of REEs into the environment are not well understood and environmental regulations are limited for this industry. However, because REE extraction and recovery is a chemically intense process, use of mineral acids, bases and organic solvents in REE extraction may result in the generation of multiple waste streams that require proper management. The project was conducted under the conditions of a *Project Chemical Hygiene Plan (CHP)*, an internal West Virginia University document, addressing key environmental and health issues. A similar document and policy is also in place at Virginia Tech.

Results

Preliminary sampling consisting of 140 aqueous AMD samples and 152 sludge samples were collected between December 2016 and June 2017. One, untreated (raw) AMD sample and at least one sludge sample were collected at each AMD treatment facility. Based on these preliminary results, a subset

consisting of 60 NAPP and 16 CAPP sites was then identified for intensive sampling which took place in Fall 2017. The following discussion summarizes the results of both sampling campaigns.

Chemical Composition of AMD and AMD Sludge

I. Statistical Analysis of the Data

Objectives:

1. Characterize REE concentrations in untreated AMD and AMD sludge across the CAPP and NAPP
2. Develop a predictive model for use as a prospecting tool for promising sludge sources

The general statistical model used in this study included the following variables:

Dependent variables (D) and Independent variables (I).

- D: REE concentration in AMD sludge
- D or I: REE concentration in untreated AMD
- I: pH
- I: Major ions: Al, Ca, Fe, Mg, Mn, Na, Si, Cl, SO₄
- I: Field parameters: pH, electrical conductivity (EC)

Hypothesis test:

Sample sizes of individual populations varied from 1 to over 10 with 10 as the nominal maximum. Neither homoscedasticity nor normality could be assumed. Thus, confidence intervals around each mean value were generated using Student's t test since it generates an independent variance for each population and adjusts each mean's precision test according to sample size, see **Table 8**. These mean values are used throughout this report to characterize REE concentrations of the CAPP and NAPP coal basins. The ratios of confidence interval to mean are summarized in **Table 9**. The results indicate higher variance in the CAPP AMD and sludge. This is probably due to the higher proportion of large, underground mine complexes in the NAPP which tend to homogenize AMD quality to a greater extent than the more isolated flow pathways typical of surface mines. CI/mean ratios for all ions were substantially lower in sludge than in AMD samples. This most likely reflects the integrating effect of sludge accumulation in cells over time while instantaneous AMD quality varies over short time intervals, a factor widely known within the AMD treatment community. Nonetheless in all cases the CI/mean ratios were all substantially less than 1 with a range of 0.05 to 0.53 indicating good to excellent sampling precision. Median values were near mean values for REE but less so for major ions, suggesting some skewness in the latter distributions.

Table 8. Summary of population sizes (n), means and confidence intervals (CI): two tailed tests and α , the probability of a type 1 error = 0.05.

REE	Raw AMD (ug/L)						AMD sludge (g/t)					
	CAPP			NAPP			CAPP			NAPP		
	mean	CI	n	mean	CI	n	mean	CI	n	mean	CI	n
Sc	3.2	1.0	53	6.4	1.6	127	12.6	1.5	143	20.9	1.0	471
Y	51.1	19.1	55	81.2	24.6	130	151.7	18.3	143	192.8	14.1	479
La	26.7	14.1	55	21.1	6.9	130	79.2	10.6	143	58.3	3.6	473
Ce	55.1	25.8	55	63.2	19.6	130	160.7	17.2	143	162.5	10.3	480
Pr	8.2	3.7	54	9.8	2.9	129	23.7	2.6	143	24.3	1.7	465
Nd	38.4	16.0	55	45.8	13.5	130	104.3	11.4	143	113.8	8.1	471
Sm	10.1	3.8	54	13.3	3.7	129	26.4	3.0	143	32.0	2.4	471
Eu	2.7	0.9	54	3.8	1.1	127	6.4	0.8	142	8.4	0.6	462
Gd	12.8	4.6	55	18.7	5.3	130	34.5	4.2	143	44.2	3.1	471
Tb	2.0	0.7	54	3.2	0.9	128	5.1	0.6	142	7.0	0.5	461
Dy	10.8	4.0	54	17.1	4.9	129	28.3	3.5	143	39.0	2.7	470
Ho	2.0	0.7	54	3.3	0.9	128	5.4	0.7	142	7.4	0.5	471
Er	5.1	1.9	54	8.4	2.5	129	14.2	1.7	143	19.9	1.4	470
Tm	0.8	0.2	53	1.3	0.3	126	1.9	0.2	133	2.8	0.2	425
Yb	3.9	1.5	54	6.5	1.8	130	10.4	1.2	143	15.1	1.0	471
Lu	0.7	0.2	53	1.1	0.3	126	1.6	0.2	133	2.3	0.1	431
TREE	232.6	95.9	55	303.4	88.6	130	666.0	72.2	143	737.8	49.1	484
Co							380.9	80.4	107	582.6	71.3	414
U							4.8	0.6	105	7.0	0.5	401
Th							6.6	0.8	103	7.5	0.3	389
% moisture							72.2	3.6	142	78.8	1.5	451
Major ions												
pH f	4.9	0.4	46	5.1	0.4	91						
Al	14.1	5.3	49	30.5	6.0	93	7.6	0.5	85	9.3	0.6	384
Ca	174.9	27.7	53	179.6	23.6	125	2.8	0.7	85	7.0	0.7	381
Fe	24.4	14.6	53	61.9	23.6	125	6.7	1.3	85	11.3	1.8	384
Mg	124.2	26.3	53	74.3	11.0	125	4.5	0.8	85	2.7	0.3	377
Mn	10.8	3.2	53	8.7	2.4	125	2.7	0.5	85	1.6	0.2	375
Na	48.4	27.4	53	550.9	198.2	125	0.2	0.0	57	0.1	0.0	299
Si	11.4	2.5	53	14.2	1.7	125	15.7	1.8	85	9.7	0.7	384
Cl	13.2	16.5	52	323.0	257.3	121	68.3	9.6	12	130.5	34.4	86
SO4	1129.3	195.3	52	1765.5	359.2	121	2.8	0.5	56	4.5	0.4	304

Table 9. Ratios of confidence interval (CI) to mean for data presented in Table 8.

REE	Raw AMD (CI/mean)		AMD sludge (CI/mean)	
	CAPP	NAPP	CAPP	NAPP
Sc	0.33	0.25	0.12	0.05
Y	0.37	0.3	0.12	0.07
La	0.53	0.33	0.13	0.06
Ce	0.47	0.31	0.11	0.06
Pr	0.45	0.29	0.11	0.07
Nd	0.42	0.3	0.11	0.07
Sm	0.37	0.28	0.11	0.07
Eu	0.34	0.28	0.12	0.07
Gd	0.36	0.29	0.12	0.07
Tb	0.33	0.27	0.12	0.07
Dy	0.37	0.29	0.12	0.07
Ho	0.34	0.27	0.12	0.07
Er	0.38	0.29	0.12	0.07
Tm	0.28	0.23	0.13	0.07
Yb	0.38	0.29	0.11	0.07
Lu	0.28	0.23	0.12	0.06
REE median	0.41	0.29	0.11	0.07
median	0.37	0.29	0.12	0.07

major ions	Raw AMD (CI/mean)		AMD sludge (CI/mean)	
	CAPP	NAPP	CAPP	NAPP
pH f	0.09	0.07		
Al	0.38	0.2	0.06	0.07
Ca	0.16	0.13	0.27	0.11
Fe	0.6	0.38	0.19	0.16
Mg	0.21	0.15	0.18	0.12
Mn	0.3	0.28	0.19	0.11
Na	0.57	0.36	0.1	0.07
Si	0.22	0.12	0.12	0.07
Cl	1.25	0.8	0.14	0.26
SO4	0.17	0.2	0.17	0.08
Median	0.26	0.2	0.17	0.11

REE Concentrations

The dominant factor controlling the TREE concentration in raw AMD is the pH of the raw water. The population is essentially bimodal, **Figure 3**. A pH of 5.5 was chosen as the boundary between these two populations. Below pH 5.5 AMD is, by definition, acidic while above 5.5 it becomes increasingly net alkaline. In fact, due to the nature of Al and Fe buffering in AMD solutions the region between pH 4.5 and 6.0 is sparsely populated since small changes in acidity result in stability at pH 3.0 to 4.5, the points where Fe^{3+} and Al^{3+} precipitate and 6.0, where Fe^{2+} oxidizes and precipitates. While the aqueous and solid phase curves are broadly similar, see **Figures 3** and **4**, regression analysis indicates that raw AMD pH predicts the TREE concentration in AMD much better than the TREE concentration in sludge ($R^2 = 0.64$ vs. 0.15 respectively). The poor correlation between AMD pH and sludge TREE concentration likely reflects the difference between an instantaneous influent water pH and the accumulated sludge which would integrate a variety of influent pH levels over time. These and additional, contaminating factors during AMD treatment will influence sludge quality. These will be discussed in a later section of this report.

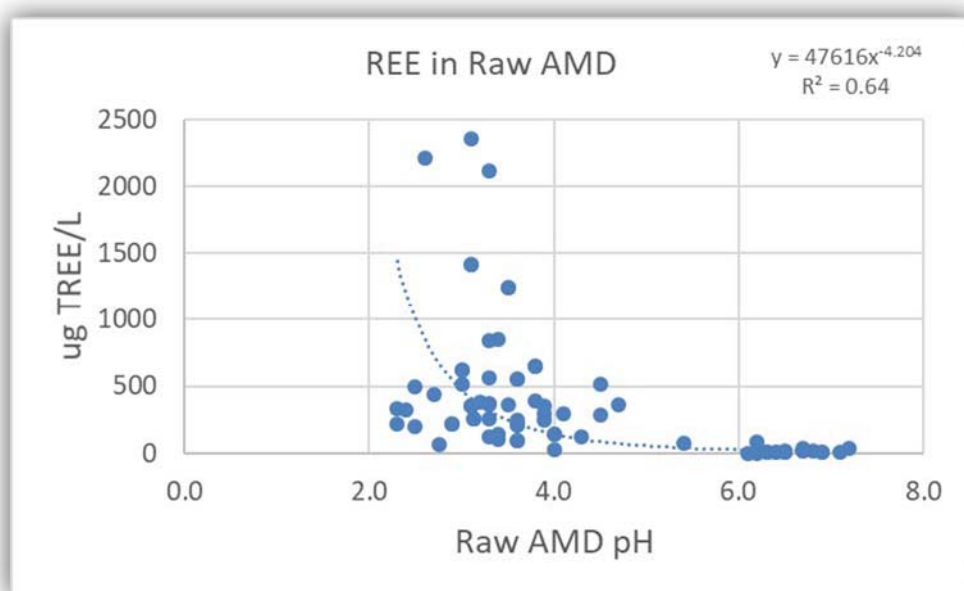


Figure 3. The relationship between the pH of raw AMD and the concentration of TREE in the aqueous phase.

REE concentrations across the 140 sampled sites indicate a strong division at pH 5.5. The acid samples averaged 355 $\mu\text{g/L}$ while at the alkaline sites the average TREE concentration was only 27 $\mu\text{g/L}$, **Table 10**. The ratio HREE/TREE was slightly higher in the alkaline water (42% vs. 38%).

For the sake of simplicity, raw AMD with a pH <5.5 will be referred to as acidic AMD, while the higher pH AMD will be referred to as alkaline AMD.

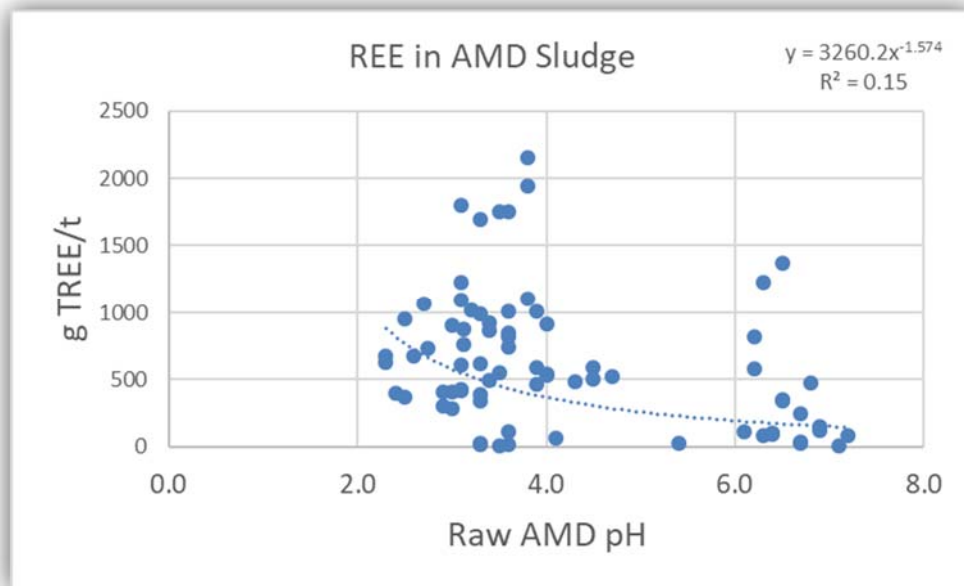


Figure 4. The relationship between the pH of raw AMD and the concentration of TREE in the resulting AMD treatment sludge.

Both raw AMD and AMD treatment sludges generated in the NAPP had marginally higher concentrations of REE than those from the CAPP, **Table 10**. NAPP sludge averaged 751 g TREE/t while CAPP sludges averaged 666 g TREE/t. The ratio of HREE to TREE was 47% in NAPP sludges and 40% in CAPP sludges. The combined ratios of HREE+critical REE/TREE were also higher in NAPP sludges, 63% vs. 56%. Across all samples, the ratio HREE/TREE was 43% while the ratio HREE+critical/TREE was 60%. Proportions of HREE and critical REEs to TREE in both coal basins compare favorably with the best REE ores on the international market.

Th and U, the naturally occurring radioactive materials (NORMs) in AMD sludge comprised less than 2% of TREE content. Co concentrations in both CAPP and NAPP sludges were nearly identical to TREE concentrations. The moisture content of sludge averaged 72 and 79% in CAPP and NAPP samples respectively, **Table 10**.

The proportion of individual REEs varies marginally across coal basins, **Table 10**. The six most common REEs comprise 82.5% of TREE and include three critical and three HREE, **Table 11**. The proportion of REE relative to TREE is similar in both untreated AMD and sludge; see **Figures 5 and 6**.

Table 10. AMD and sludge REE content in central (CAPP) and northern (NAPP) Appalachian coal basins. Additional parameters include U, Th, Co and sludge moisture content. T, L and HREE refer to total, light (green shading) and heavy (purple shading) REE. Critical REEs are highlighted in red.

n =	AMD ($\mu\text{g/L}$)			Sludge (g/t)		
	CAPP	NAPP	All	CAPP	NAPP	All
	55	130	185	144	485	629
La	26.7	21.1	23.9	79.2	58.3	68.7
Ce	55.1	63.2	59.1	160.7	162.5	161.6
Pr	8.2	9.8	9.0	23.7	24.3	24.0
Nd	38.4	45.8	42.1	104.3	113.8	109.0
Sm	10.1	13.3	11.7	26.4	32.0	29.2
Eu	2.7	3.8	3.3	6.4	8.4	7.4
Sc	3.2	6.4	4.8	12.6	20.9	16.7
Y	51.1	81.2	66.1	151.7	192.8	172.3
Gd	12.8	18.7	15.7	34.5	44.2	39.3
Tb	2.0	3.2	2.6	5.1	7.0	6.0
Dy	10.8	17.1	14.0	28.3	39.0	33.6
Ho	2.0	3.3	2.7	5.4	7.4	6.4
Er	5.1	8.4	6.7	14.2	19.9	17.0
Tm	0.8	1.3	1.1	1.9	2.8	2.3
Yb	3.9	6.5	5.2	10.4	15.1	12.8
Lu	0.7	1.1	0.9	1.6	2.3	2.0
TREE	233.5	304.2	268.9	666.4	750.6	708.5
LREE	141.3	157.0	149.1	400.8	399.2	400.0
HREE	92.3	147.1	119.7	265.6	351.4	308.5
HREE/TREE	39.5%	48.4%	44.5%	39.9%	46.8%	43.5%
HREE+critical/TREE	57.1%	64.7%	61.4%	56.5%	63.1%	60.0%
U				4.8	7.0	5.9
Th				6.6	7.5	7.0
U+Th/TREE				1.7%	1.9%	1.8%
Co				666.0	737.8	701.9
% moisture				72%	79%	75%

The proportion of individual REEs varies marginally across coal basins, **Table 11**. The six most common REEs comprise 82.5% of TREE and include three critical and three HREE, **Table 12**. The proportion of REE relative to TREE is similar in both untreated AMD and sludge; see **Figures 5** and **6**.

Table 11. The proportion of individual REE in untreated AMD and AMD sludge in the CAPP and NAPP coal basins. T, L and HREE refer to total, light (green shading) and heavy (purple shading) REE. Critical REEs are highlighted in red.

	AMD ($\mu\text{g/L}$)			Sludge (g/t)		
	CAPP	NAPP	All	CAPP	NAPP	All
n =	55	130	185	144	485	629
La	11.5%	6.9%	8.9%	11.9%	7.8%	9.7%
Ce	23.6%	20.8%	22.0%	24.1%	21.6%	22.8%
Pr	3.5%	3.2%	3.4%	3.6%	3.2%	3.4%
Nd	16.4%	15.1%	15.7%	15.7%	15.2%	15.4%
Sm	4.3%	4.4%	4.3%	4.0%	4.3%	4.1%
Eu	1.2%	1.3%	1.2%	1.0%	1.1%	1.0%
Sc	1.4%	2.1%	1.8%	1.9%	2.8%	2.4%
Y	21.9%	26.7%	24.6%	22.8%	25.7%	24.3%
Gd	5.5%	6.1%	5.8%	5.2%	5.9%	5.6%
Tb	0.9%	1.0%	1.0%	0.8%	0.9%	0.9%
Dy	4.6%	5.6%	5.2%	4.2%	5.2%	4.7%
Ho	0.9%	1.1%	1.0%	0.8%	1.0%	0.9%
Er	2.2%	2.8%	2.5%	2.1%	2.7%	2.4%
Tm	0.3%	0.4%	0.4%	0.3%	0.4%	0.3%
Yb	1.7%	2.1%	1.9%	1.6%	2.0%	1.8%
Lu	0.3%	0.4%	0.3%	0.2%	0.3%	0.3%
TREE	100.0%	100.0%	100.0%	100.0%	100.0%	100.0%

Table 12. REE in both CAPP and NAPP basins ranked according to proportion of TREE.

rank	REE	Proportion of TREE	cumulative proportion
1	Y	24.3%	24.3%
2	Ce	22.8%	47.1%
3	Nd	15.4%	62.5%
4	La	9.7%	72.2%
5	Gd	5.6%	77.8%
6	Dy	4.7%	82.5%
7	Sm	4.1%	86.6%
8	Pr	3.4%	90.0%
9	Er	2.4%	92.4%
10	Sc	2.4%	94.8%
11	Yb	1.8%	96.6%
12	Eu	1.0%	97.6%
13	Ho	0.9%	98.5%
14	Tb	0.9%	99.4%
15	Tm	0.3%	99.7%
16	Lu	0.3%	100.0%

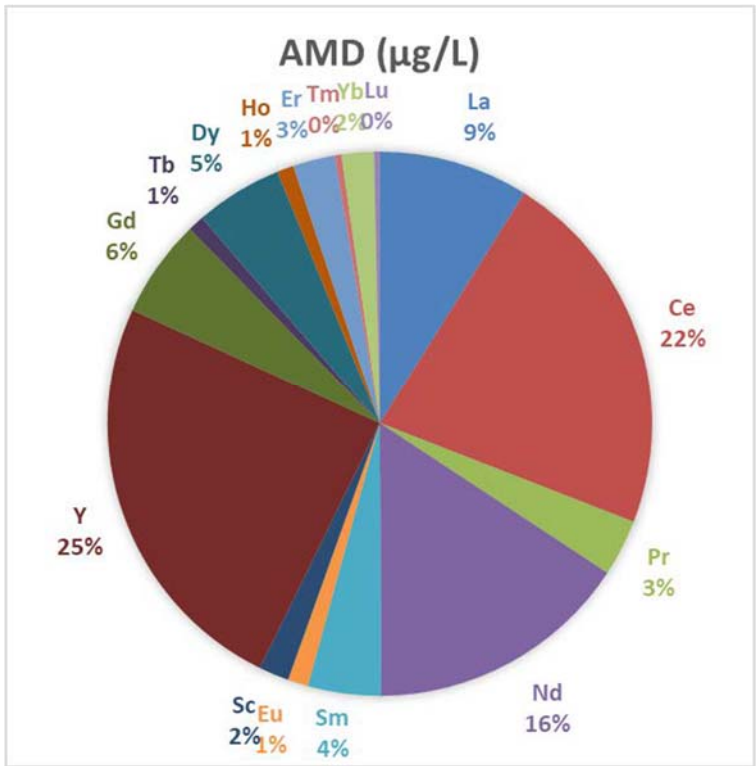


Figure 5 The proportion of individual REE in untreated AMD.

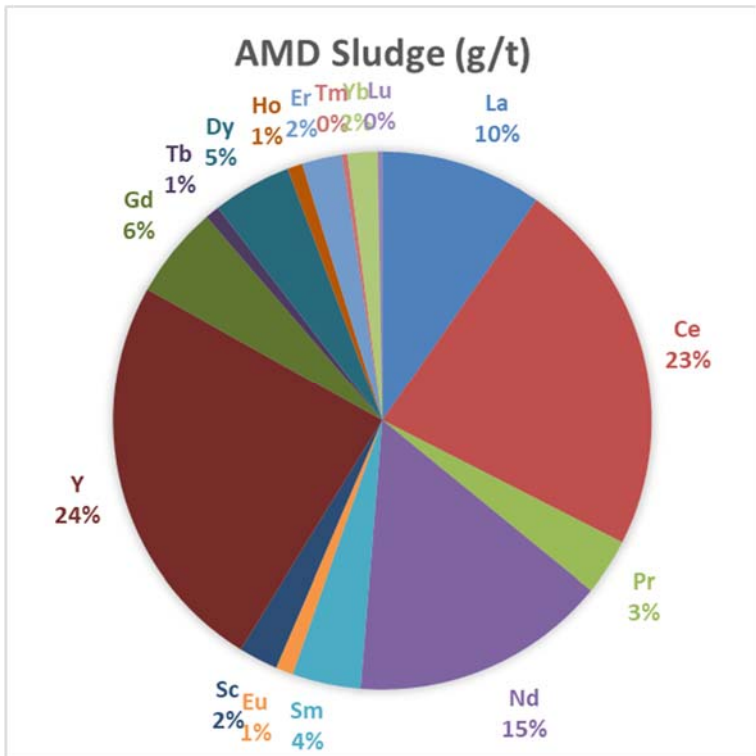


Figure 6. The proportion of individual REE in AMD sludge.

The process of conventional AMD treatment concentrates REE by an average 2635x on a mass basis over all samples. The concentration factor in the CAPP was higher than in the NAPP (2853x vs 2468x), **Table 13**. The concentration factors of all REE except Sc ranged between 2100x and 2900x except Sc which was 3480x, **Figure 7**.

Table 13. Conventional AMD treatment increased REE concentration from aqueous phase (AMD) to solid phase (sludge) at rates specific to each element and was nominally affected by coal basin.

	Concentration factor		
	CAPP	NAPP	All
La	2961	2760	2873
Ce	2915	2572	2732
Pr	2886	2476	2663
Nd	2717	2481	2589
Sm	2620	2410	2500
Eu	2384	2211	2283
Sc	3931	3256	3480
Y	2972	2373	2604
Gd	2705	2368	2505
Tb	2561	2205	2342
Dy	2614	2278	2408
Ho	2721	2240	2420
Er	2793	2376	2533
Tm	2311	2173	2226
Yb	2671	2342	2466
Lu	2229	2139	2174
TREE	2853	2468	2635

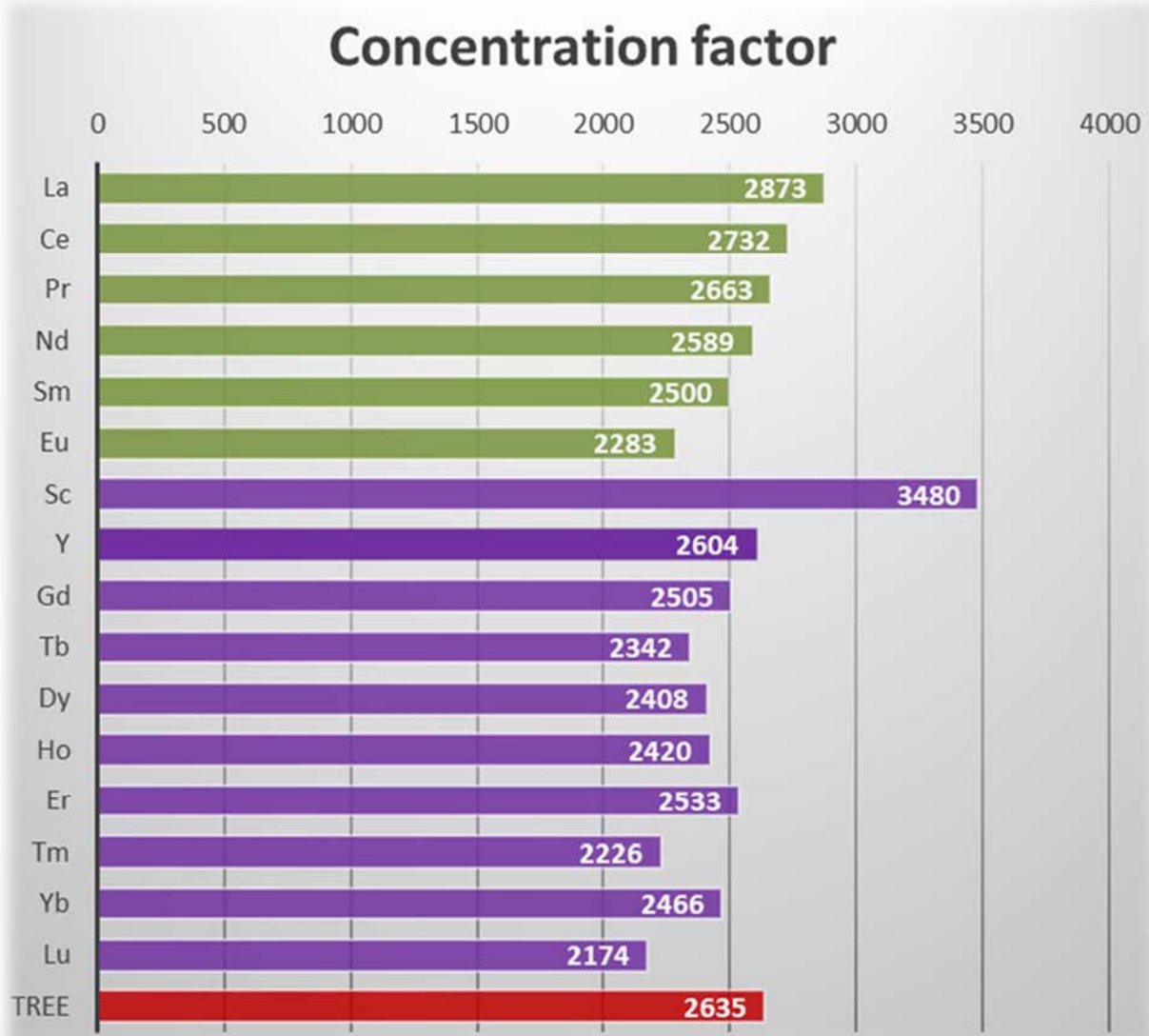


Figure 7. Concentration factor indicates the change in concentration from aqueous (AMD) to solid (sludge) phase because of AMD treatment. The results are determined on a mass basis. The data include CAPP and NAPP coal basins. Green=LREE, Purple=HREE. TREE represents the overall concentration factor.

Capacity of AMD to supply REE in the CAPP and NAPP coal basins

I. Stored REE resource

The initial survey yielded 140 AMD sludge storage sites to visit and characterize. Generally, one to two samples each of sludge and raw AMD were collected for analysis. As discussed earlier, these sites were down-selected to 16 CAPP and 60 NAPP sites for further investigation. Sludge volumes were then estimated using Google Earth. Sludge cell surface was estimated and each cell was assumed to have a depth of 10 feet unless specific depth information was available. Moisture content was used to correct to sludge mass on a dry weight basis. Analytical results were then used to determine the mass of individual REEs at each site. Basket REE and contained values were calculated for each sludge source; see **Table 14**. This approach accounts for site variations of each REE and their availability as sludge. Sites not permitting access or which did not dispose sludge in surface cells were not included in the volumetric estimations. It is understood that, perhaps, most sludge is disposed in ways that render them unavailable such as injection into deep mine voids or subsequent burial of sludge cells in subsequent spoil or refuse lifts. It is expected that determination of the economic value of AMD sludge will affect operators' sludge handling decisions and result in higher rates of availability. The findings indicate 350 tons in place with an estimated contained value of \$79 million, **Table 15**. The basin-wide basket price was found to be \$237.73/kg TREE and the contained value for one ton of dry sludge was \$129.16. The grade of NAPP sludges was higher than the CAPP sludges. Contained values of CAPP and NAPP sludges were \$107 and \$135/ton dry weight basis respectively. There was much more sludge in the NAPP resulting in an overall contained value of \$58 million vs. \$22 million in the CAPP sites. The estimated TREE mass in NAPP sludge was 255 tons vs. 95 tons in the CAPP. Sampling for an earlier project identified an additional 44.5 tons of TREE at three additional sites in the NAPP. This would increase the REE content of sampled sludge in place to 395 tons with a contained value of \$87.5 million.

Table 14. Results of sludge cell sampling, 76 sites in CAPP and NAPP. DW = dry weight basis; CV = contained value; SL = sludge.

site code	coal basin	TREE g/t	Basket price \$/kg TREE DW	CV \$/t SL DW	SL volume m ³ DW	On site sludge		
						SL DW (t)	TREE (t)	CV
SL 1 1	CAPP	963.6	\$ 136.53	\$ 131.56	1,254	2,759	2.7	\$ 362,955
SL 1 5	CAPP	900.7	\$ 148.01	\$ 133.32	1,526	3,357	3.0	\$ 447,591
SL 1 10	CAPP	283.4	\$ 370.05	\$ 104.88	30,710	67,562	19.1	\$ 7,085,909
SL 18 5	CAPP	398.3	\$ 265.44	\$ 105.71	34,444	75,777	30.2	\$ 8,010,565
SL 32 1	CAPP	733.7	\$ 131.97	\$ 97.02	532	1,170	0.9	\$ 113,548
SL 33 1	CAPP	1013.3	\$ 124.47	\$ 126.13	673	1,481	1.5	\$ 186,751
SL 35 1	CAPP	1104.7	\$ 117.92	\$ 130.27	4,921	10,826	12.0	\$ 1,410,279
SL 35 10	CAPP	547.6	\$ 228.53	\$ 125.15	7,776	17,107	9.4	\$ 2,140,979
SL 39 1	CAPP	1368.8	\$ 71.08	\$ 97.30	2,003	4,407	6.0	\$ 428,765
SL 40 1	CAPP	501.1	\$ 176.23	\$ 88.96	28	62	0.0	\$ 5,480
SL 45 5	CAPP	592.7	\$ 130.86	\$ 77.56	1,389	3,056	1.8	\$ 236,997
SL 46 1	CAPP	914.7	\$ 155.13	\$ 141.89	154	339	0.3	\$ 48,072
SL 46 5	CAPP	530.2	\$ 156.34	\$ 82.89	4,968	10,930	5.8	\$ 905,971
SL 85 1	CAPP	815.1	\$ 69.07	\$ 56.30	629	1,384	1.1	\$ 77,903
SL 92 2	CAPP	820.8	\$ 139.45	\$ 114.46	213	469	0.4	\$ 53,638
SL 93 2	CAPP	1022.3	\$ 104.21	\$ 106.53	407	895	0.9	\$ 95,390
	CAPP		\$ 157.83	\$ 107.50	91,627	201,579.4	95.1	\$ 21,610,792

site code	coal basin	TREE g/t	Basket price \$/kg TREE DW	CV \$/t SL DW	SL volume m ³ DW	On site sludge		
						SL DW (tons)	TREE (t)	CV
SL 2 1	NAPP	412.8	\$ 952.46	\$ 393.14	3,566	7,845	3.2	\$ 3,084,244
SL 2 2	NAPP	428.5	\$ 850.48	\$ 364.41	2,990	6,578	2.8	\$ 2,397,119
SL 2 5	NAPP	421.0	\$ 790.34	\$ 332.74	3,702	8,144	3.4	\$ 2,709,985
SL 3 1	NAPP	611.6	\$ 280.23	\$ 171.40	199	438	0.3	\$ 75,041
SL 4 1	NAPP	673.6	\$ 290.60	\$ 195.75	3,577	7,869	5.3	\$ 1,540,448
SL 6 1	NAPP	624.8	\$ 257.35	\$ 160.80	1,865	4,103	2.6	\$ 659,780
SL 8 1	NAPP	374.9	\$ 203.64	\$ 76.35	1,164	2,561	1.0	\$ 195,510
SL 9 1	NAPP	1228.8	\$ 133.47	\$ 164.01	990	2,178	2.7	\$ 357,203
SL 10 1	NAPP	678.6	\$ 427.67	\$ 290.43	826	1,817	1.2	\$ 527,771
SL 11 1	NAPP	955.1	\$ 114.92	\$ 109.76	505	1,111	1.1	\$ 121,947
SL 12 1	NAPP	461.8	\$ 152.04	\$ 70.21	196	431	0.2	\$ 30,276
SL 20 1	NAPP	23.1	\$ 15.50	\$ 0.36	39,748	87,446	2.0	\$ 31,317
SL 21 1	NAPP	114.4	\$ 324.96	\$ 37.29	-	-	0.0	\$ -
SL 21 5	NAPP	151.4	\$ 462.65	\$ 70.04	27,705	60,951	9.2	\$ 4,269,305
SL 23 1	NAPP	127.4	\$ 187.46	\$ 23.88	2,225	4,895	0.6	\$ 116,906
SL 26 2	NAPP	1063.1	\$ 198.87	\$ 199.30	2,478	5,452	5.8	\$ 1,086,516
SL 30 1	NAPP	19.9	\$ 281.72	\$ 6.41	32,723	71,991	1.4	\$ 461,310
SL 30 SS	NAPP	5.4	\$ 187.78	\$ 28.57	951	2,092	0.0	\$ 59,774
SL 31 1	NAPP	584.6	\$ 193.93	\$ 113.37	195	429	0.3	\$ 48,635
SL 48 1	NAPP	543.0	\$ 284.36	\$ 154.40	54	119	0.1	\$ 18,343
SL 48 5	NAPP	305.6	\$ 216.47	\$ 66.35	866	1,905	0.6	\$ 126,401
SL 49 1	NAPP	408.2	\$ 131.84	\$ 53.85	5,426	11,937	4.9	\$ 642,861
SL 50 1	NAPP	924.4	\$ 108.15	\$ 99.98	89	196	0.2	\$ 19,575

site code	coal basin	TREE g/t	Basket price \$/kg TREE DW	CV \$/t SL DW	SL volume m ³ DW	On site sludge		
						SL DW (tons)	TREE (t)	CV
SL 51 1	NAPP	1691.1	\$ 160.03	\$ 270.63	58	128	0.2	\$ 34,533
SL 51 5	NAPP	1747.8	\$ 147.25	\$ 257.48	14,932	32,850	57.4	\$ 8,458,216
SL 53 1	NAPP	845.8	\$ 172.47	\$ 145.88	55	121	0.1	\$ 17,652
SL 54 5	NAPP	744.1	\$ 201.83	\$ 150.18	1,338	2,944	2.2	\$ 442,077
SL 57 2	NAPP	496.1	\$ 273.08	\$ 136.09	118	260	0.1	\$ 35,330
SL 58 5	NAPP	862.3	\$ 192.30	\$ 93.09	9,639	21,206	18.3	\$ 1,974,074
SL 59 1	NAPP	758.2	\$ 281.74	\$ 181.64	901	1,982	1.5	\$ 360,046
SL 59 2	NAPP	758.2	\$ 290.26	\$ 220.06	305	671	0.5	\$ 147,660
SL 64 2	NAPP	876.0	\$ 83.99	\$ 73.58	2,707	5,955	5.2	\$ 438,173
SL 65 1	NAPP	989.2	\$ 192.90	\$ 190.88	799	1,758	1.7	\$ 335,537
SL 65 5	NAPP	1096.3	\$ 194.65	\$ 213.40	11,020	24,244	26.6	\$ 5,173,578
SL 66 1	NAPP	1803.9	\$ 194.02	\$ 388.87	852	1,874	3.4	\$ 728,894
SL 66 4	NAPP	1947.1	\$ 194.81	\$ 379.33	1,720	3,784	7.4	\$ 1,435,367
SL 67 1	NAPP	2149.4	\$ 90.27	\$ 194.02	128	282	0.6	\$ 54,637
SL 68 1	NAPP	862.3	\$ 155.10	\$ 130.25	5,883	12,943	11.2	\$ 1,685,797
SL 69 1	NAPP	389.9	\$ 230.71	\$ 89.95	235	517	0.2	\$ 46,506
SL 69 5	NAPP	1011.8	\$ 243.13	\$ 245.99	1,606	3,533	3.6	\$ 869,137
SL 70 1	NAPP	109.9	\$ 357.03	\$ 39.28	59,520	130,944	14.4	\$ 5,143,646
SL 70 P	NAPP	16.9	\$ 850.99	\$ 35.95	13,371	29,416	0.5	\$ 1,057,378
SL 74 2	NAPP	1161.4	\$ 134.80	\$ 156.56	325	715	0.8	\$ 111,944
SL 77 2	NAPP	1751.0	\$ 109.34	\$ 191.45	1,183	2,603	4.6	\$ 498,260
SL 78 1	NAPP	61.6	\$ 476.20	\$ 32.09	9,213	20,269	1.2	\$ 650,344
SL 79 1	NAPP	1231.3	\$ 221.86	\$ 273.16	121	266	0.3	\$ 72,717
SL 100 1	NAPP	525.7	\$ 258.84	\$ 136.07	1,700	3,740	2.0	\$ 508,910
SL 102 20	NAPP	27.0	\$ 16.50	\$ 0.45	10,785	23,727	0.6	\$ 10,569
SL 106 1	NAPP	354.9	\$ 319.61	\$ 113.43	5,556	12,223	4.3	\$ 1,386,463
SL 107 1	NAPP	248.2	\$ 424.12	\$ 105.27	2,941	6,470	1.6	\$ 681,099
SL 108 1	NAPP	85.7	\$ 35.11	\$ 3.01	16,995	37,389	3.2	\$ 112,507
SL 108 10	NAPP	90.3	\$ 33.67	\$ 3.04	375	825	0.1	\$ 2,509
SL 109 1	NAPP	100.4	\$ 341.58	\$ 34.29	5,752	12,654	1.3	\$ 433,980
SL 110 1	NAPP	345.8	\$ 246.48	\$ 85.23	2,288	5,034	1.7	\$ 429,023
SL 112 1	NAPP	33.1	\$ 417.99	\$ 13.84	37,912	83,406	2.8	\$ 1,153,960
SL 117 1	NAPP	479.4	\$ 146.30	\$ 76.82	13,073	28,761	13.8	\$ 2,209,266
SL 118 2	NAPP	618.9	\$ 207.40	\$ 134.84	7,626	16,777	10.4	\$ 2,262,246
SL 119 1	NAPP	343.7	\$ 275.77	\$ 94.77	600	1,320	0.5	\$ 125,103
SL 120 1	NAPP	25.1	\$ 26.07	\$ 0.65	10,655	23,441	0.6	\$ 15,340
SL 120 5	NAPP	85.7	\$ 259.13	\$ 22.21	6,961	15,314	1.3	\$ 340,095
SL BR	NAPP	26.3		17.8	50,764	111,681	2.9	\$ 1,990,017
SL MV	NAPP	432.2		251.7	1,242	2,732	1.2	\$ 687,810
SL DL	NAPP	1450.4		191.1	12,417	27,317	39.6	\$ 5,220,718
NAPP		631.1	\$ 258.40	\$ 134.94	391,288	860,834	255	\$ 58,022,837
			average all CAPP, NAPP		Sum all CAPP, NAPP			
			\$ 237.23	\$ 129.16	482,915	1,062,413	350	79,633,629

Table 15. Summary of basinal REEs content and value in the sludge resource.

Sludge cells sampled, this project		76
Sludge volume (Dry)	482,915	m ³
Sludge mass (Dry)	1,062,413	tons DW
average TREE grade	663	g/t
TREE mass	350	tons
REE Basket Price (MREO)	\$ 237.23	/kg TREE
estimated CV	\$ 79,633,629	

II. Annual REE production

AMD is generated at sites ranging from ephemeral discharges of less than 5 gpm to massive, continuous discharges exceeding 2500 gpm. Only a fraction of the Appalachian Basin's AMD production is treated. Estimates range between 33% to 50%. The untreated portion is generated by pre-law (SMCRA 1977: PL 95-87) mining operations and enters groundwater, streams and rivers and contributes to regional stream impairment. Identified in statute as abandoned mine lands or AMLs they are a potential REE resource and could be developed given appropriate economic incentives but currently those incentives do not exist. To account for access limitations, annual REE production was estimated based on state surveys and data sets. It was then assumed that only one half of that resource could be developed as an REE reserve base. Surveyed sites represented a fraction of regional AMD production.

AMD reporting is incomplete at best. For example, even regulated AMD discharges are generally not required to report flow (Q). The treated effluent is monitored for regulated parameters such as Fe, Mn, Al, pH and, perhaps a few other ions. Raw water quality is not reported. In addition, abandoned discharges are even more difficult to quantify. Flows are precipitation driven and in the Upper Ohio River Basin, annual precipitation over the past 20 years has ranged from a low of 36 inches/year to a high of 64 inches/year. During our sampling period, precipitation in the region was near average: ~45 in./yr. Mine discharges vary seasonally and in response to precipitation and recharge events; therefore, one year surveys are estimates at best. Also, large underground mine complexes can exceed 20 square miles. After mining, flooding of these voids can take many years when there is little to no discharge. Other discharges upwell into stream and riverbeds making direct flow measurement problematic. Nonetheless, our research program as well as state and Federal agencies have made some progress toward quantifying AMD production in the Appalachian basin. These have been aggregated to an estimate of 94,838 L/sec. An alternative approach to estimating AMD discharges was recently published by Stewart et al.⁹ It relies on an estimate of coal mined acreage in the Appalachian basin and an average net infiltration rate yielding an estimated AMD production rate of 418,000 L/sec. This likely represents the upper bounds for basinal AMD discharge. Given the limitations of both approaches, we present two estimates for basinal AMD discharge, **Table 16**. However, the lower, more conservative value will be used in the following analyses.

Table 16. Two estimates of AMD production in the northern and central Appalachian coal basins (L/sec).

State	State records, author's observation	Stewart et al., 2017 ⁹
	LOW ESTIMATE	HIGH ESTIMATE
PA	51,469	Total, Appalachian Basin
WV	24,127	
OH	18,925	
MD	317	
Total	94,838	418,000

AMD sludge density was determined hygrometrically; see **Table 17** and yielded a mean value of 2.2 t/m³.

Resource valuation was based on prices for mixed rare earth oxides (MREO) and did not assume refinement to individual REEs. This is a conservative assumption and the separability and refining costs of REE are the subject of our ongoing bench scale project (DE-FE0026927). More reliable estimates of these two important parameters are not currently available. In this context, two parameters are used to estimate value: Basket price and contained value **Table 18**. The average basket price and contained value were used to estimate basinal resource value.

Table 17. Sludge density was determined hygrometrically and was found to vary within narrow limits. Confidence intervals represent the range in which 95% of the population's samples are likely to occur. They were determined using the student's t statistic and the parameters listed in the table.

parameter	value
upper confidence level	2.24 t/m ³
mean	2.20 t/m ³
lower confidence level	2.16 t/m ³
confidence interval	0.041
sample size	9
alpha	0.05
standard deviation	0.053

Table 18. Basis for determining REE basket price and contained value. Oxide prices (MREO) were used to estimate resource value.

Basket Price (\$/kg TREE DW)	
CAPP	\$ 157.83
NAPP	\$ 258.40
Avg. all	\$ 237.23
Contained REE Value (\$/ton sludge DW)	
CAPP	\$ 168.03
NAPP	\$ 165.86
Avg. all	\$ 166.31

Table 19 summarizes values used to estimate REE reserves and contained values. Note that prices for MREO are used as the basis for value estimation. The reserve base assumes that 50% of the annual AMD production is accessible.

Table 19. Parameters and values used for REE reserve and value estimation. DW=Dry weight.

Basis for reserve estimation		
Parameter	value	units
AMD REE conc.	0.269	mg TREE/L
Sludge REE conc.	709	g TREE/t
sludge density	2.20	t/m ³ DW
REE Basket Price (MREO)	\$ 237.23	/kg
sludge solids %	24.5%	
accessability	50%	

The above values were used to estimate annual AMD-based REE production in the Appalachian Basin, **Table 20**. The low AMD production estimate yields 808 ton REE/year with a contained value of \$192 million. The high AMD production estimate yields 3,563 ton REE/year with a contained value of \$845 million.

Prediction of sludge TREE from field survey data

The *overall objective* of this section is to better understand what drives TREE concentrations in acid mine drainage and treatment sludge. The *specific objectives* of the current analyses are to:

1. Model TREE in raw AMD and treatment sludge from landscape and survey-level water chemistry data;
2. Model TREE in raw AMD as a function of detailed water chemistry data; and
3. Model TREE in treatment sludge from detailed water chemistry and treatment characteristics.

Table 20. Estimated annual NAPP and CAPP REE production from AMD.

All Sites	Sampled		
	sites (n=140)	est. total APP ¹	est. total APP ²
Total Q (L/sec)	6,221	94,838	418,000
% total APP Q		6.56%	1.49%
Total TREE flux (kg/yr)	53,029	808,408	3,563,086
MREO ³ Basket Price(\$/kg REE DW)	\$ 237.23	\$ 237.23	\$ 237.23
est. contained value	\$ 12,579,978	\$ 191,778,717	\$ 845,270,972

¹ APP basin AMD discharge (Q) per this study
² APP basin AMD discharge (Q) per Stewart et al., 2017
³ Mixed Rare Earth Oxides

Results of backward deletion (*F*-ratios; *p*-values) were used to identify the minimum adequate model relating TREE concentrations (log [x]-transformed) in raw AMD to pH, discharge, specific conductance, source (refuse, underground flooded, underground non-flooded, surface mining), coal formation (Kanawha, Allegheny, Monongahela, New River, Pocahontas, Conemaugh) and basin (Central

Appalachian, Northern Appalachian). Change in residual variance and degrees of freedom (*df*) represent increases in residual variance and *df* following removal of insignificant terms from the most simplified model.

Backward deletion (*F*-ratios; *p*-values) was also used to identify the minimum adequate model relating TREE concentration in treatment sludge as a function of major ions and treatment characteristics across sites with high sludge concentrations relative to AMD concentrations. Residual variance and degrees of freedom (*df*) change represent increases in residual variance and *df* following removal of insignificant terms from the most simplified model.

The above formed the basis for developing a simple model for use as a survey tool allowing prediction of sludge REE concentration as a function of the field parameters pH and electrical conductivity.

Dependent variable:

$$Y = \text{predicted sludge TREE concentration (g TREE/t sludge DW)}$$

Independent variables:

X_1 = field pH

X_2 = field electrical conductivity (EC)

$X_{3,4}$ = Chemical treatment method

The model was validated by comparing estimated sludge TREE against observed TREE, **Figure 8**. The modest correlation coefficient ($R^2 = 0.57$) indicates a useful prospecting tool that can be used to identify promising sludge deposits using field survey tools and help focus expensive and time consuming chemical analysis.

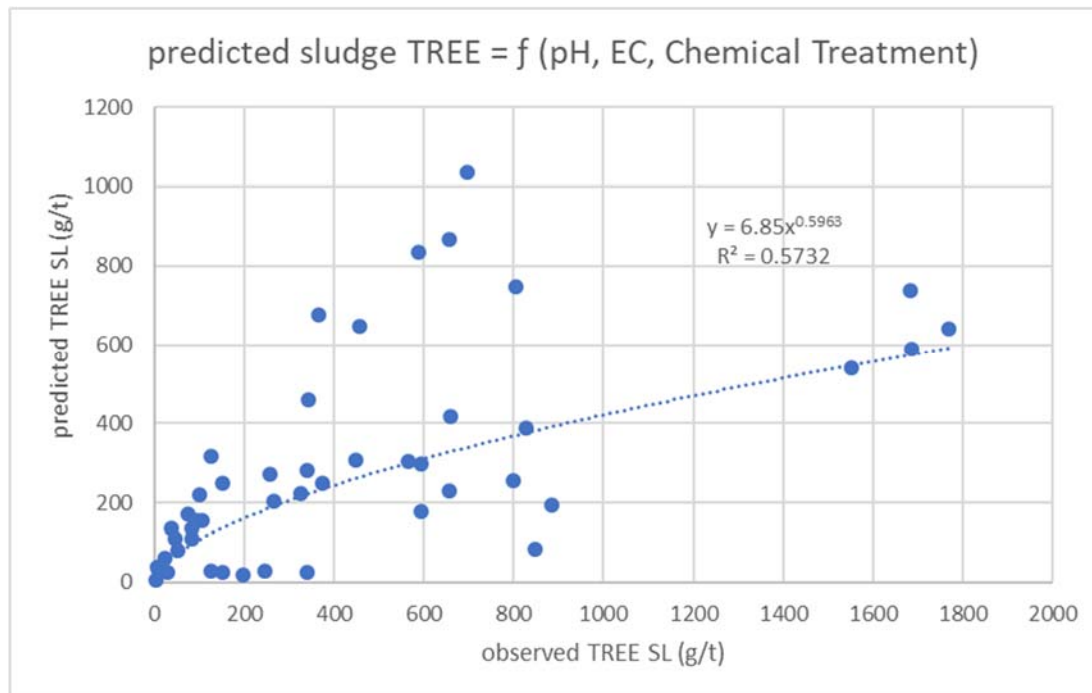


Figure 8. Predicted sludge TREE. The model uses the field parameters pH and EC to estimate the TREE concentration in AMD sludge. SL = sludge.

III. Acid Leaching Trials

Over the course of the project, over 600 individual leaching test runs were completed. Initially, XRF was used to determine the elemental content for 150 unique sludge samples that were later evaluated in various leaching tests. Using the appropriate analytical settings, XRF produced measurable assays for 29 different elements, including Ba, Sb, Sn, Mo, Nb, Zr, Sr, Rb, Bi, As, Pb, W, Zn, Cu, Ni, Co, Fe, Mn, Cr, V, Ti, Ca, K, Al, P, Si, Cl, S and Mg. It should be noted that this specific XRF unit is not optimized for REE analysis and as such, they were not included in the analytical suite. **Figure 9** shows the average elemental distribution for all samples (only the top 5 elements are shown). Note the category 'other' is the difference between detected elements and total mass, thus H and O are included in 'other' and likely account for a large portion of total mass. While **Figure 10** shows the maximum assay recorded from the population of sludge samples for each element. Iron was the predominant species, with an average content of 16.4% and a maximum of 62.2% in one specific specimen (SL-30-R), a flooded, net alkaline deep mine, pH 6.2. As expected, other major species included Ca, S, Si, Al, Mn, Mg, Cl and K. XRF also detected trace amounts of other elements which are also noted in **Figure 10**.

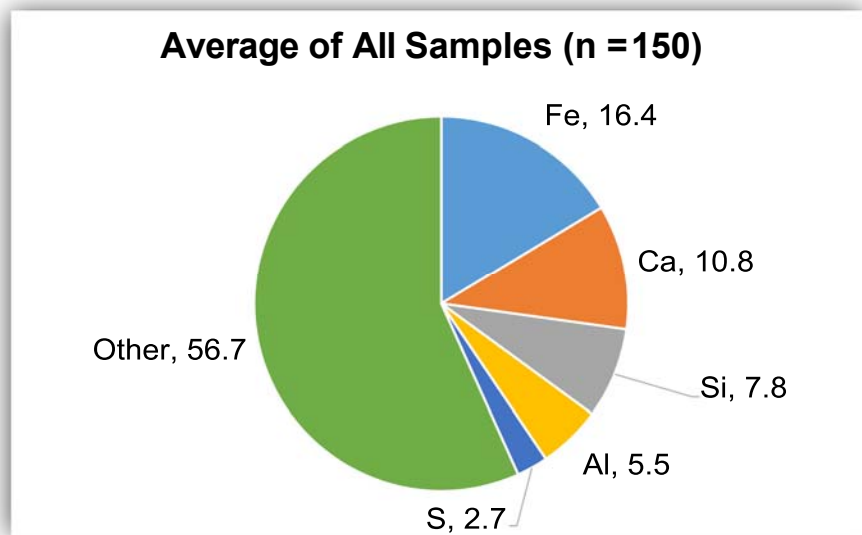


Figure 9. Average assay for all sludge samples, as determined by handheld XRF.

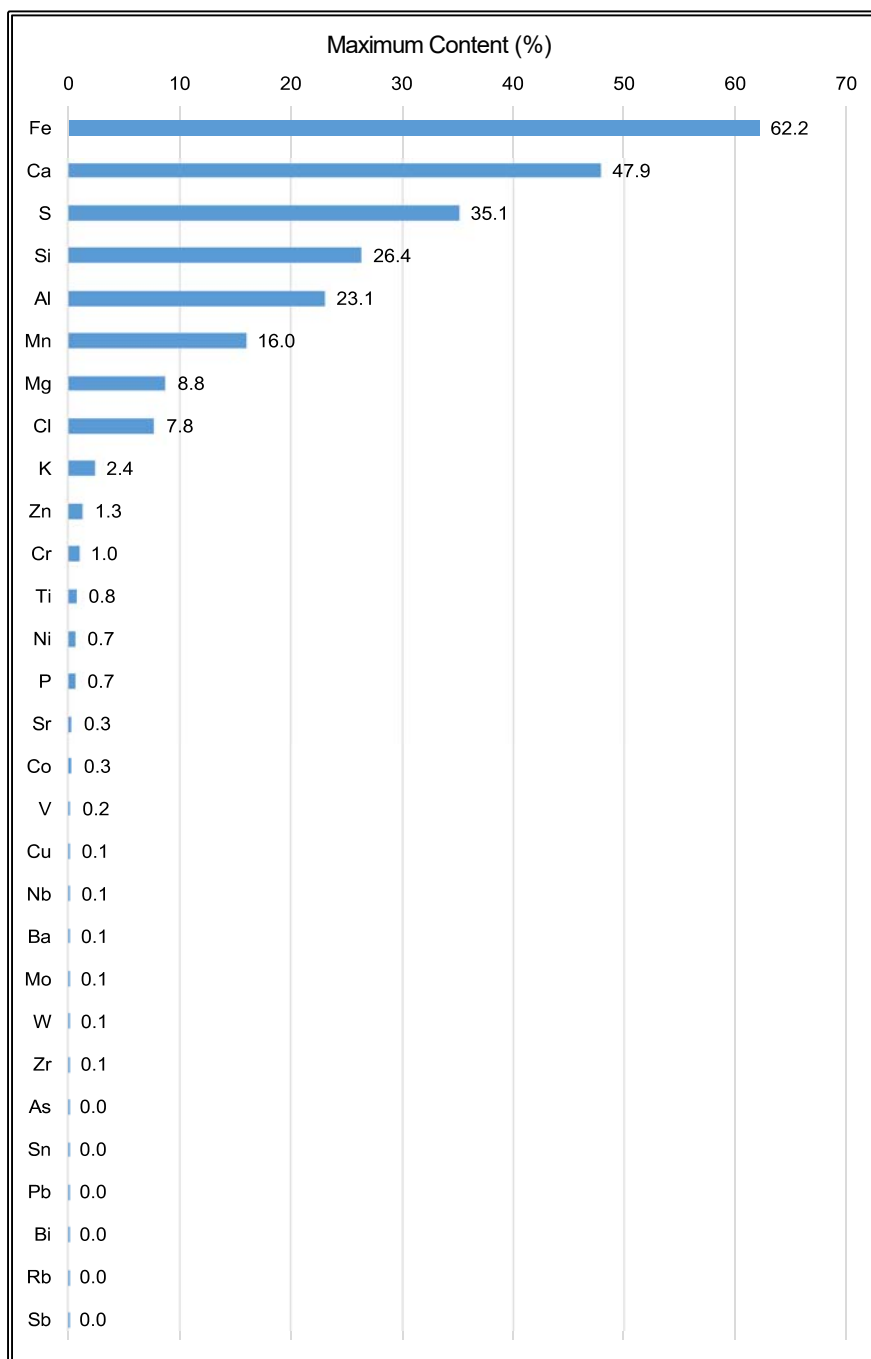


Figure 10. Maximum elemental concentration determined from full population of sludge samples (n=150).

While the data from this handheld XRF did not have sufficient precision for high-fidelity quantitative analyses, it can be used for rough comparisons between sludge samples. To this end, the XRF data was used to classify the specimens based on their primary element (i.e. the element with the highest concentration) and this classification was subsequently used to explain and interpret the leaching test results. The breakdown between the primary, XRF based, species classification is shown in **Figure 11**, while **Figure 12** shows the elemental distribution for the samples in each classification group. As

indicated here, iron is the dominant element in approximately one-third of the samples and this specific group of samples has a much smaller fraction of the remaining major elements (<15% Si, Ca, Al and Mg combined). Likewise, another third of the samples are calcium-rich, while about 20% are silicon-rich. The remaining 10% are classified as either aluminum-, manganese-, or sulfur-rich. While the Ca-rich and Si-rich samples have large differences between the primary species and the next closest species, the Al- rich samples are much more uniformly dispersed. Altogether, these XRF results coincide with expectations, as Fe, Ca, Si and Al are routinely listed as the predominant major metals in AMD and AMD sludge. Differences in sludge composition coincide with the composition of the raw water and the treatment chemical. For example, high Fe samples are associated with low raw water pH while overtreatment with lime will yield a high Ca sludge. Dominantly Al/Si samples tend to occur in the raw water pH range 3.5 to 5.0. Elemental concentrations were determined using XRF.

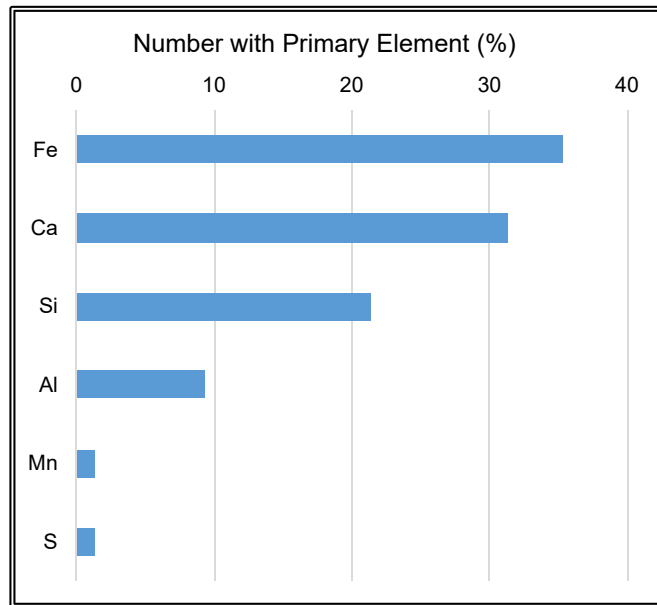


Figure 11. Maximum elemental concentration determined from full population of sludge samples (n=140).

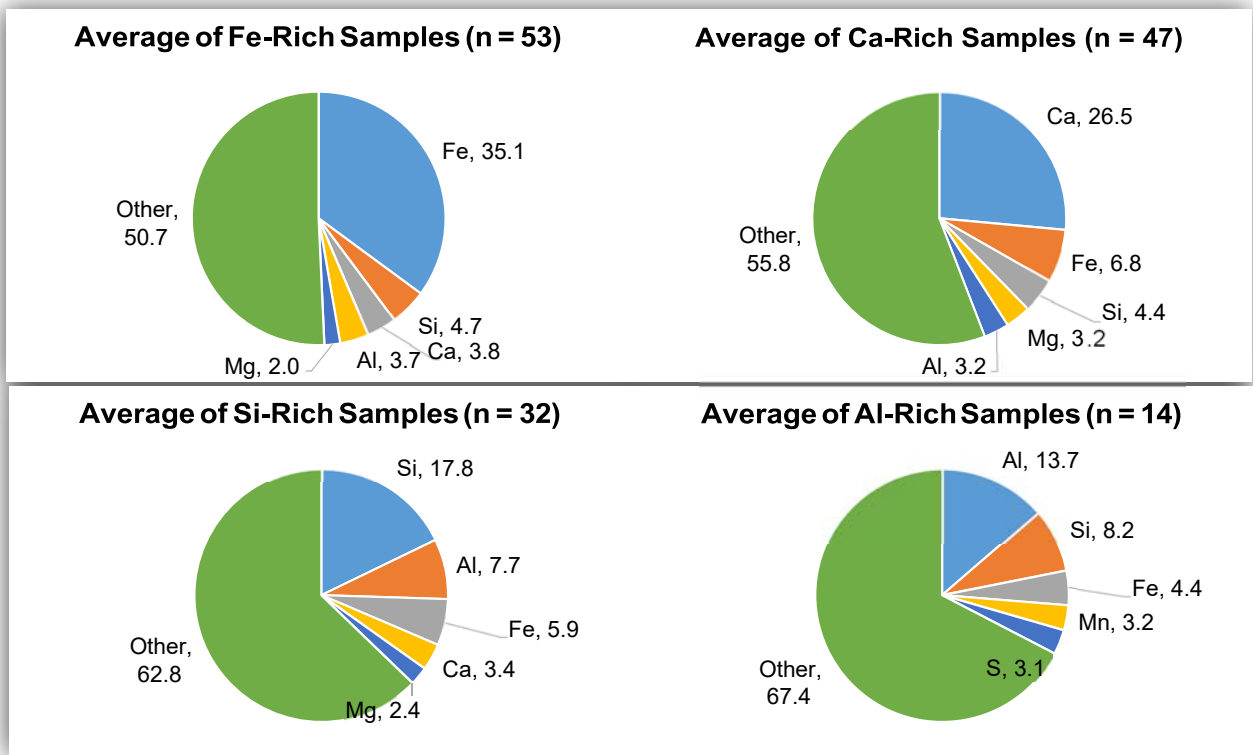


Figure 12. Average assay for sludge samples, itemized by primary species classification group.

Analysis of the moisture data showed that the average moisture of all samples was approximately 67% with a range of 20% to 99%. **Figure 13** shows this distribution of data classified by major elemental species. While the Si, Fe and Ca-rich specimens show very little distinction about the minimum, maximum and average the aluminum samples clearly show an elevated moisture content relative to the other groups. This result may be distorted due to the relatively small sample size (n = 14) of Al-rich specimens when compared to the other groups that have 30 to 50 samples. The distribution of the other samples appears to be reduced due to several anomalously low points, which are not present in the Al-rich population. In either case, the data shows that the moisture content does not vary considerably between the different classifications of sludge specimens.

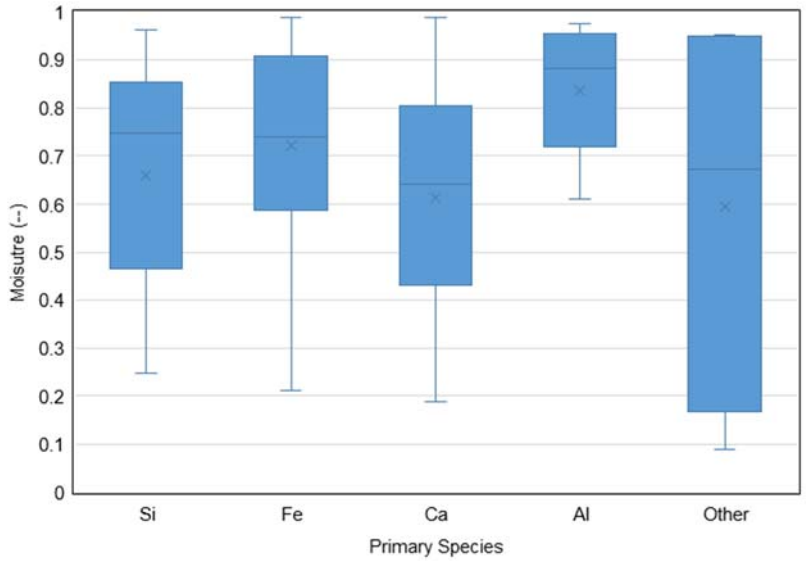


Figure 13. Sludge moisture data categorized by major elemental species. The vertical lines indicate data ranges while the boxes represent the upper and lower quartiles around the median value (horizontal lines across each box).

After the initial training runs this series included 10 repeat test runs over three days on a single bucket of sample collected from one site. **Figure 14** summarizes the results from this test series. The left panel shows a standard test result, i.e. measured pH versus mass-normalized acid dose on a semi-log X axis, while the right panel shows the standard deviation of the measured pH (as a percent of the mean) plotted as a function of the normalized acid dose. In addition, a pie chart showing the XRF results is included as an inset. This data indicates that the test is reproducible, particularly for acid doses less than 1 g/g and corresponding pH values greater than 1.0. The variability in the test, as indicated by the standard deviation, increases considerably below these thresholds. Nevertheless, it should be noted that the absolute standard deviation (c.f. the standard deviation normalized to the mean) stays relatively consistent across all pH and acid dose values.

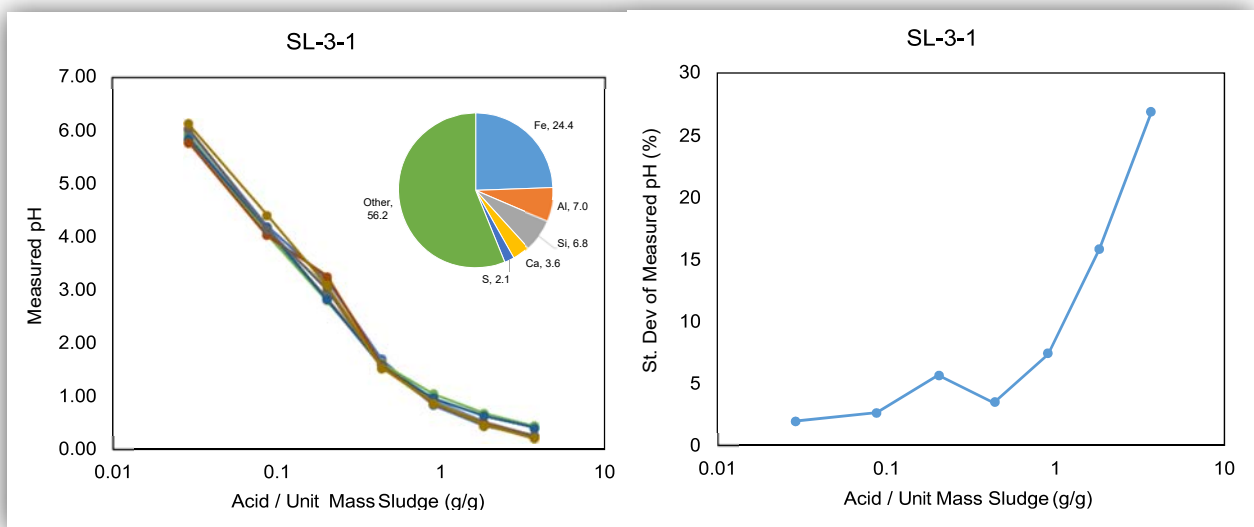


Figure 14. Acid consumption test results for test series #1 - test repeatability.

Given the high-test reproducibility, subsequent test series were conducted using only three replicate tests for each desired condition.

As part of the standard test procedure (described in **Table 6**), a sludge to liquid ratio of 1:1 was used for most tests. Test Series #2 evaluated this standard parameter by determining the influence of solids concentration on acid consumption. These results are shown in **Figure 15**. The left panel shows the measured pH as a function of the raw acid dose, while the right panel shows the results after normalizing the x-axis to the dry sludge mass, per Equation 1. While the 1.5:1 sample showed some variability at the very low acid doses, these two plots otherwise clearly show the impact of the dry mass normalization procedure in correcting for different solids concentrations. The position of the sharp pH drop varies considerably with respect to raw acid dose (left panel), with a low value of ~40 mL for an S:L ratio of 0.5:1 and a high value of ~130 mL for an S:L ratio of 1.5:1. However, the position of the sharp pH drop coincides to a value of ~1.8 g/g when the data is mass normalized. Altogether, this result confirms that any solid to liquid ratio is suitable for routine analysis, provided that the data is normalized to the dry sludge mass.

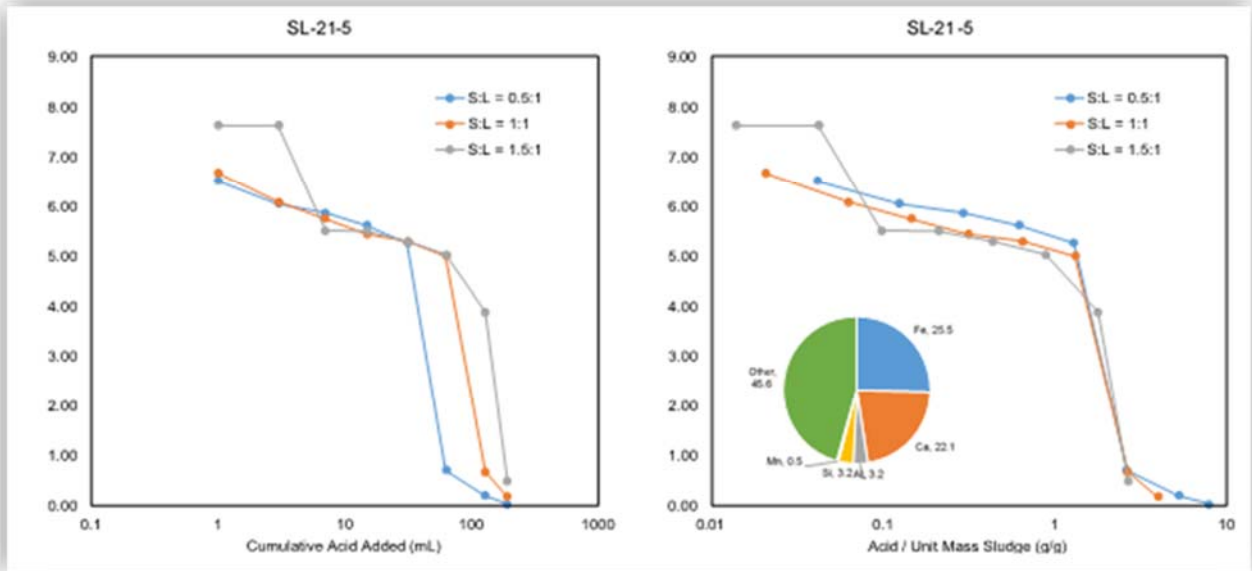


Figure 15. Acid consumption test results for test series #2 – solids concentration. The x axis represents measured pH.

The third parametric test series evaluated the difference in acid consumption with respect to the acid type, namely considering hydrochloric, nitric and sulfuric acid. These comparisons were repeated for three different test specimens, including two Al-rich samples and one Mn-rich sample. Overall, the results in **Figure 16** show very little variability between the various samples and the variability that is present is not consistent between the test specimens. For example, in the SL-51-1 tests, all three acids produced very similar results with a slight vertical offset between the three acid types. While nitric and hydrochloric acid fall within the same error bounds, sulfuric acid produced a slightly lower pH across all acid doses. A similar pattern is observed for SL-40-1; however, in this case, the difference between sulfuric and the other two acids is much more pronounced. For the final sample, SL-67-1, sulfuric and nitric largely overlap, but hydrochloric is notably elevated.

These results remain inconclusive in suggesting that one acid is universally superior to the other two; however, in all cases, nitric acid was not anomalously high or low. This result thus confirms that nitric acid is suitable for the larger parametric evaluation in this study.

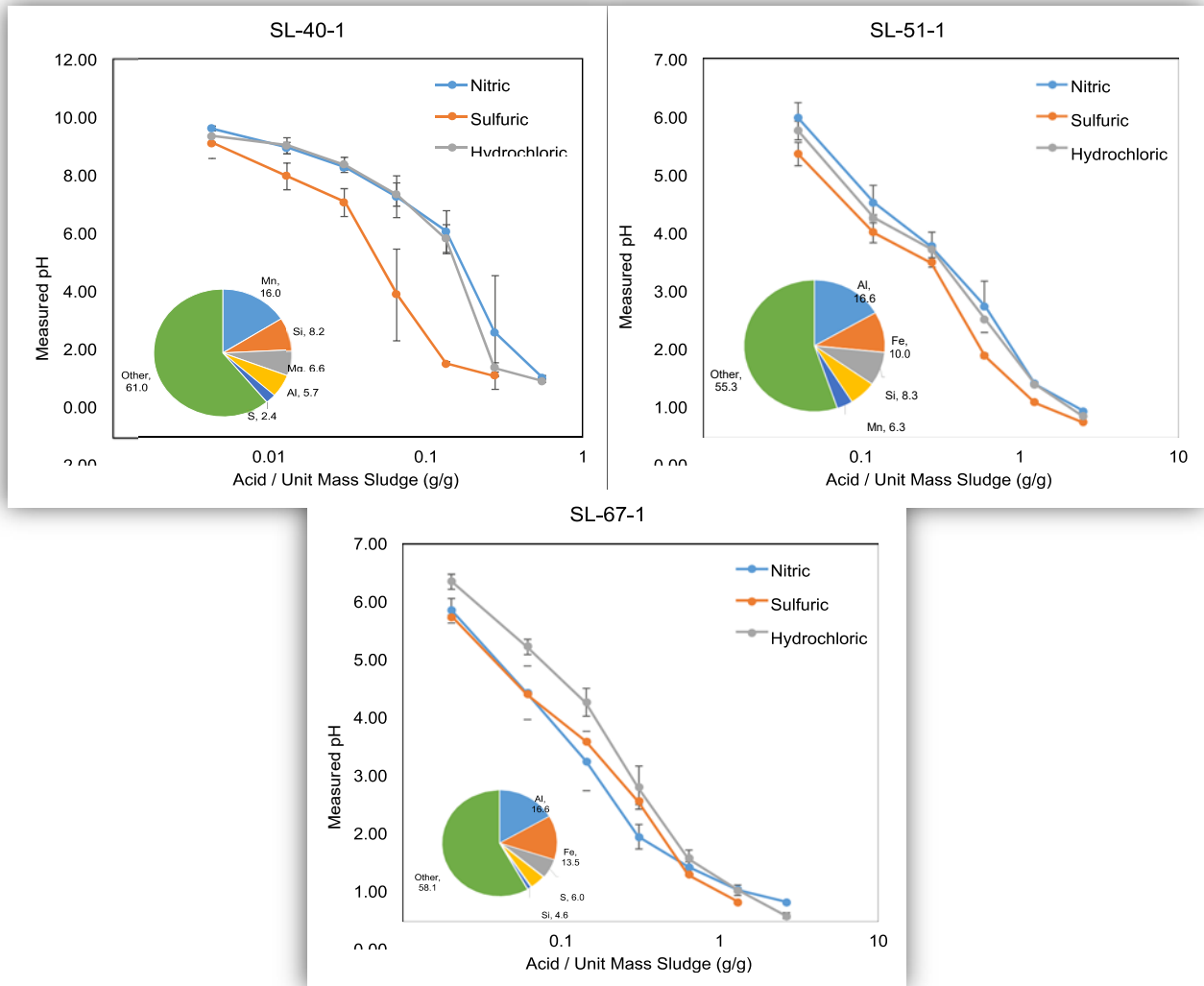


Figure 16. Acid consumption test results for test series #3 - acid comparison.

As part of the detailed sampling campaign in this study, multiple buckets of sample, often 8 to 12, were recovered from select sites to determine what variation in REE content and acid consumption can be expected within a given site. The results of these “Intra-Site Variation” acid leaching tests (Series #4) are shown in **Figure 17**. Please note that the XRF insets are omitted from this figure, as XRF analysis was not performed on each individual site subsample. With few exceptions, this data largely indicates that material from the same site is consistent. Data from SL-66-1, SL-51-1 and SL-67-1 follow similar trends and typically only have one or two outlier samples that deviate from mean. SL-51-1 also had one sample (SL-51-1f) that had considerably low-test reproducibility and thus resulted in large error bars as shown on the plot. Despite this high-test uncertainty, the sample averages still fall within the bounds of the other data sets. On the contrary, SL-40-1 did not show the same level of consistency as the other sites.

Many of these tests had considerably high error bars and the amount of acid needed to reach a target pH value spans more than one order of magnitude for some specific points. For example, to reach a target pH of 3.0, the amount of acid varied from less than 0.1 g/g to nearly 1.0 g/g, depending on the specific test specimen. This result can be explained by the field sampling approach, as the subsamples were recovered from two distinct zones in the water treatment system. Samples a through i were recovered from a downstream sludge pond, while j through l were recovered further upstream on the sludge flow path. This difference in location likely contributes to the large discrepancy in acid consumption.

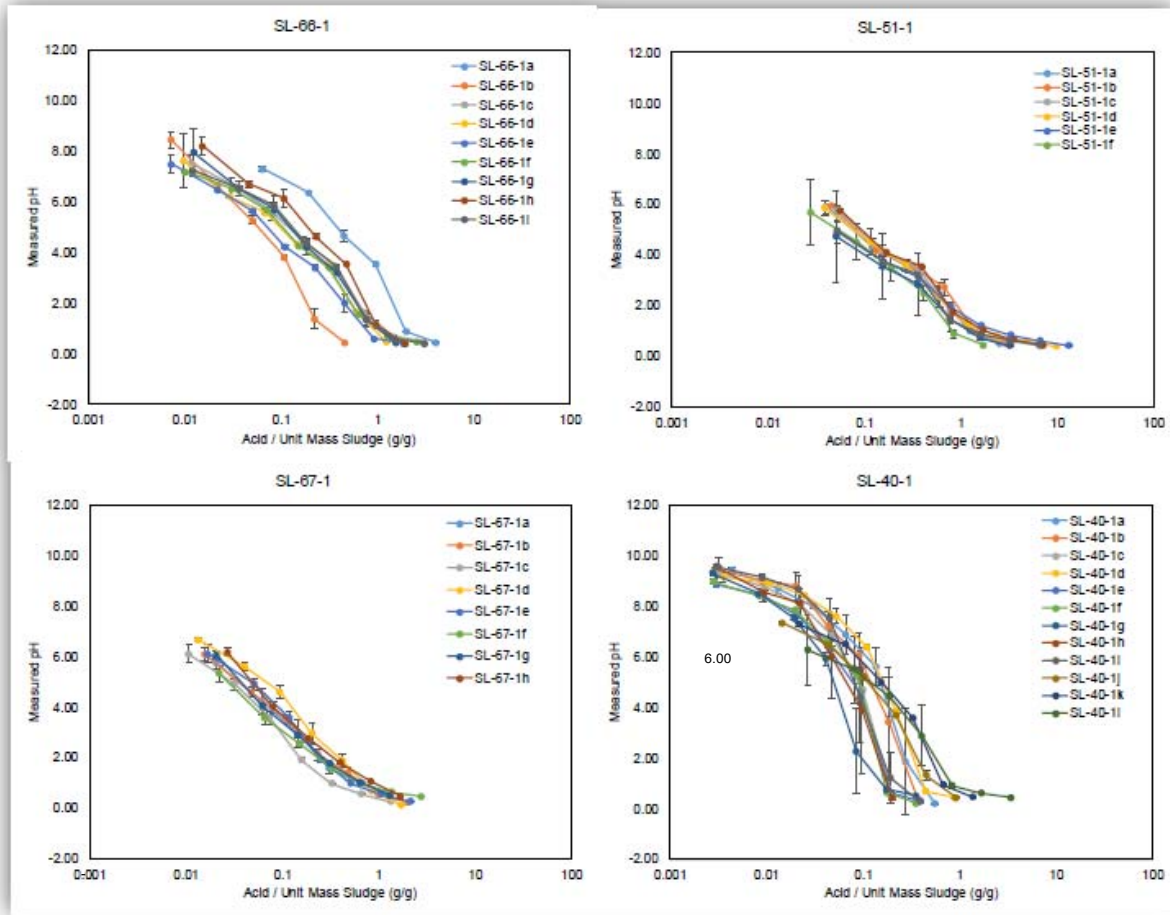


Figure 17. Acid consumption test results for test series #4 - intra-site variation.

While intra-site variation was not evaluated for other sites, this specific test series does provide some quantitative assessment of variability that can be used in rigorous error propagation calculations in the future. Furthermore, these data indicate that the site location alone does not mitigate the test variability, particularly in cases like SL-40-1 where sludge was sampled from multiple zones.

The principal outcome from this acid leaching study is the site variation data collected in Test Series #5. In this series, the standard acid leaching test (which by convention includes 3 replicates) was performed on one sample from each of the 140 sites sampled in the initial exploratory campaign. The results from all tests are shown in **Figure 18**. While individual results cannot be interpreted from this plot, it does indicate the range of values recorded throughout the course of testing. For example, while most samples have starting pH (i.e. asymptotic y-intercept) that is near neutral, a second cohort has a starting pH value of 12.0 to 13.0. The high starting pH samples are mostly resultant from overdosed treatment and have considerable amounts of free lime. The acid consumption in these samples shows a very consistent pattern that includes a very steep decline in pH after that free lime is presumably depleted. Moreover, another group of samples has a very low starting pH (<4.0) and minimal response to additional acid addition.

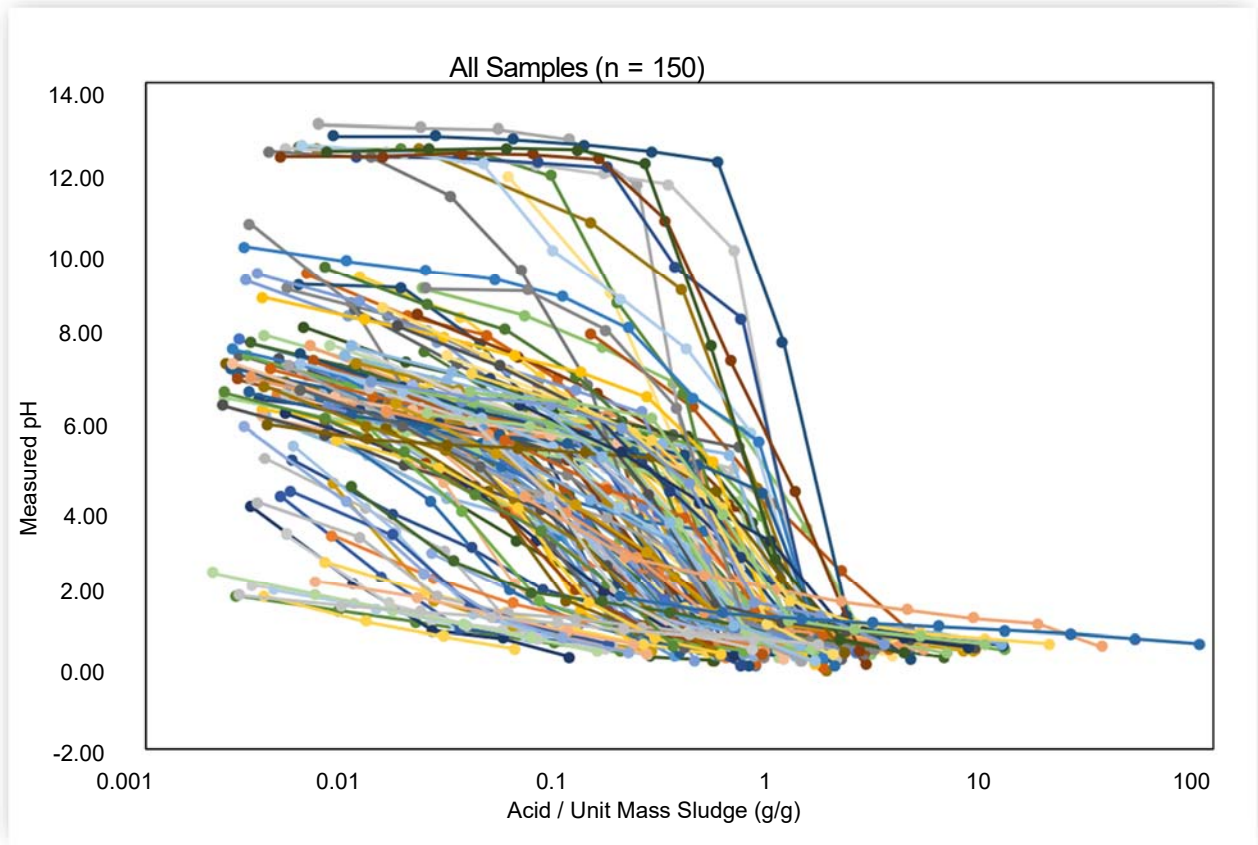


Figure 18. Acid consumption test results for test series #5 - site-to-site variation.

Figure 19 shows these same results classified by primary elemental species as determined by the handheld XRF. The categorization does show that there are unique trends observed for each sludge classification; however, the data also indicate primary species alone cannot account for all the variation

in the data set. The most significant difference is observed between the Fe-rich and Ca-rich samples. None of the Ca-rich samples have a starting pH below 6.0 and the only samples with a starting pH above 12.0 are in the Ca-rich group. The Fe-rich samples tended to have a lower starting pH and most of the samples with a starting pH lower than 4.0 were in the Fe-rich group. Interestingly, the Si-rich group shows some similarities between both the Fe-rich and Ca-rich groups and it should be noted that, on average, samples in the Si-rich group had equal parts Fe and Ca; refer to **Figure 12**.

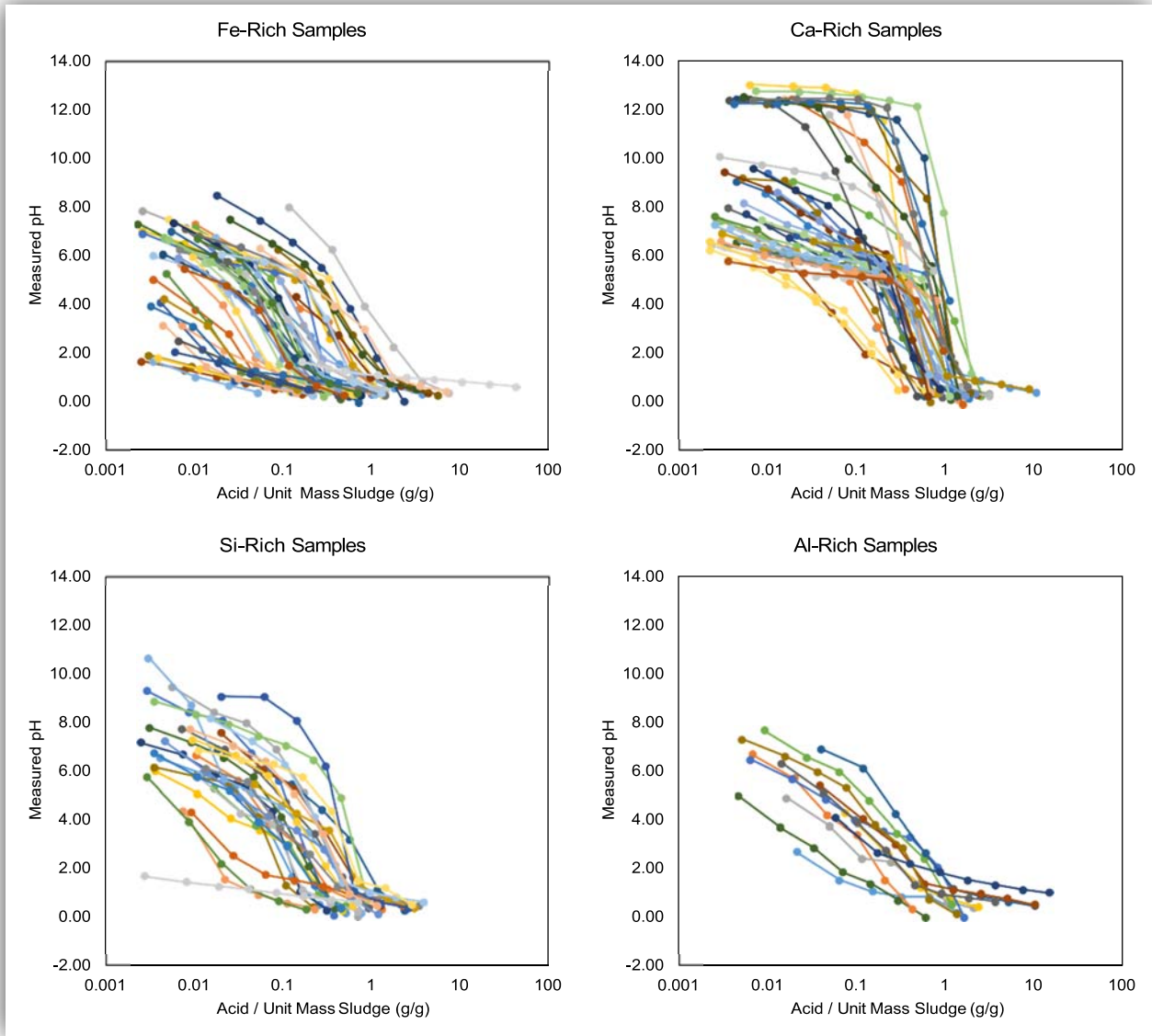


Figure 19. Acid consumption test results for test series #5 - site-to-site variation, classified by major elemental species.

V. Data Modeling and Analysis

Given the magnitude of the data set and difficulty in direct quantitative comparisons of acid consumption curves, an empirical modeling approach was used to simplify the dataset by providing a limited number of fitting parameters that could be assessed directly. After evaluating several mathematical functions, Equation 2 was selected as the model to fit each acid consumption curve. All 150 test runs in Test Series #5 as well as the 38 test runs in Test Series #4 were fit to the empirical model by using a nonlinear optimizer to minimize the sum of squares error (SSQE) between the predicted and experimental values. The results from each fitting exercise are shown in the Appendix. Summary data is included here for discussion and analysis.

Overall, the empirical model provided exceptional fit to most of the dataset. Examples of the best fit and the worst fit (as indicated by SSQE) are shown in **Figure 20**. The poor fit in the SL-36-1 sample can be explained by the shape of the acid consumption curve. This data set contains two inflection points (likely due to two major buffering ions), which is difficult to model using Equation 2. Nevertheless, the overall trend is still captured and more importantly, this double-asymptote behavior was only present in less than 10 the data sets. Most of the data sets showed exceptional fit to the empirical model.

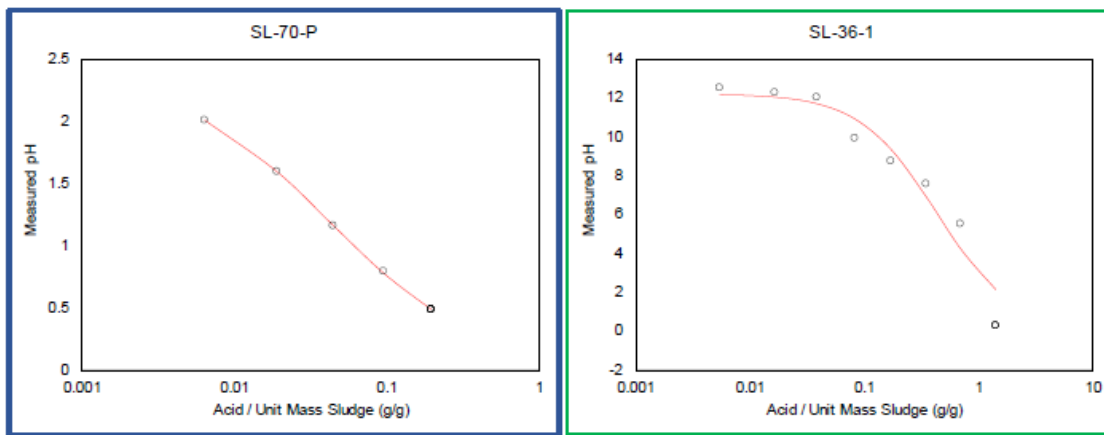


Figure 20. Example of best and worst data fits.

One advantage to this fitting equation is that the three model parameters directly correspond to geometric features of the curve. This benefit is depicted in **Figure 21**, which shows relatively extreme values for each of the fitting parameters. Recall, pH_{Max} indicates the position of the high asymptote, α is the slope of the transition and d_{50} is the x-axis location of the inflection point.

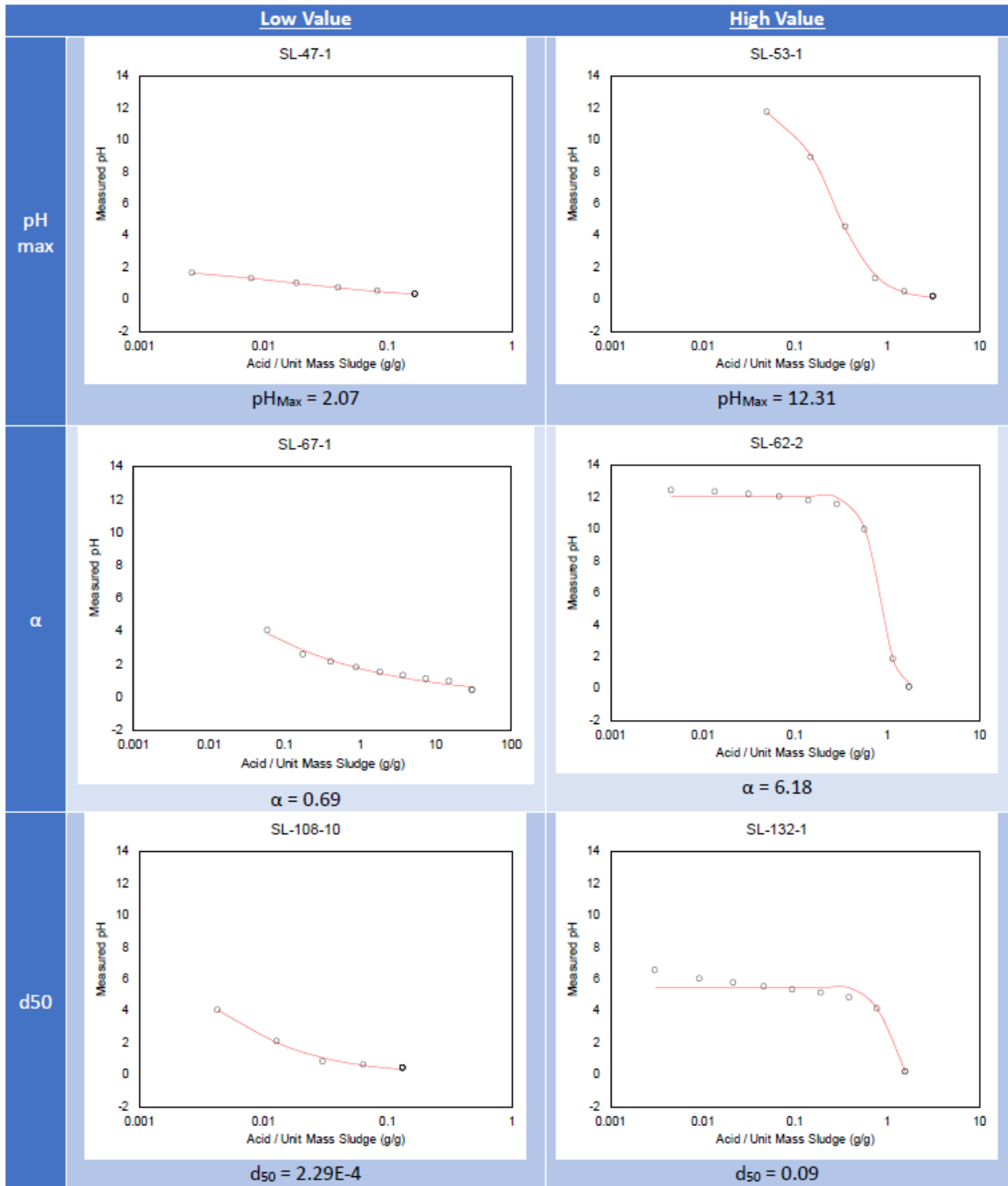


Figure 21. Examples of extreme values (and the resultant curves) for each of the three fitting parameters.

Initially, the model parameters were used to quantitatively assess the variation in the in intra-site variation data, depicted in **Figure 17**. The distribution of model parameters from each site sub-sample is shown in **Figure 22**. These results provide some quantitative basis for the visual trends observed in the raw data. For example, all curves in the SL-66-1 set have very similar parameters, except for one low and one high outlier. These outliers are shown and quantified in the pH_{Max} and d_{50} data sets. These model fits also confirm large variability in other parameters, including α in SL-40-1 and pH_{Max} in SL-51-1. Interestingly, the model data indicate substantial overlap between the different sites, suggesting that, at least for these samples, the intra-site variation is just as significant as the site-to-site variation.

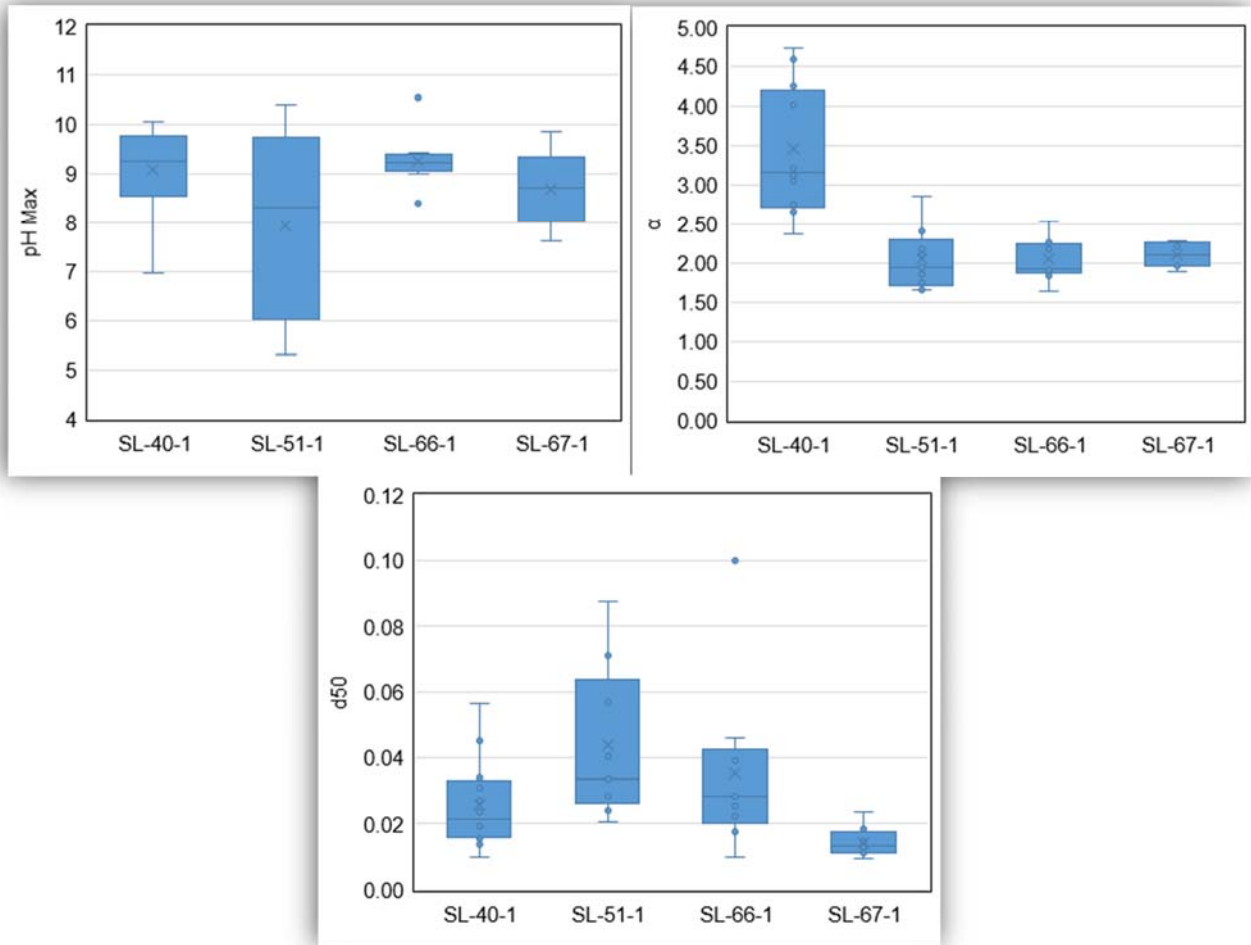


Figure 22. Distribution of model fitting parameters determined from test series #4 - intra-site variation.

A similar analysis was performed on the Test Series #5 data set and categorized by primary elemental species. These results are shown in **Figure 23** and largely confirm the visual observations from the categorized raw data in **Figure 19**. For example, the distribution of pH_{max} values has significant overlap between the Si, Fe and Ca-rich specimens; however, of these three, the Fe-rich samples were the only group to include low values, < 5.0 and the Ca-rich samples were the only to include high values > 11.0 . The Al-rich and other samples have relatively wide distributions, likely due to the low number of samples within these classifications. With respect to the α and d_{50} parameters, most elemental groups

cover a very similar range of values, approximately 1.0 to 4.0 for α and 0 to 0.02 for d_{50} . The Ca-rich samples are clear exceptions to this trend, as both the α value and the d_{50} value are elevated above the other sample classifications. This elevated d_{50} value indicates that Ca-rich samples tend to require a high acid dose before a noticeable pH drop. Likewise, the high α value indicates that the rate of the pH drop is quite high. Fundamentally, this empirical result is further evidence that the Ca-rich samples correspond to AMD that has been over-treated and thus has significant free lime that must be neutralized during acid leaching.

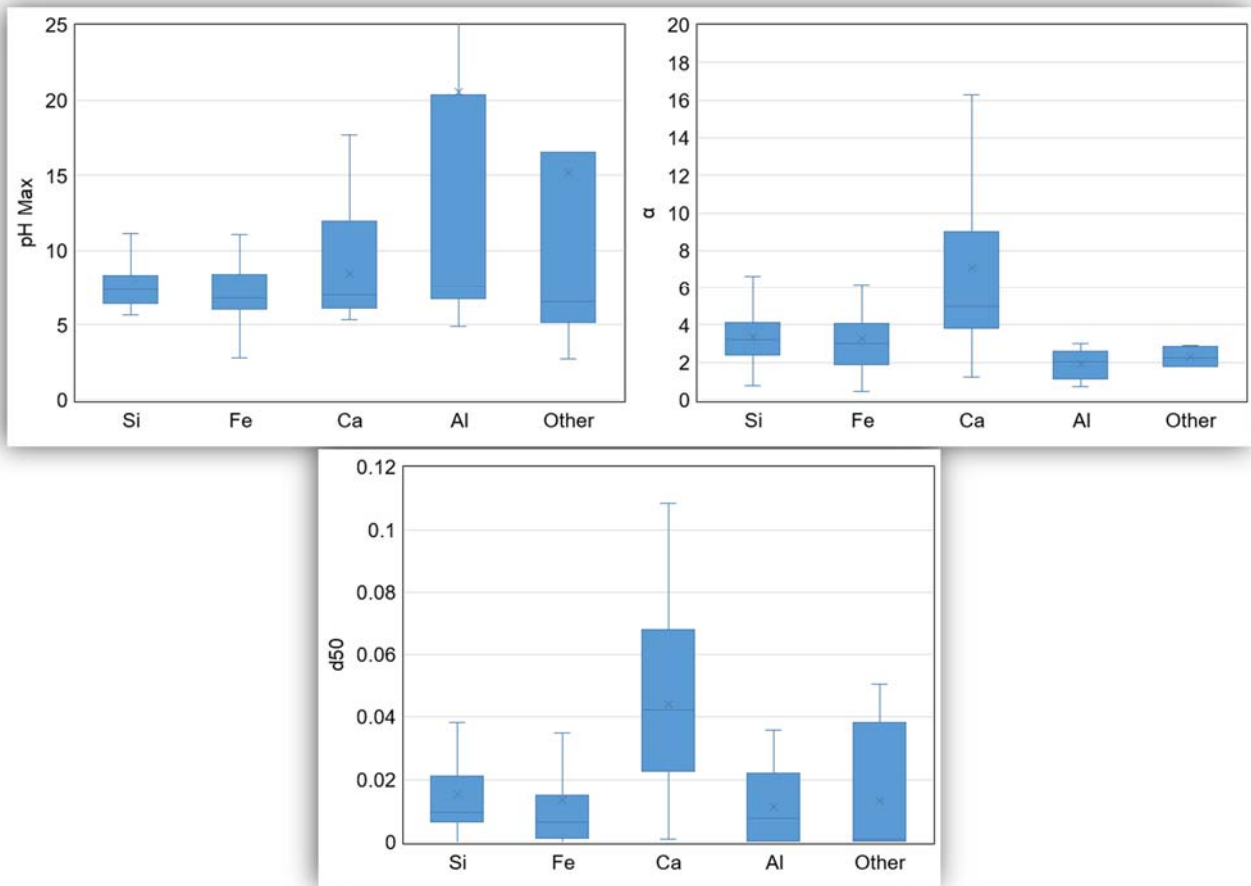


Figure 23. Distribution of model fitting parameters determined from test series #5 – site to site variation, categorized by primary elemental species.

Attempts to directly correlate the model parameters to observable sludge parameters largely proved unsuccessful. To this end, **Figure 24** shows the three fitting parameters plotted individually against the elemental assays of Fe, Ca, Si and Al and similarly **Table 21** shows a matrix of Pearson’s coefficients for the fitting parameters, moisture and major elemental assays. These data show that most data series have little or no correlation to the other series. One exception is Ca, which has a significant positive correlation to both α (Pearson’s = 0.64) and d_{50} (Pearson’s = 0.72). These results are expected, given the plurality of supporting evidence in **Figures 19** and **23**. Furthermore, these results suggest that the acid consumption curve is difficult to predict from raw sludge data alone. With the current state of

knowledge, the acid consumption data is easier to determine experimentally than to predict fundamentally.

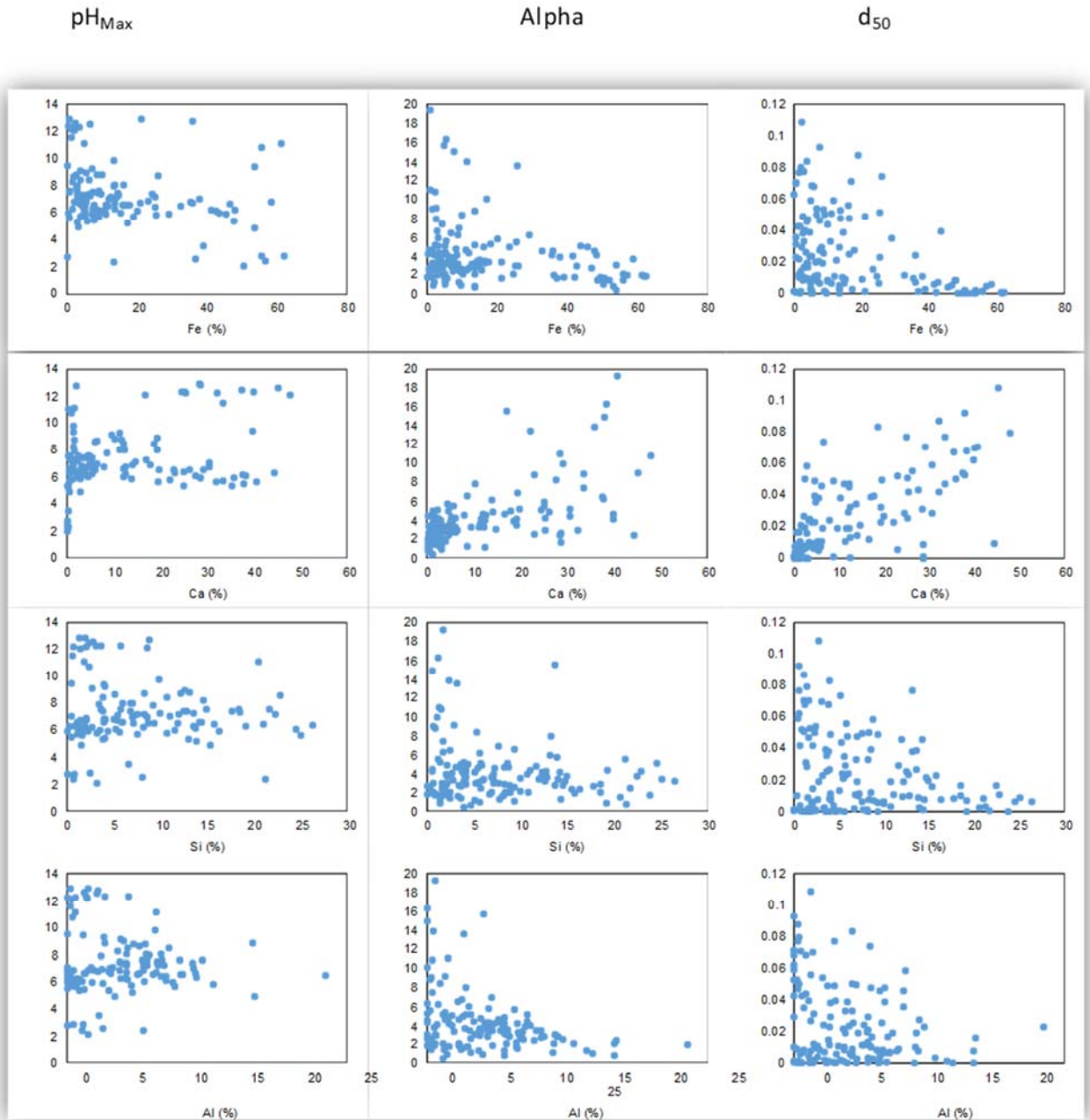


Figure 24. Cross-Plots showing the three fitting parameters (pH_{Max} , alpha and d_{50}) plotted against Fe, Ca, Si and Al assay values.

Table 21. Pearson's correlation coefficient for fitting parameters and sludge elemental assays.

	pH _{Max}	alpha	d ₅₀	Moisture	Fe	Ca	Si	Mn	Mg	Al
pH _{Max}	1.00	-0.13	-0.16	0.16	0.20	-0.11	-0.05	-0.09	0.24	-0.11
alpha	-0.13	1.00	0.66	-0.26	-0.23	0.64	-0.21	-0.20	0.06	-0.34
d ₅₀	-0.16	0.66	1.00	0.02	-0.38	0.72	-0.28	-0.07	0.33	-0.20
Moisture	0.16	-0.26	0.02	1.00	0.03	-0.26	-0.01	0.31	0.14	0.27
Fe	0.20	-0.23	-0.38	0.03	1.00	-0.40	-0.40	-0.22	-0.32	-0.45
Ca	-0.11	0.64	0.72	-0.26	-0.40	1.00	-0.43	-0.29	0.31	-0.41
Si	-0.05	-0.21	-0.28	-0.01	-0.40	-0.43	1.00	0.13	-0.28	0.53
Mn	-0.09	-0.20	-0.07	0.31	-0.22	-0.29	0.13	1.00	0.31	0.24
Mg	0.24	0.06	0.33	0.14	-0.32	0.31	-0.28	0.31	1.00	-0.26
Al	-0.11	-0.34	-0.20	0.27	-0.45	-0.41	0.53	0.24	-0.26	1.00

One interesting observation is the relationship between the measured starting pH measured in the lab (prior to any acid addition) and the pH_{Max} model value shown as a parody plot in **Figure 25**. While the model parameter is intended to be indicative of the starting pH, it is not a direct equivalency, as Equation 2 is undefined at an acid dose of 0 g/g. Nevertheless, **Figure 25** shows that there is fair agreement between the measured pH and the model parameter, with the model parameter slightly overestimating the measured pH in most cases. One group of samples showed a relatively low measured pH (4 to 7) but a relatively high model pH_{Max} (9 to 13).

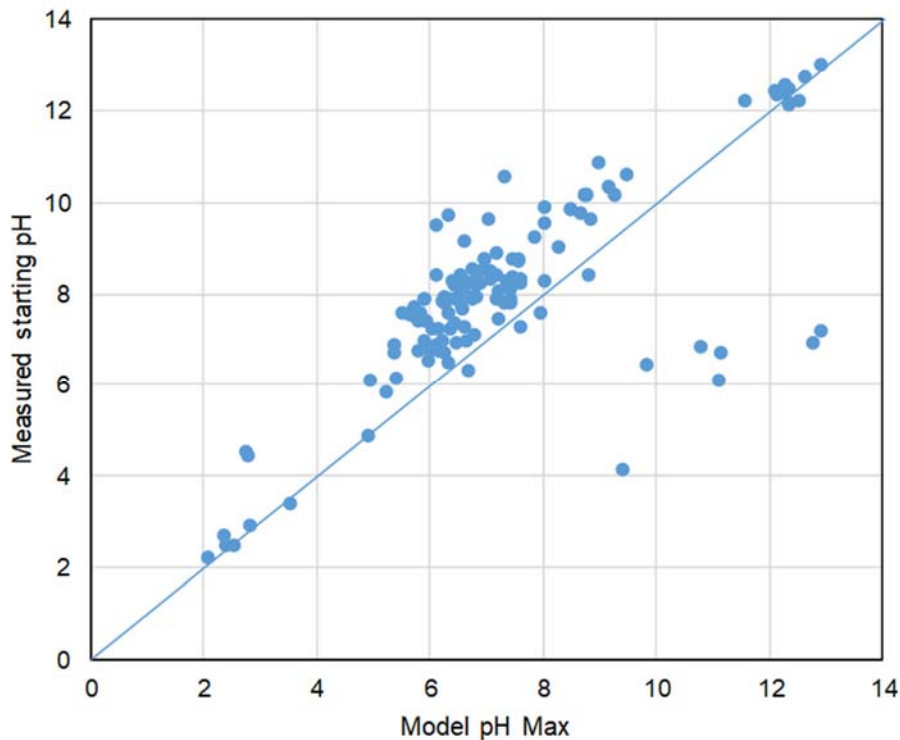


Figure 25. Parody plot showing measured starting pH versus pH_{Max} model parameter.

VI. Discussion and Implications

The cumulative results of the acid leaching tests provide a quantitative evaluation of the acid doses needed to reach target leach pH values and provide some indication of the variability that can be expected from site to site. While the variation due to test reproducibility, solid concentration and acid type are small and manageable, the intra-site variation (particularly on sites processing different types of material) can be significant and should be assessed empirically in future studies. Nevertheless, the site-to-site variation and the variation between sludges with different elemental compositions proved to be the most significant in the analysis. While the full acid consumption curve can be adequately modeled with a three-parameter non-linear equation, the actual fitting parameters cannot be readily predicted from the composition and moisture data. A more fundamental assessment may provide a pathway to this end, but that activity was out of the scope of this study.

The models and analysis from these tests can be used to guide future exploration efforts by deemphasizing sludge classes that are high acid consumers and are likely cost prohibitive to process by acid leaching. For example, one method to utilize and apply the current data set is to assign a target acid dose (perhaps based on an economic or process design metric), use the model parameters to solve for the output pH for each sludge sample and classify the resultant pH data based on primary elemental species.

An example of this analysis is shown in **Figure 26** for arbitrary acid doses of 0.1 g/g (left panel) and 0.5 g/g (right panel). The results are depicted as the distribution of output pH values, categorized by primary species. If one assumes a target pH of < 3.0, the results in **Figure 26** indicate that most Fe-rich samples can reach that target at the 0.1 g/g acid dose. A smaller number of Si and Al-rich samples meet this target; however, only the outlier Ca-rich samples qualify. At the higher acid dose of 0.5 g/g, nearly all Si, Fe and Al-rich samples meet the pH < 3.0 target, as well as approximately 50% of the Ca-rich samples. The poor response of Ca-rich sludges with acid addition is, doubtless, due to unreacted lime ($\text{Ca}(\text{OH})_2$) from the AMD treatment process in the Ca-rich sludges. With the full population of sample data and model parameters, this analysis can easily be repeated using different acid doses and target pH values as dictated by the recovery process design and process economics. In any case, this data shows that future exploration targets should prioritize Fe-rich samples and deemphasize Ca-rich samples based on the relative level of acid consumption between these two groups.

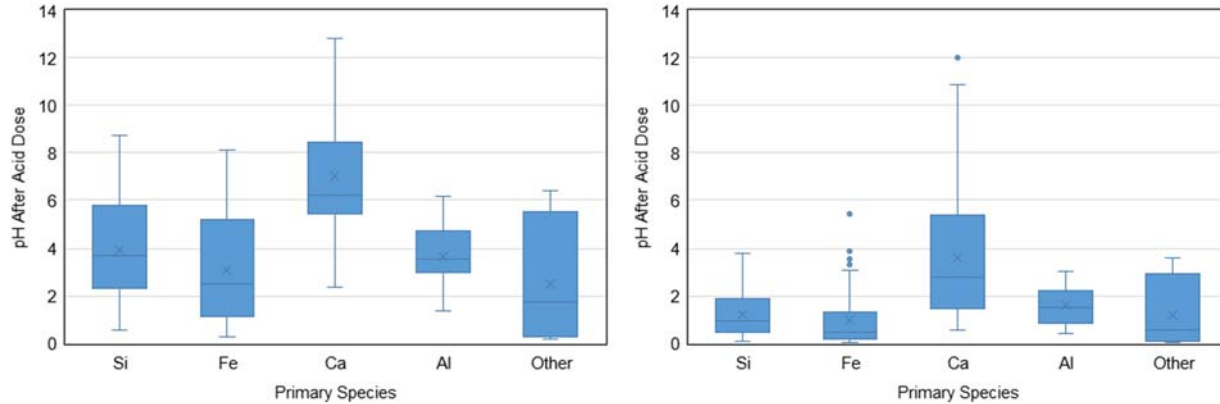


Figure 26. Distribution of output pH values categorized by primary elemental species. Output pH was predicted using Equation 2 at an arbitrary acid dose of 0.1 g/g (left panel) and 0.5 g/g (right panel). All other fitting parameters were derived from the raw data for each sludge sample.

VII. XRD analysis of sludge samples

Drying Methods

The objective was to study the crystal structures of the sludge samples. X-ray diffraction (XRD) was used to identify the solid phase and crystallinity of the sludge samples. Dried powder samples were required to perform characteristic tests. Because AMD sludge is essentially precipitated metal hydroxide floc the drying temperature method may affect the crystal structure of sludge samples, potentially causing the amorphous and soluble metal hydroxides to dehydrate to less soluble and more crystalline oxyhydroxides and oxides. To determine the optimal drying method, an initial study investigated the XRD pattern resulting from ambient-temperature desiccator-drying and standard laboratory oven-drying.

Figure 27 shows the XRD spectra of sludge samples treated by ambient-temperature desiccator-drying and standard laboratory oven-drying. It was easily visible the XRD patterns of sludge samples with oven-drying were like desiccator-drying samples. This result demonstrated the oven-drying method did not have a significant influence on the diffraction peaks of sludge samples. Therefore, the oven-drying method was chosen for all future experiments and characterization tests.

Moreover, XRD patterns can be used to study the crystalline–amorphous state of dried sludge samples. As shown in **Figure 27**, the sharp peaks formed in the X-ray diffraction patterns of SL-1-1 and SL-1-10 clearly show the crystalline characteristics of corresponding sludge samples. Besides the presence of sharp peaks, the broader patterns in SL-1-5 exhibited the co-existence of crystalline and amorphous characteristics.

Furthermore, the main types of crystalline minerals present in sludge samples can be determined using the XRD patterns. Also shown in **Figure 27**, a significant amount of quartz was detected in SL-1-1, SL-1-5 and SL-1-10. In addition, magnetite and zinc oxide were found in SL-1-1, while zirconium oxide was present in SL-1-5. Magnetite, zinc oxide and zirconium oxide were all found in SL-1-10, resulting in the highly crystalline characteristics of SL-1-10 sludge sample. However, no clear peaks of quartz were found in SL-3-1. It will be analyzed in future tests based on the elemental composition results.

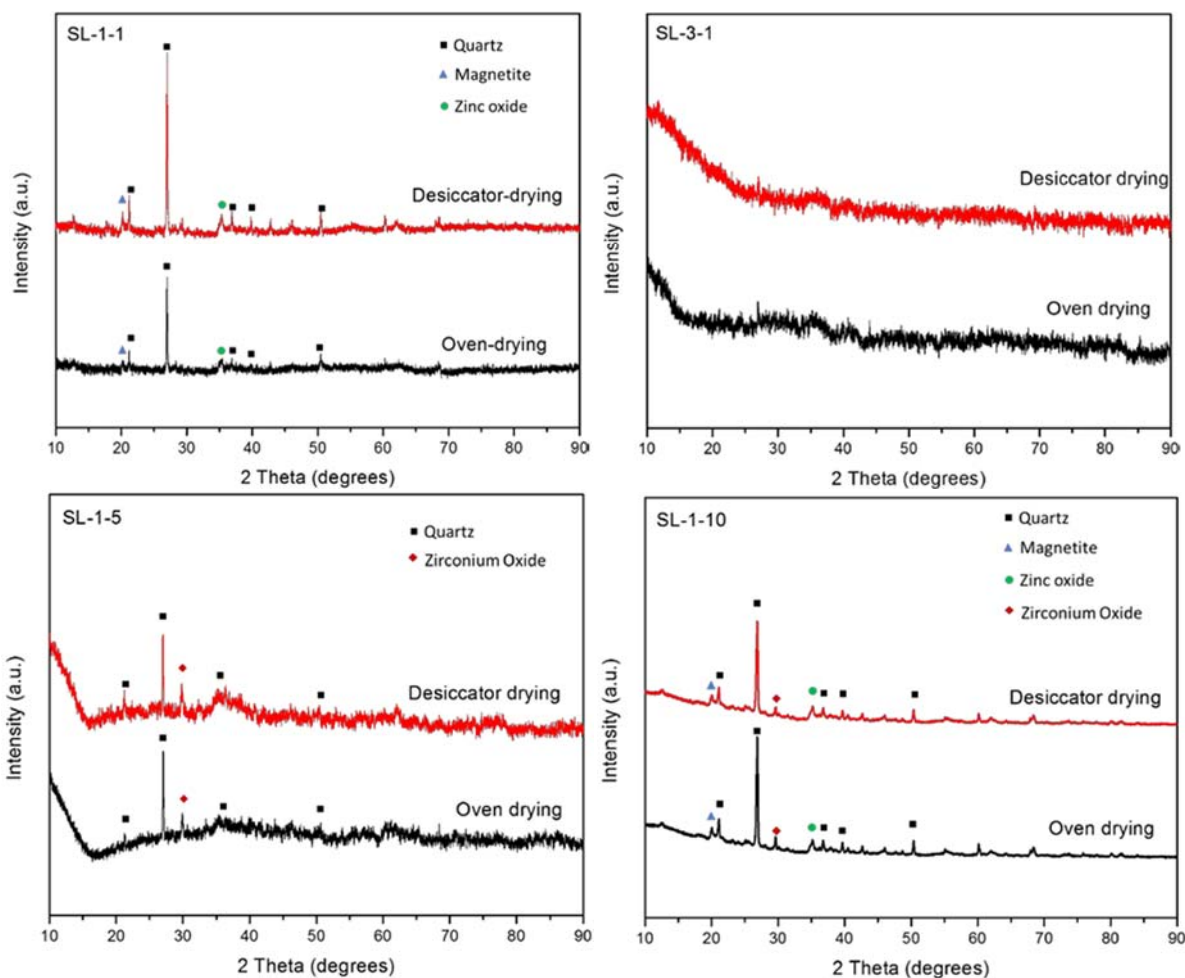


Figure 27. Characteristic results from drying method test; a.u. = arbitrary units.

Step-by-Step XRD/Crystalline Protocol

Based on the initial study of drying methods, the massive XRD tests were performed by following the step-by-step process outlined below, including a general sample preparation process (drying and grinding) and the XRD test procedure.

1. Mix the sludge thoroughly.
2. Depending on the sludge moisture content, filter approximately 50-100 mL of the mixed sludge.
3. Dry sludge residue sample in an oven at 60 °C until sample weight reaches a stable value.
4. After drying, grind each sample into a fine powder, place each in a plastic container and store in a desiccator for XRD testing. It is to be noted, the final powder samples used for XRD testing are to be kept at low moisture and uniform particle size.
5. Samples will be identified by powder XRD using the *Scintag X1* automated powder diffract meter equipped with a Peltier detector with CuK α radiation. Generally, step scans are run over the range of 10 to 90° with 0.008° stepping intervals and 15.2 second step time. The step time will be extended for any sample showing weak or no peaks within the initial measurement interval.
6. After XRD characterization, the obtained spectra are interpreted with the aid of search/matching

software and compared with standard reference patterns.

7. Chemicals found to be present and study results of the solid phase and crystalline structures of the samples are then recorded and shared with project participants.

For some sludge samples with amorphous characteristics, the observed XRD patterns were not definitive and did not allow interpretation using standard reference patterns. Therefore, a modification of the testing procedure was necessary. To obtain definitive data information, the XRD tests were performed with smaller step size and extended scan time. Generally, the scan time was 30 minutes for poorly crystalline samples compared with 15-18 minutes for the sludge samples with crystalline characteristics.

XRD spectra are included in Appendix A and the mineralogy tables are in Appendix B. In the following discussion, the appendix is indicated by the letter preceding the figure number.

Appendix A, Section A1 shows the XRD spectra of sludge samples collected during first pass sampling. A summary of the identified patterns for corresponding sludge samples is shown in **Appendix B, Section B1**. More than 117 sludge samples were characterized by XRD. The presence of sharp patterns clearly shows the crystalline characteristics of corresponding sludge samples. In many cases, only the broaden patterns or none patterns are detected. It is due to the metal hydroxides were highly hydrated, amorphous solids resulting in apparently uniform composition. Repeated tests were conducted for some of the sludge samples with amorphous characteristics to obtain more credible data. For those sludge samples that XRD has yielded almost no crystal structures, further assistance from other characteristic analysis will be required.

Appendix A, Section A2 shows the XRD spectra of sludge samples collected during second pass sampling from same site but different depth. The identified patterns for corresponding sludge samples are shown in **Appendix B, Section B2**. To easily find the difference with respect to chemical composition and solid phase, the summary plot of XRD spectra for samples taken from same site but different depth is also provided, as shown in **Section A2**. During the report period for second pass characterization, twelve (12) sample series, total 108 sludge samples were analyzed by XRD.

References

¹Skousen, J.G. and Ziemkiewicz, P.F. (eds.) 1995. Acid Mine Drainage Control and Treatment. National Mine Land Reclamation Center Publication. 27 ch. 254 pp.32. - in 2nd edition.

²Skousen, J., Zipper, C.E., Rose, A., Ziemkiewicz, P.F., Nairn, R., McDonald, L.M. and Kleinmann, R.L. 2017. Review of passive systems for acid mine drainage treatment. Mine Water and the Environment. 36: 133-153. DOI 10.1007/s10230-016-0417-1. <http://link.springer.com/article/10.1007/s10230-016-0417-1>

³ Lenter, C.M., McDonald, L.M., Skousen, J.G. and Ziemkiewicz, P.F. 2002. The Effects of Sulfate on the Physical and Chemical Properties of Actively Treated Acid Mine Drainage Floc. *Mine Water and the Environment* 21: 114-120 Springer-Verlag.

⁴ Donovan, J.J. and Ziemkiewicz, P.F. 1994. Early Weathering Behavior of Pyritic Coal Spoil Piles Interstratified with Chemical Amendments. Proceedings, International Land Reclamation and Mine Drainage Conference and the Third International Conference on the Abatement of Acidic Drainage, Pittsburgh PA, April 24-29, 1994.

⁵ Ziemkiewicz, P.F. and Meek, F.A. 1994. Long term Behavior of Acid Forming Rock: Results of Twelve Year Field Studies. Proceedings, International Land Reclamation and Mine Drainage Conference and the Third International Conference on the Abatement of Acidic Drainage, Pittsburgh PA, April 24-29, 1994.

⁶ Ziemkiewicz, P.F. and Lovett, R.J. 1994. The Rate of Pyrite Dissolution: Comparison of Field and Laboratory Studies. Proceedings, International Land Reclamation and Mine Drainage Conference and the Third International Conference on the Abatement of Acidic Drainage, Pittsburgh PA, April 24-29, 1994.

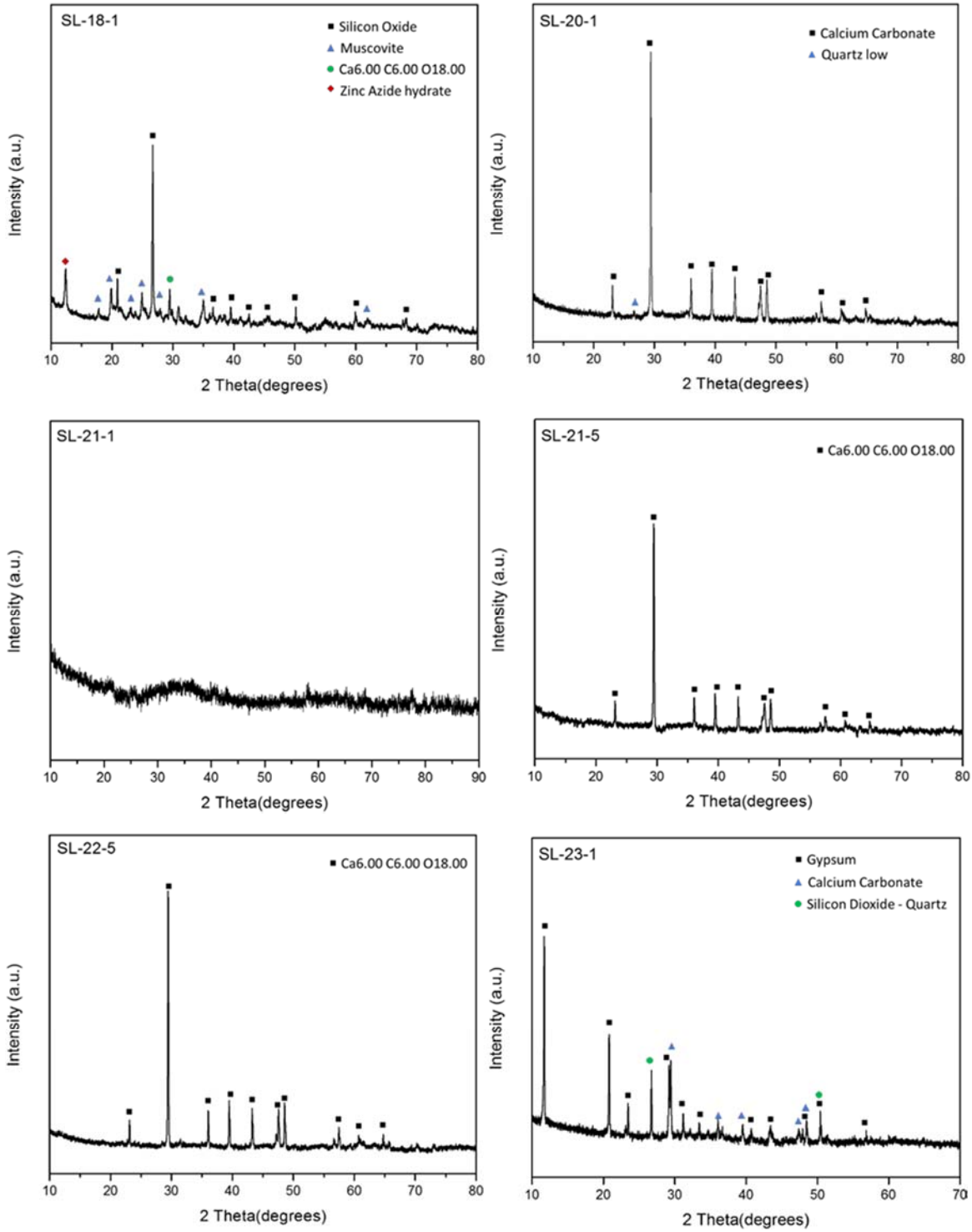
⁷ Ziemkiewicz, P.F. and Lovett, R.J. 1992. Factors Controlling Carbonate Dissolution in Acid-Forming Rock: Implications for Acid Mine Drainage Prevention Strategies. American Chemical Society Symposium Series: Sulfide Oxidation.

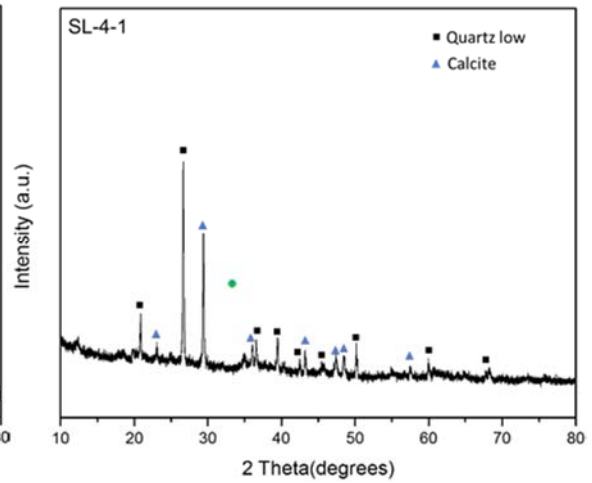
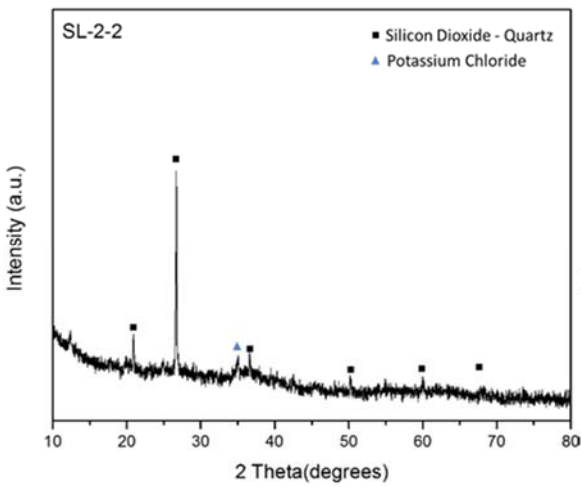
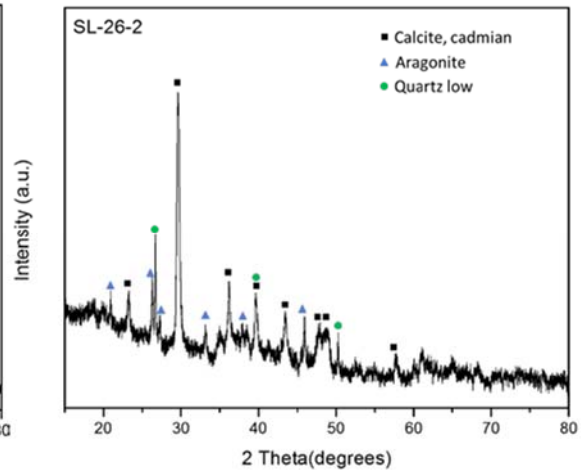
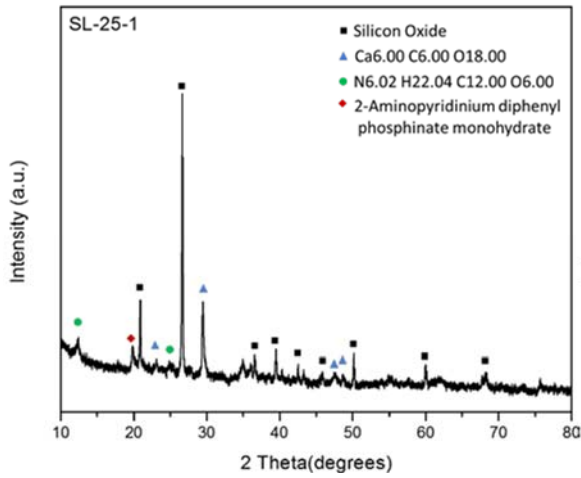
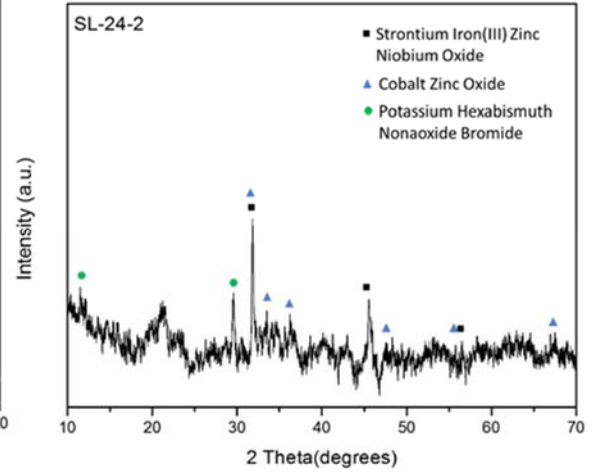
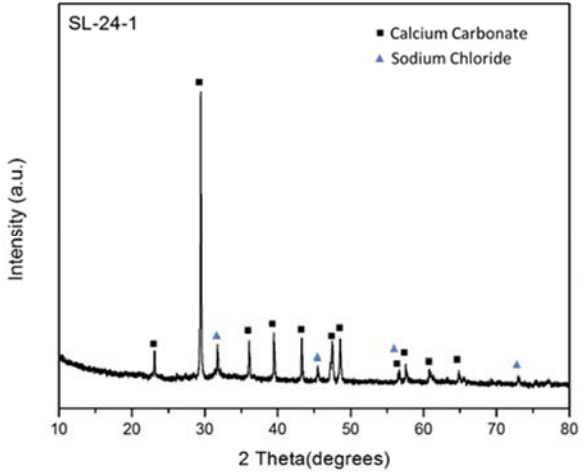
⁸ Ziemkiewicz, P.F. and Lovett, R.J. 1992. Quality and Quantity of Alkaline Amendments Needed to Prevent Acid Mine Drainage. 204th National American Chemical Society Meeting, Washington, D.C. August 1992.

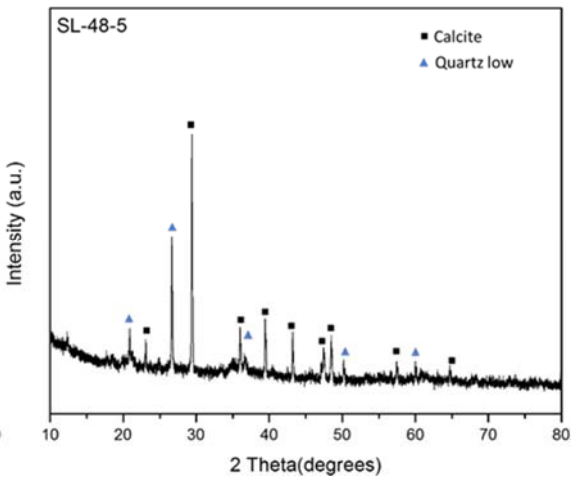
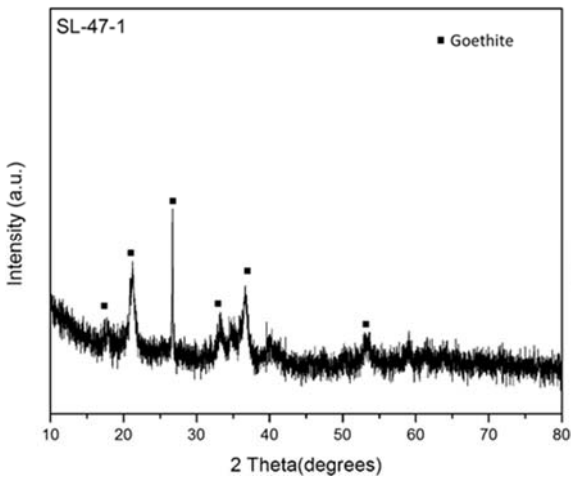
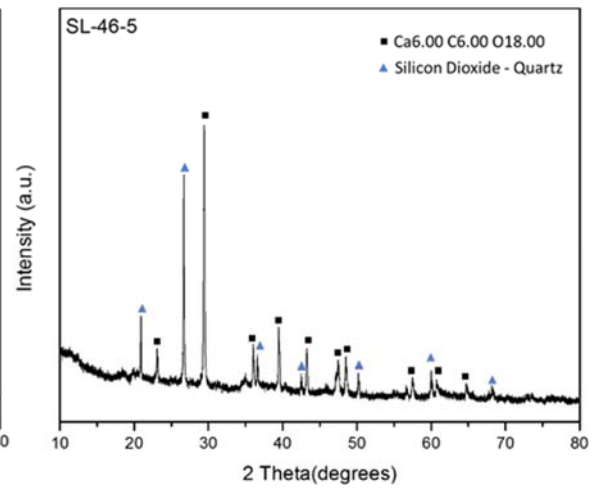
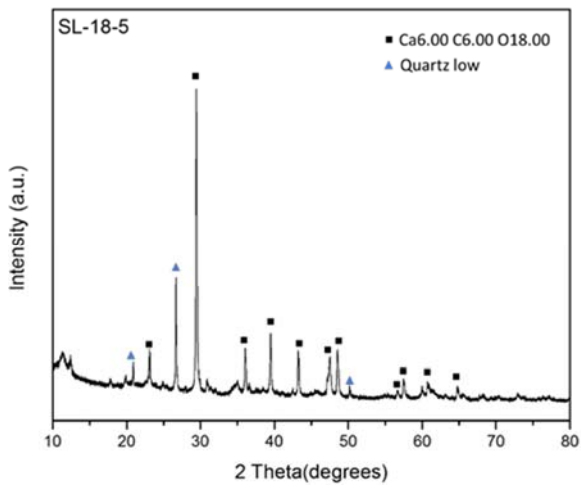
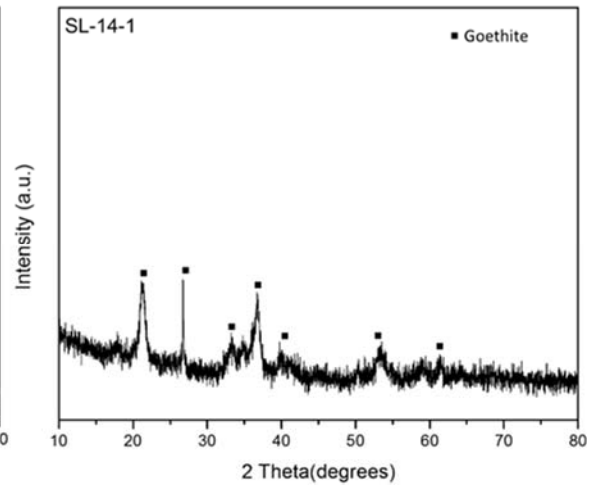
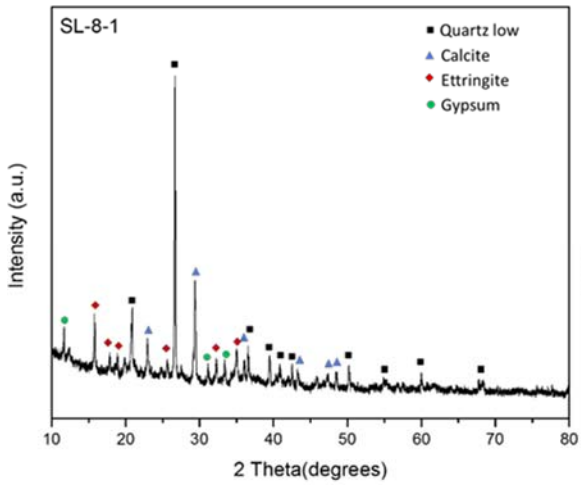
⁹ Stewart, B.W., Capo, R.C., Hedin, B.C., Hedin, R.S. 2017. Rare earth element resources in coal mine drainage and treatment precipitates in the Appalachian Basin, USA. *Int'l J. Coal Geology*. 169 (2017) 28-39.

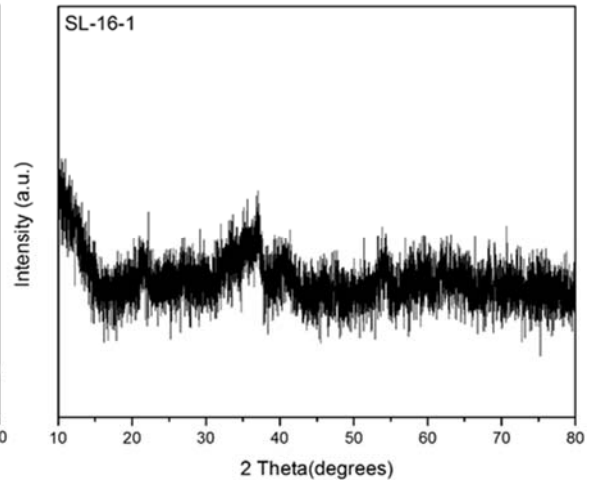
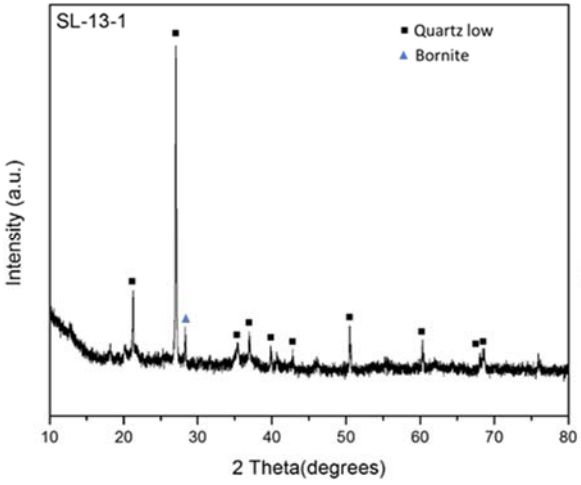
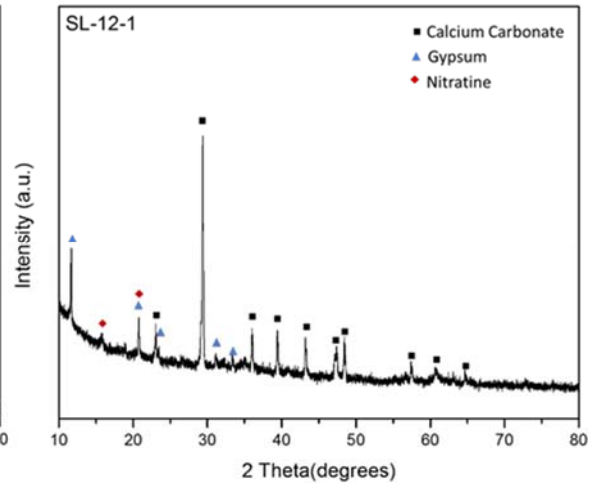
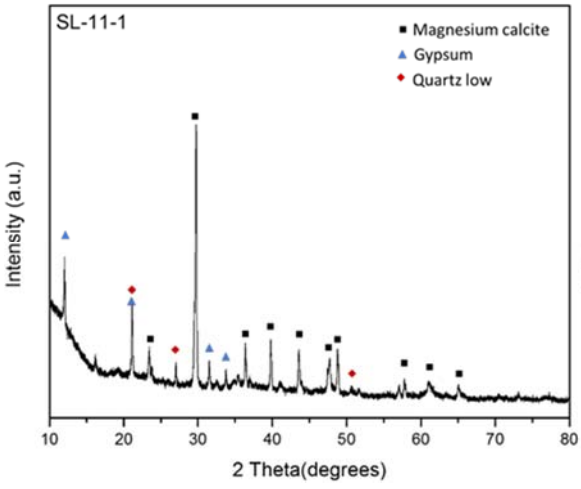
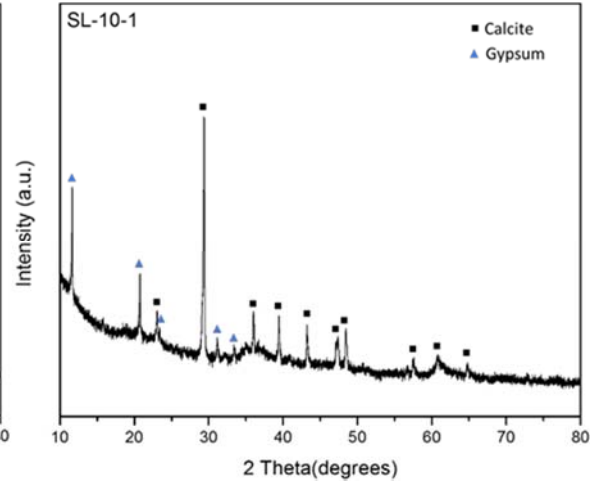
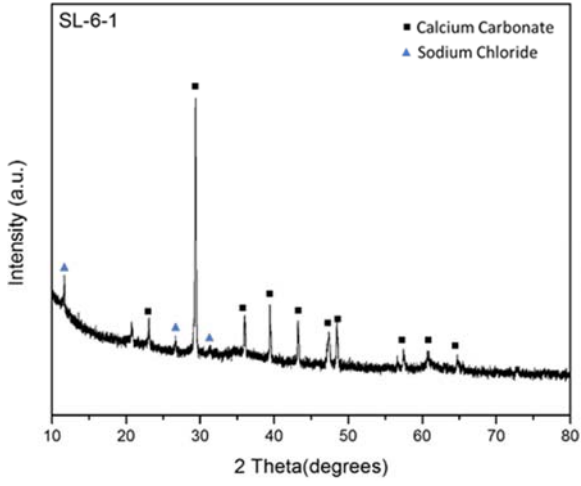
Appendix A. XRD Spectra

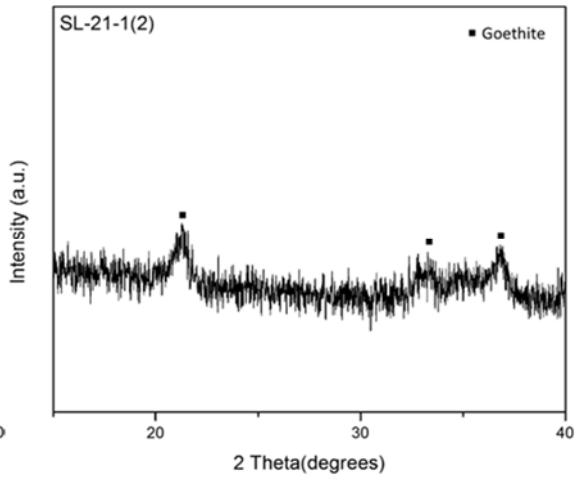
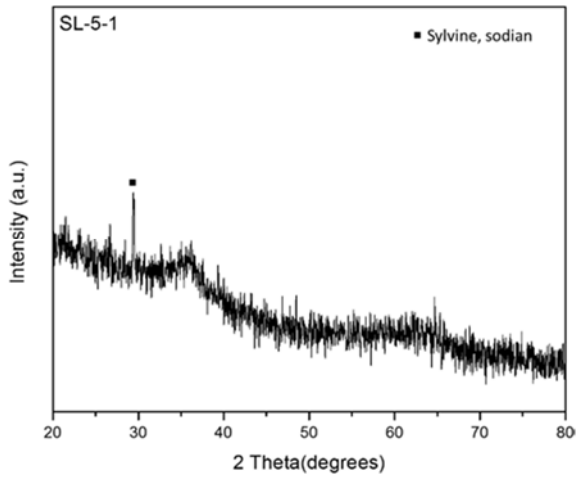
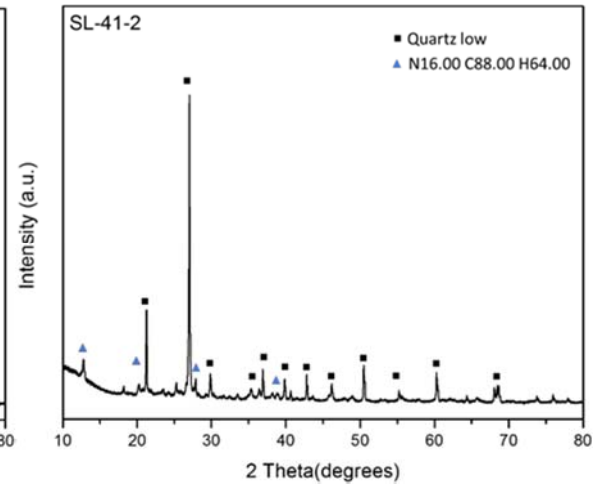
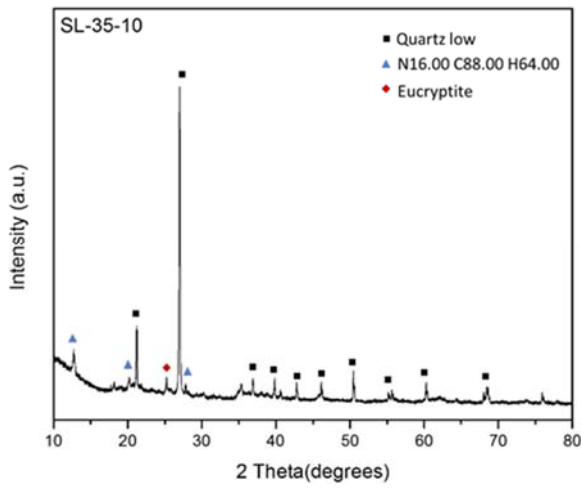
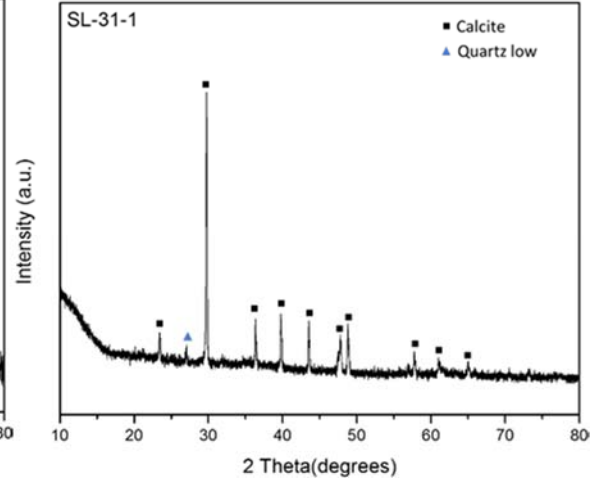
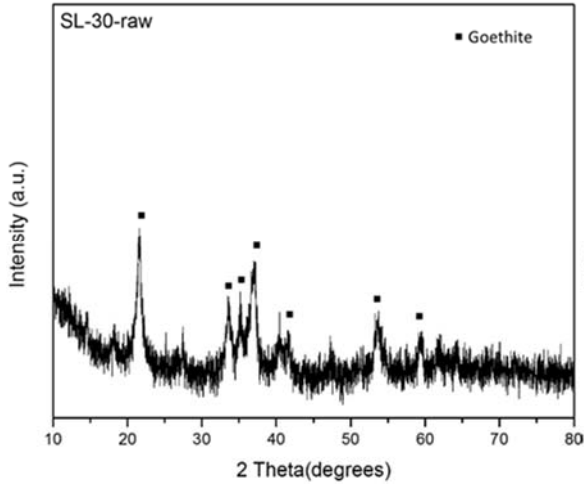
Section A1: XRD spectra of dried sludge samples collected during first pass sampling.

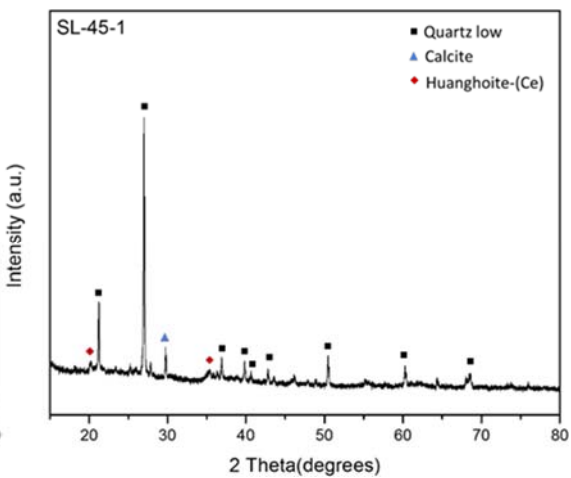
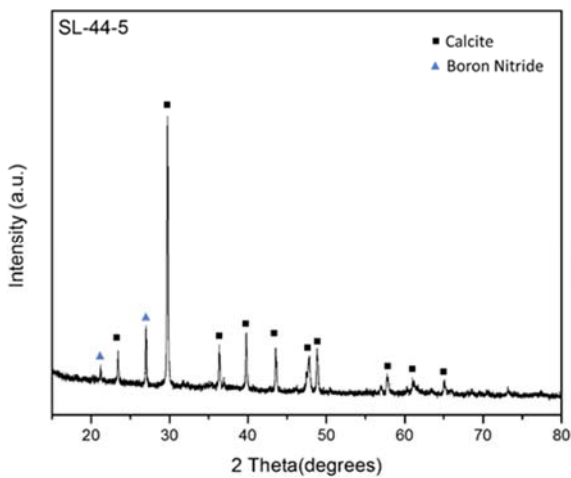
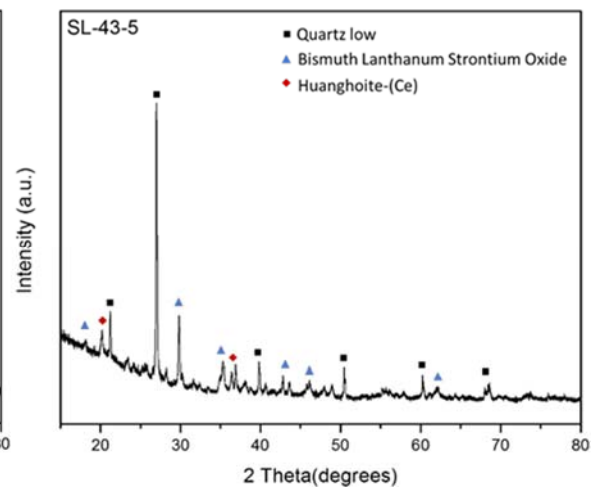
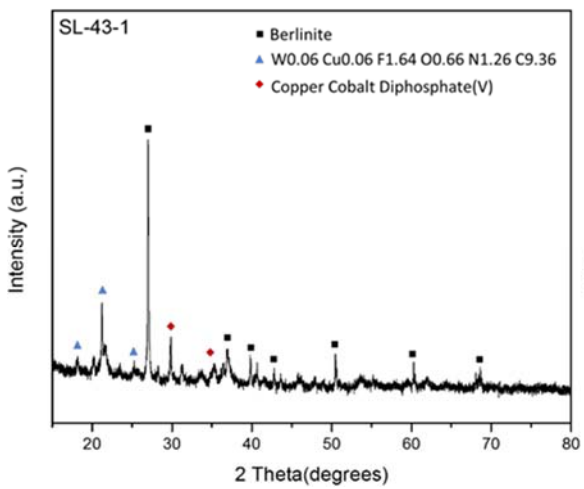
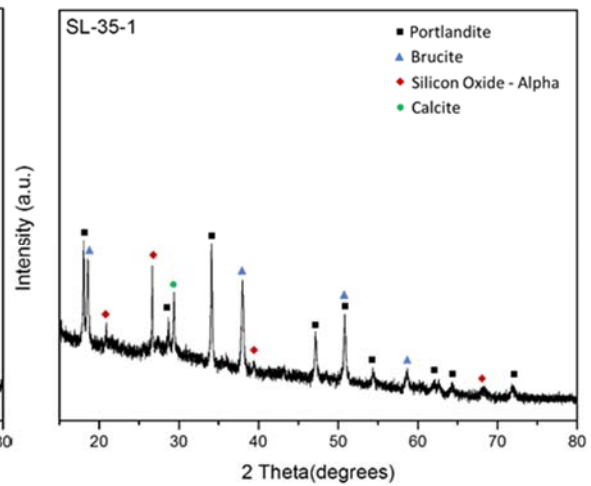
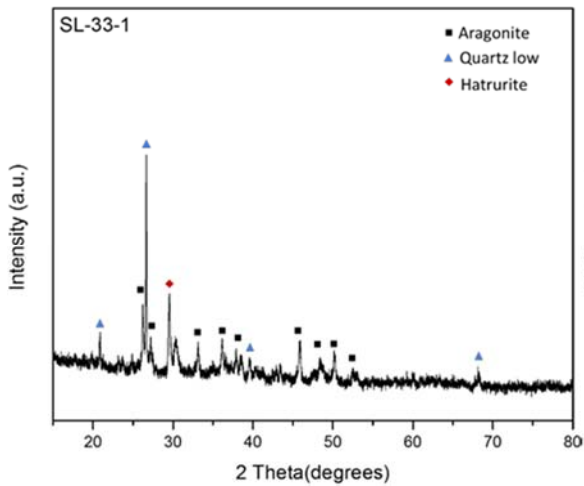


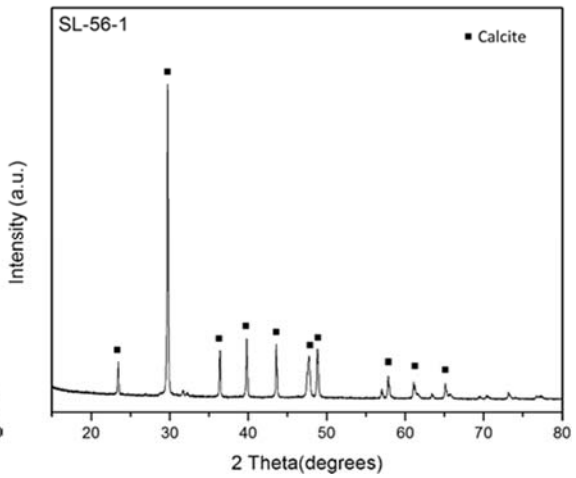
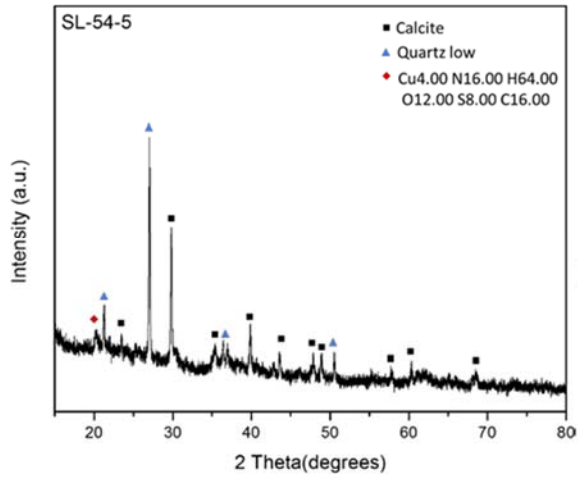
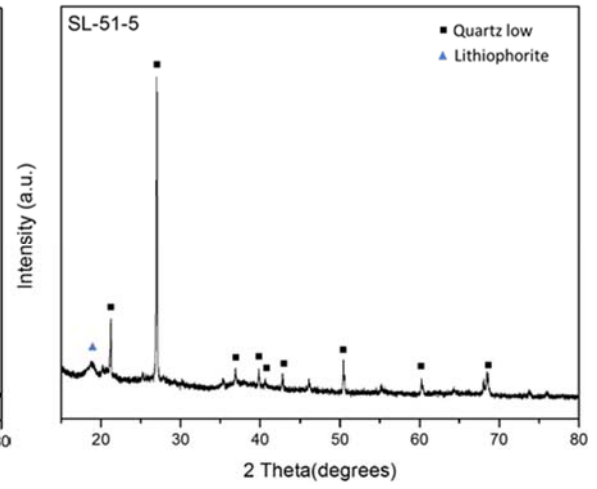
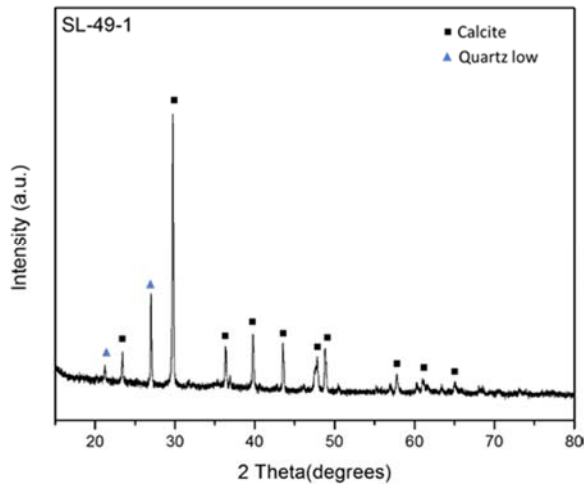
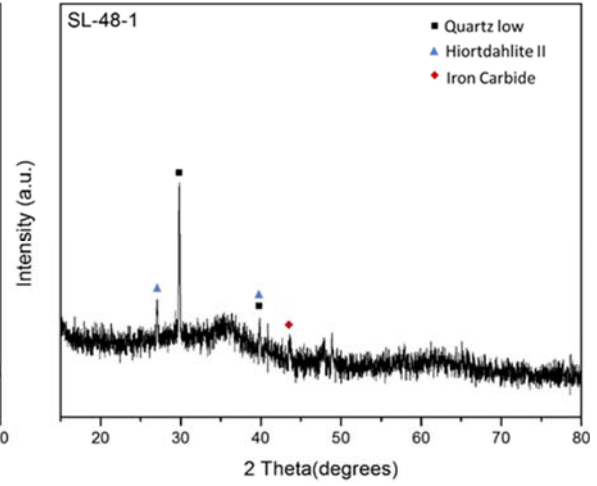
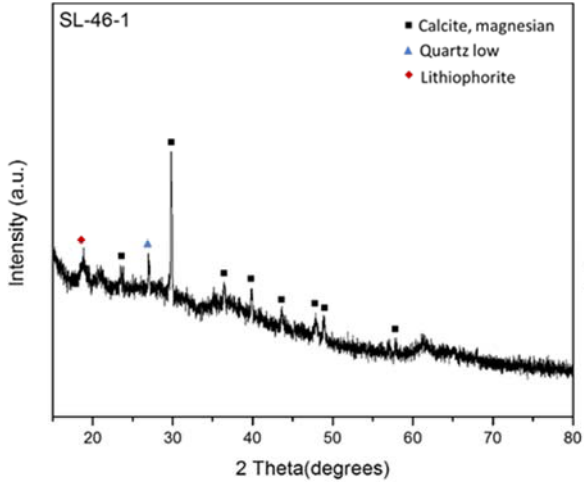


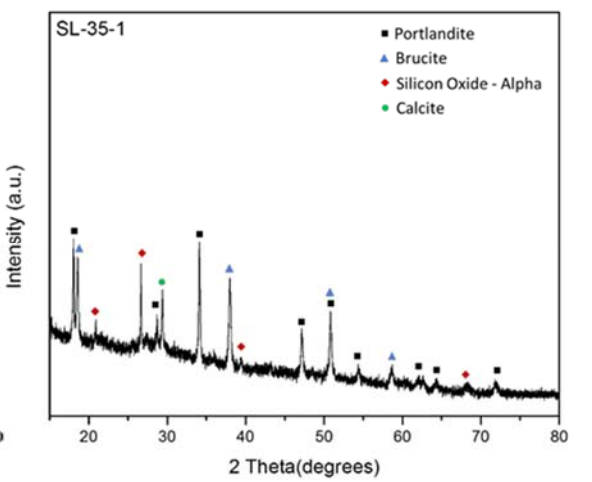
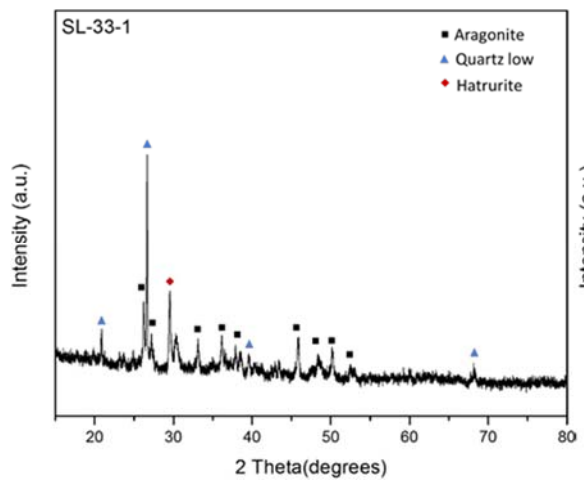
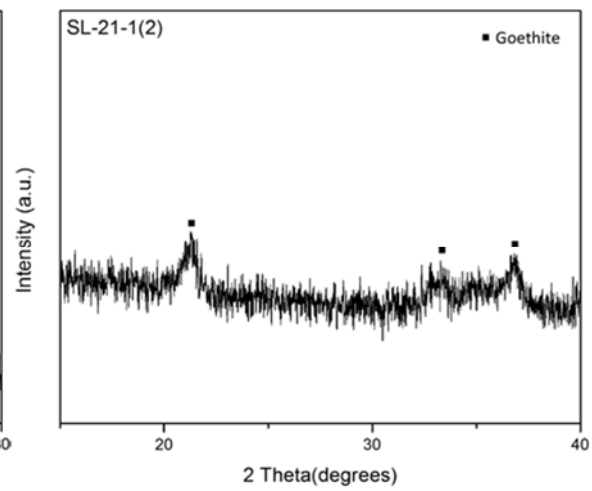
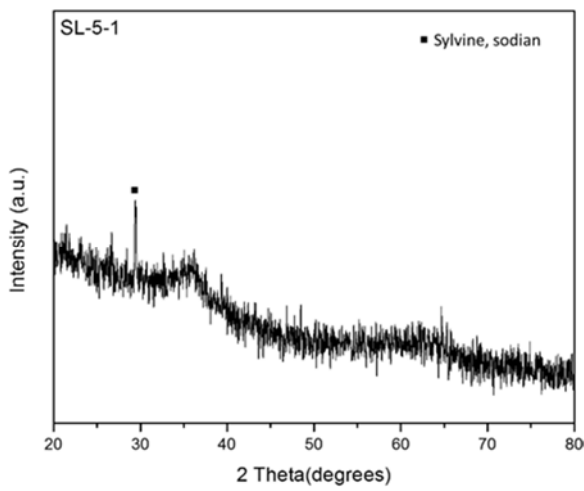
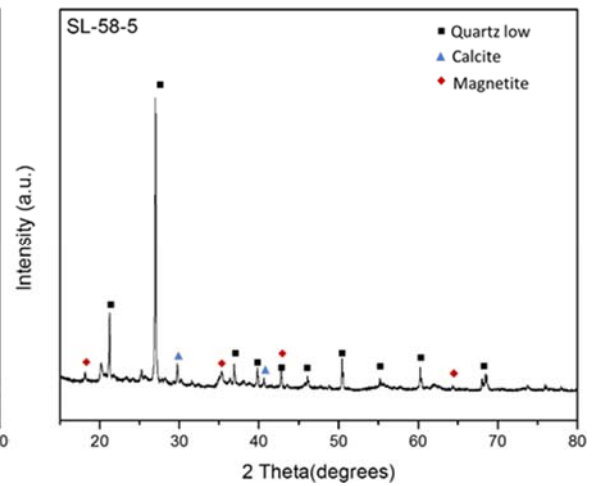
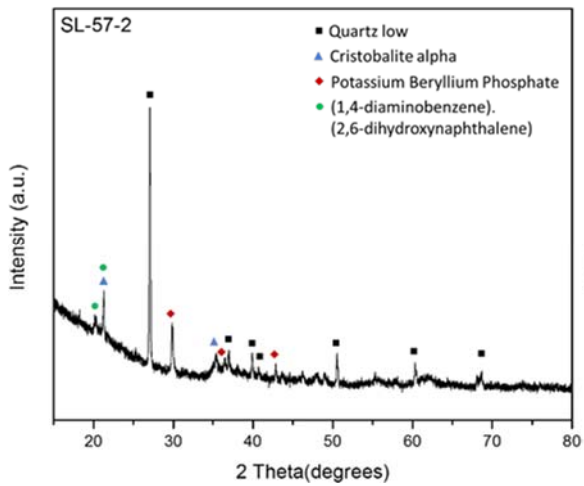


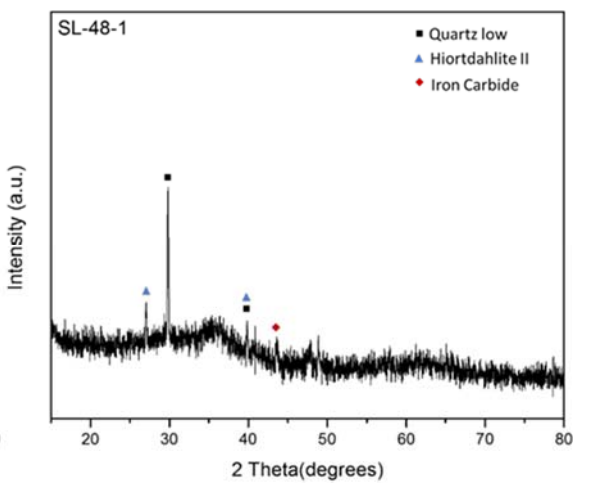
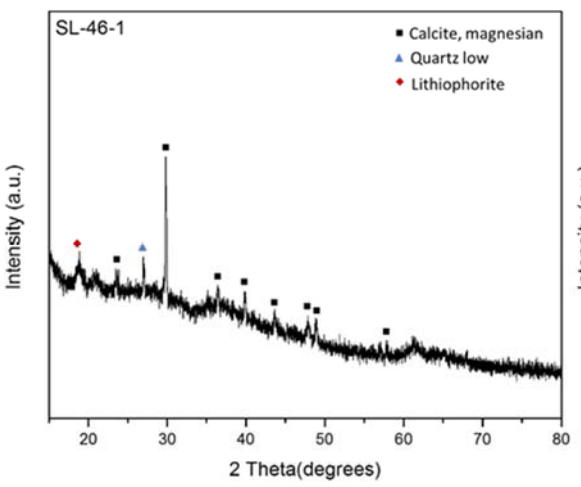
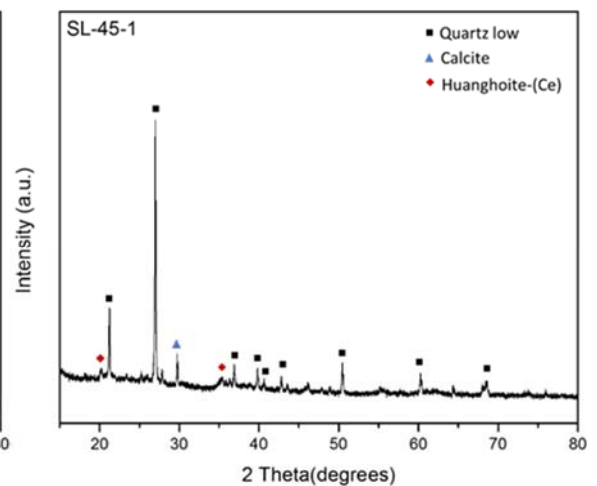
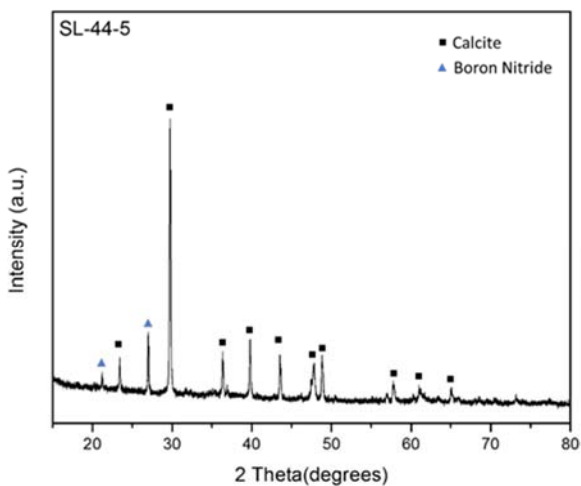
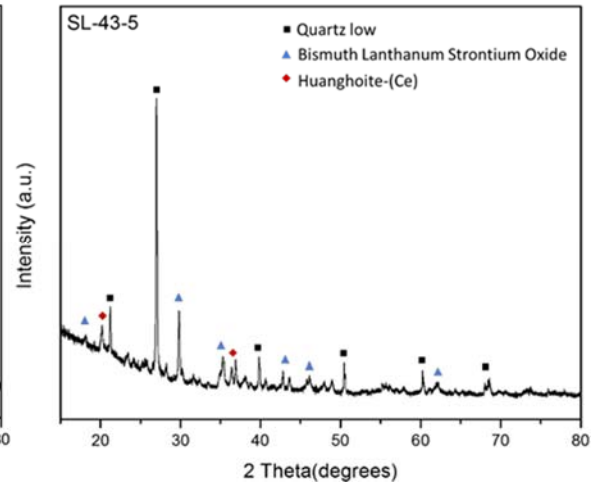
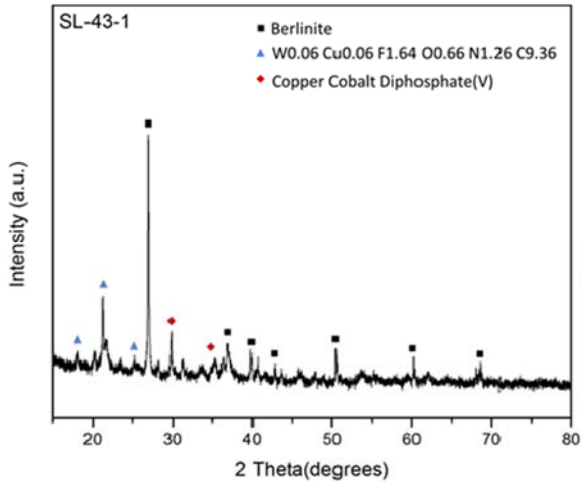


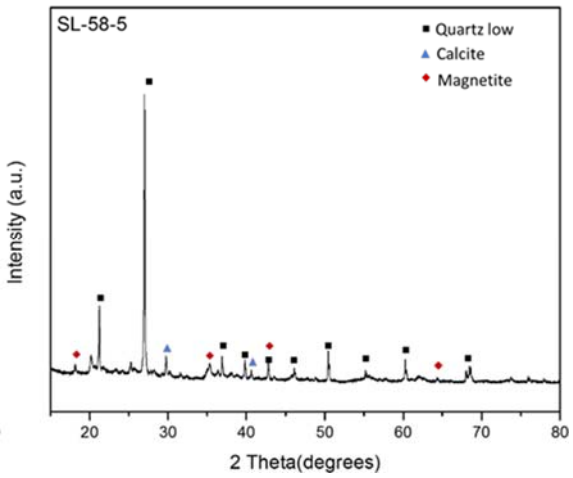
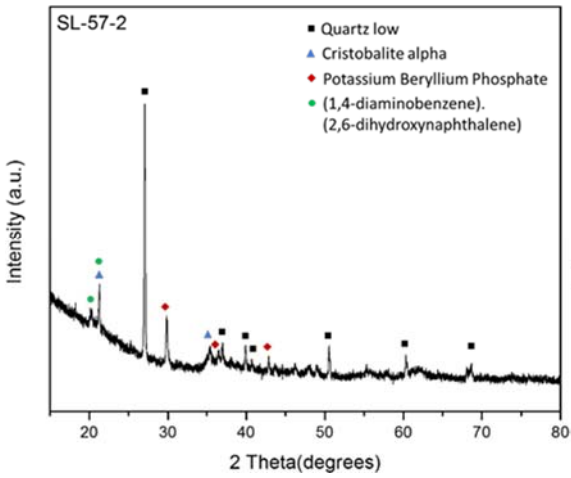
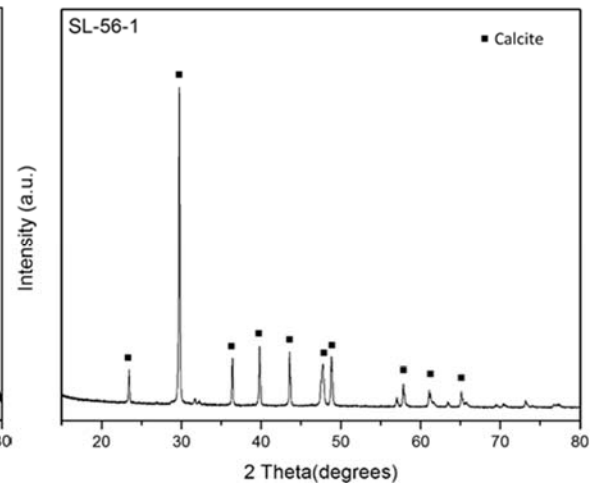
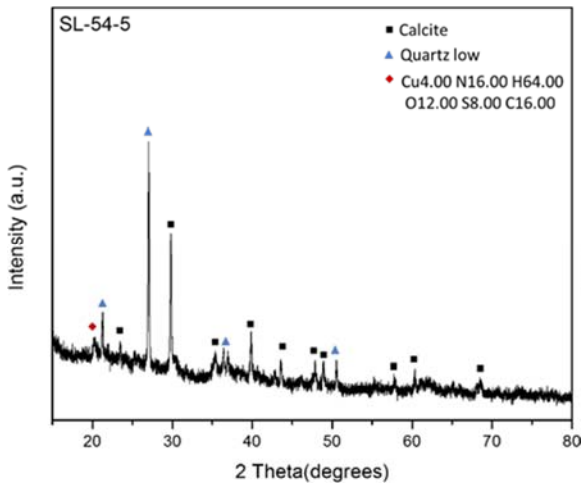
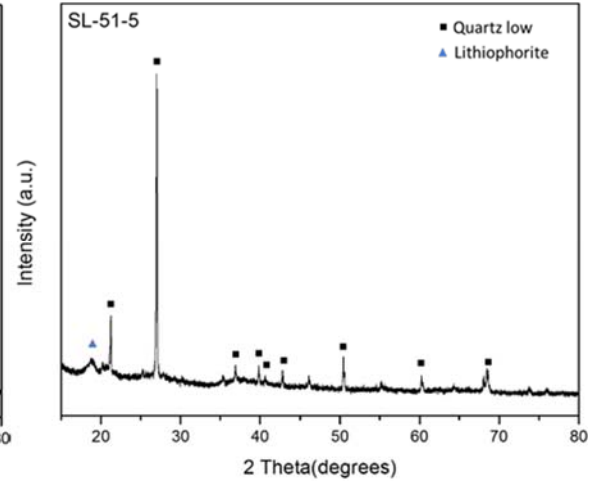
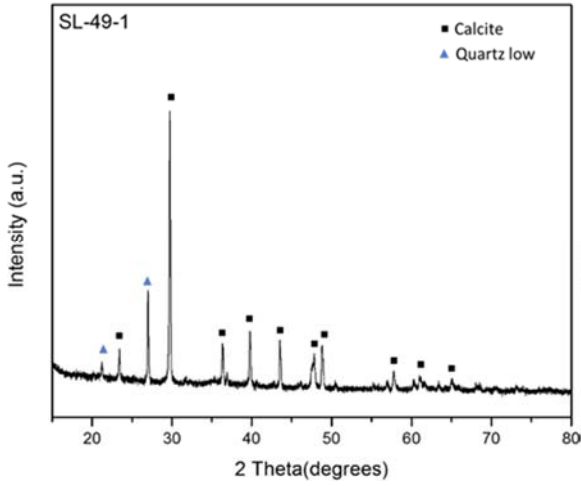


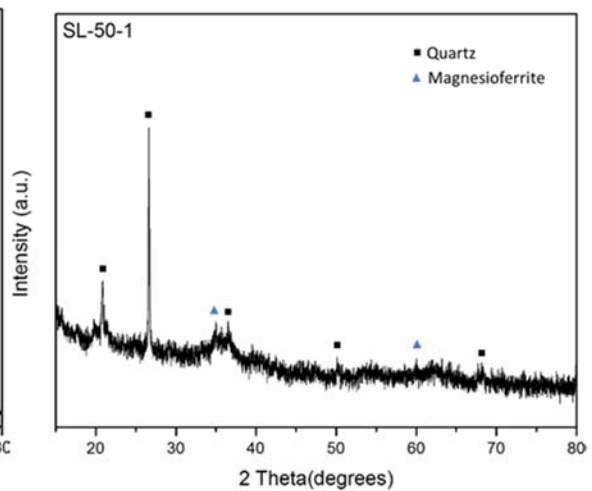
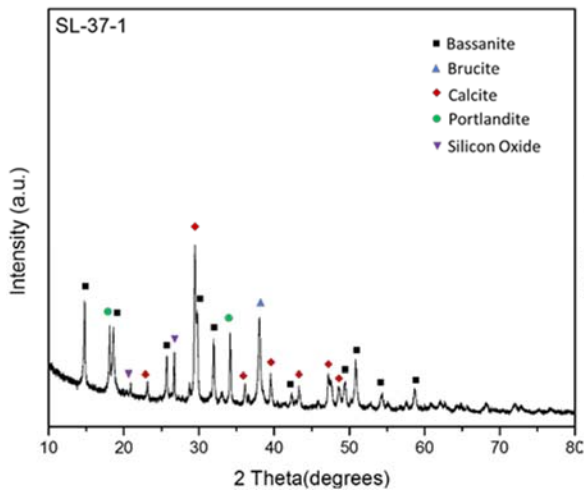
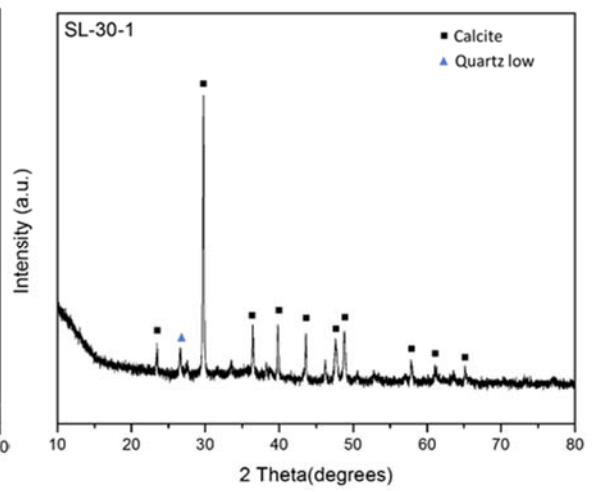
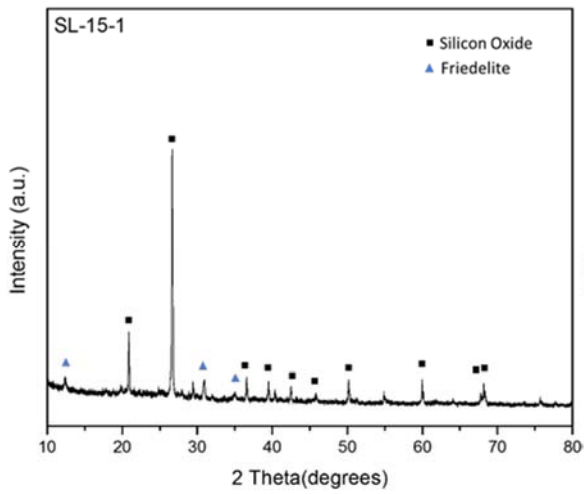
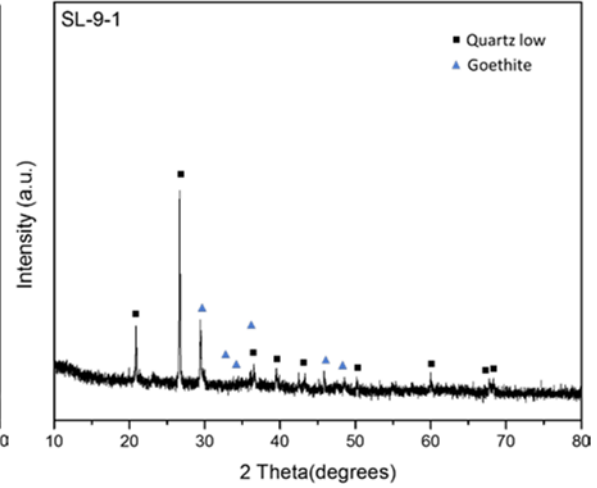
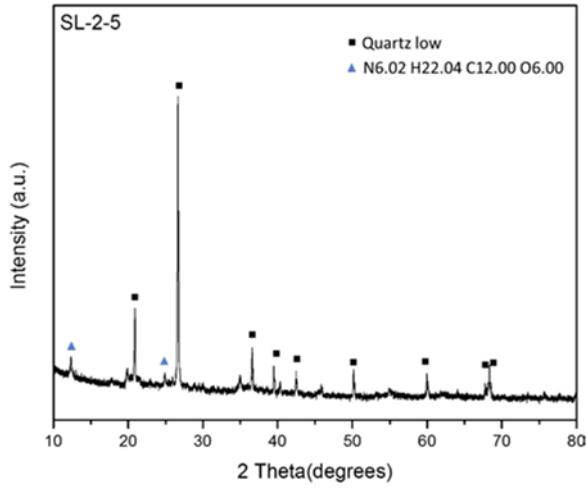


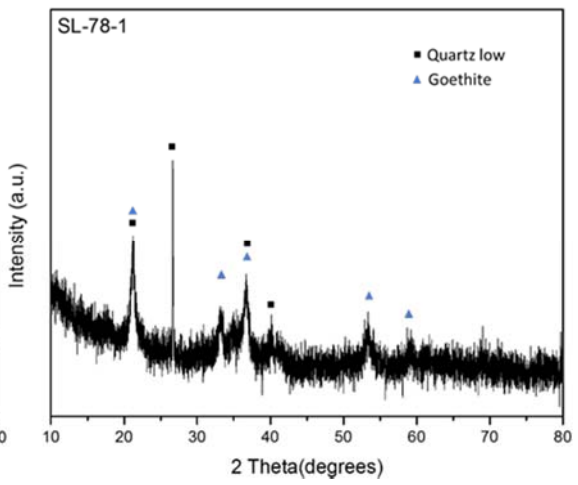
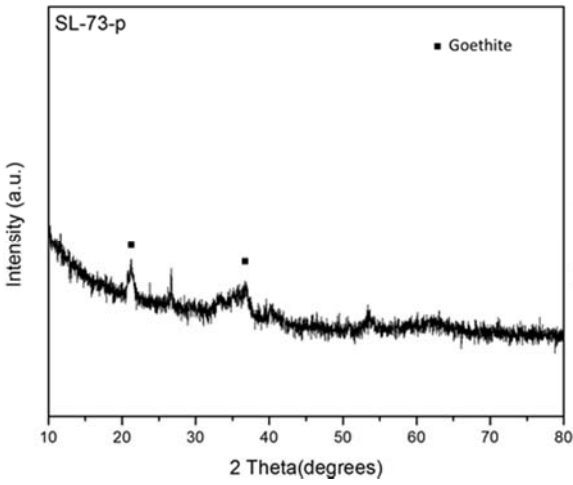
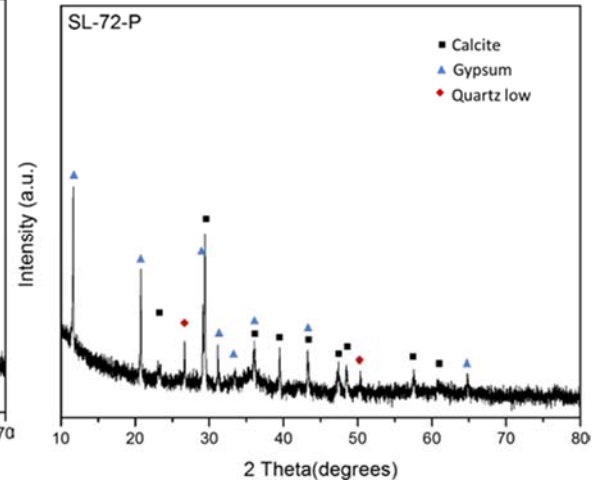
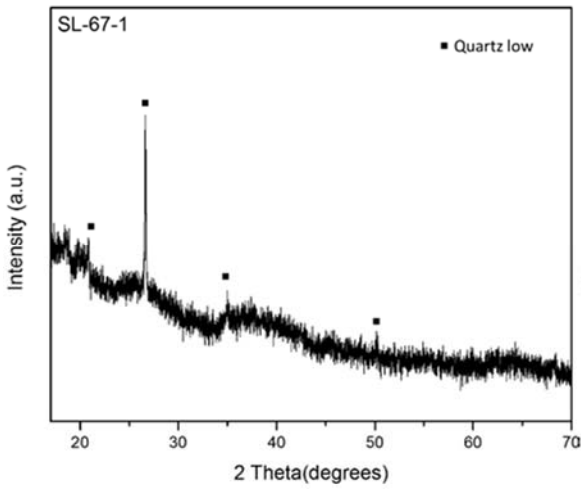
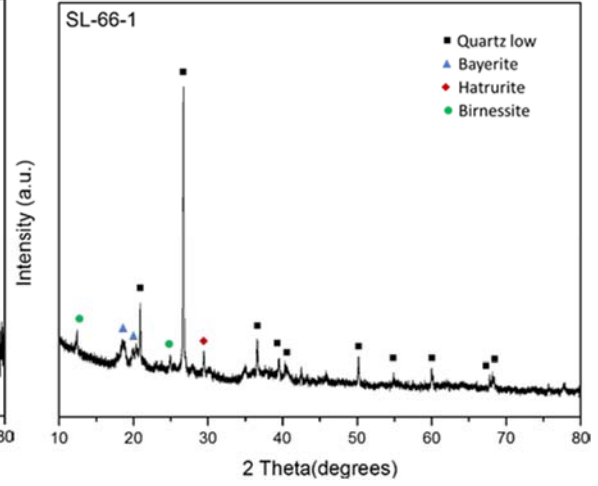
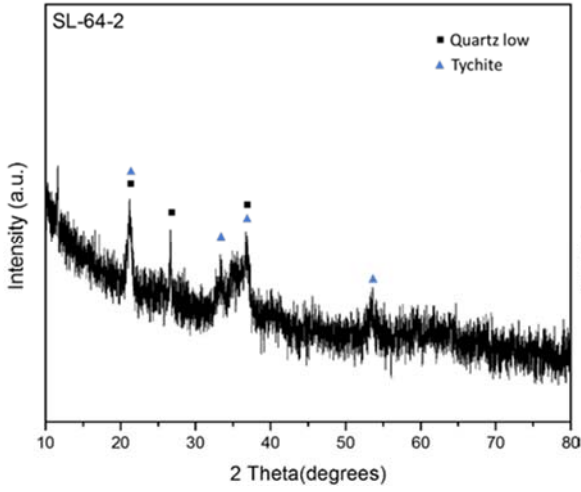


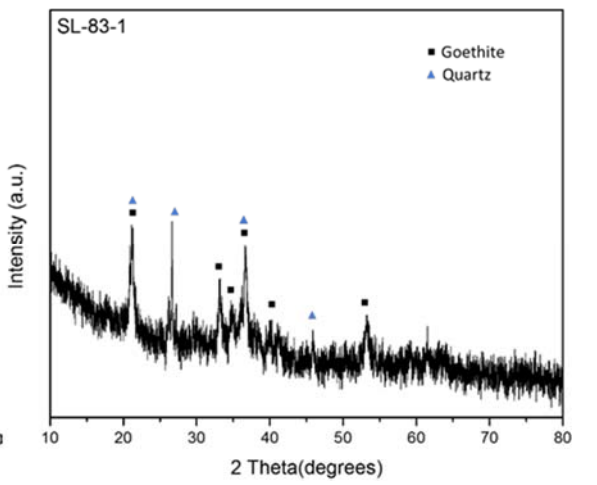
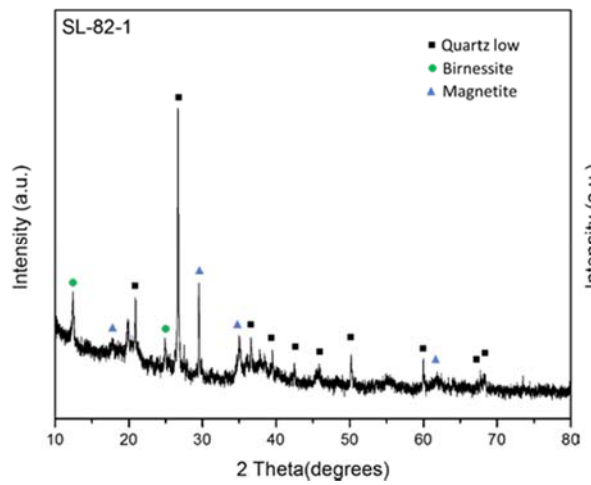
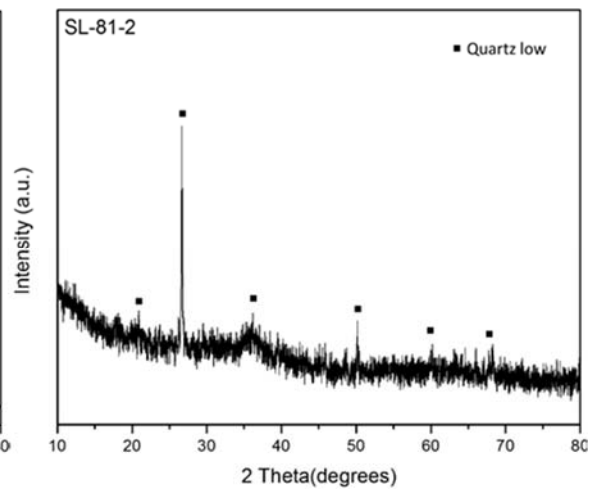
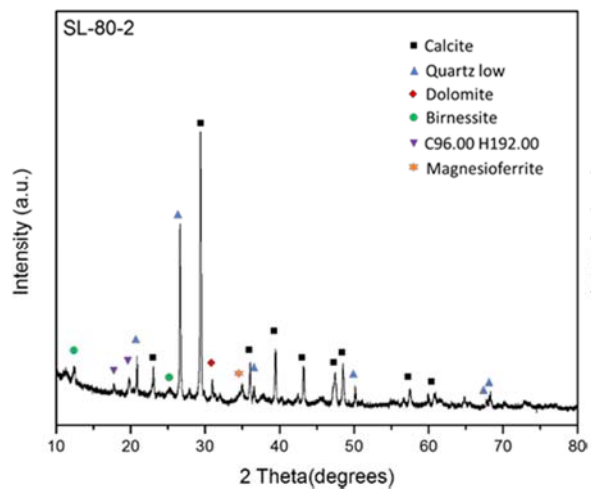
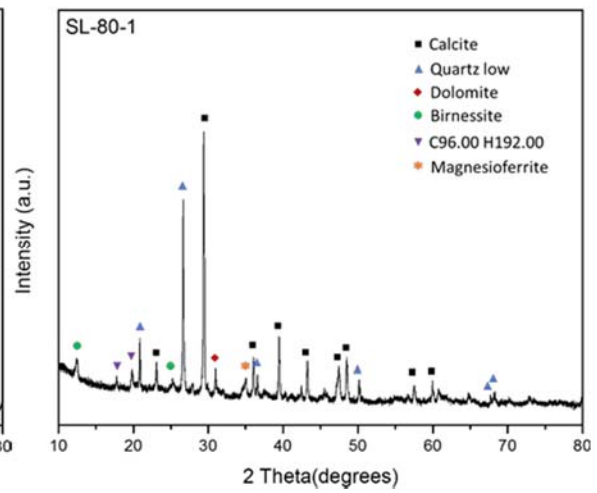
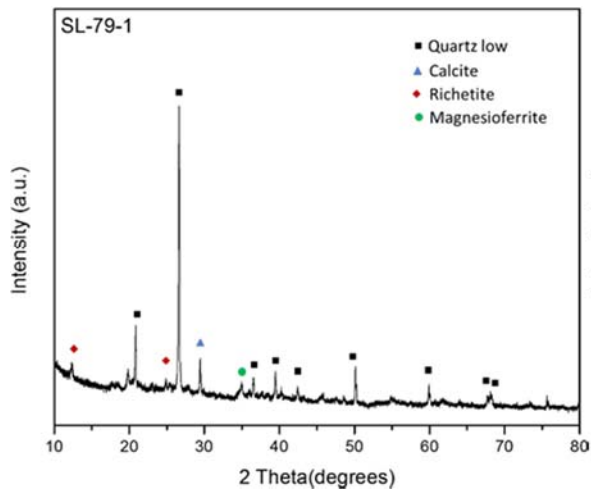


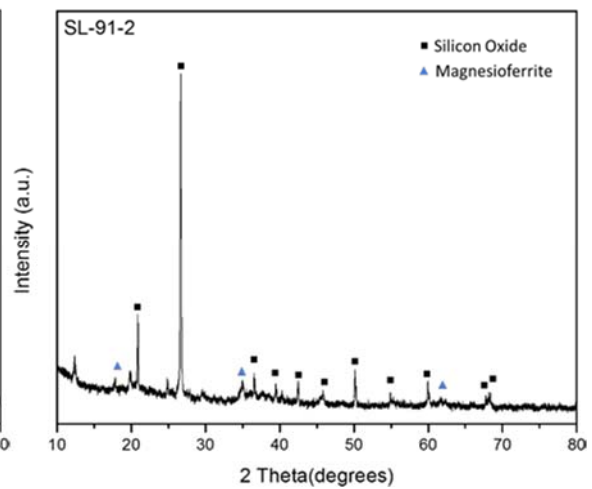
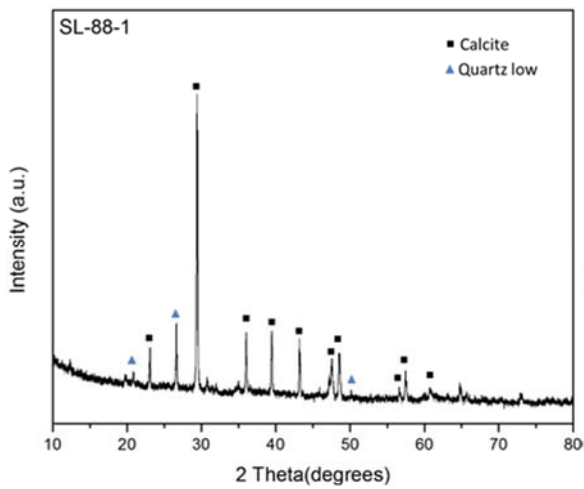
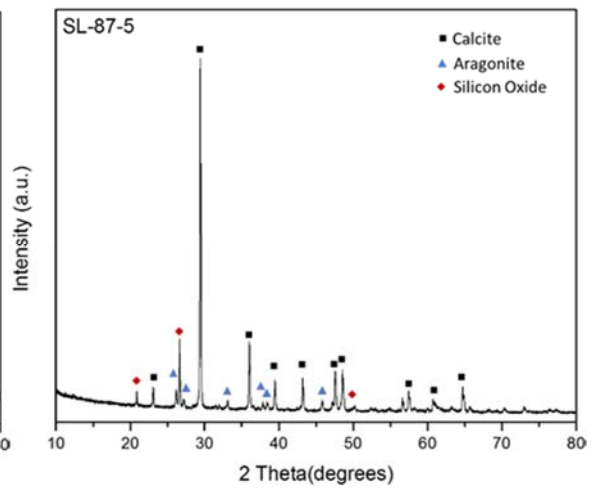
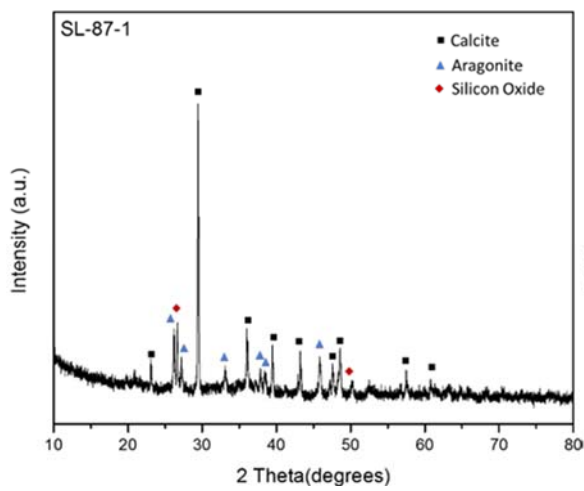
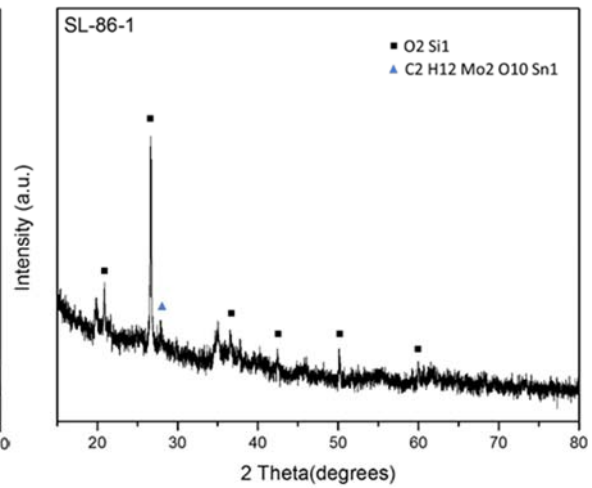
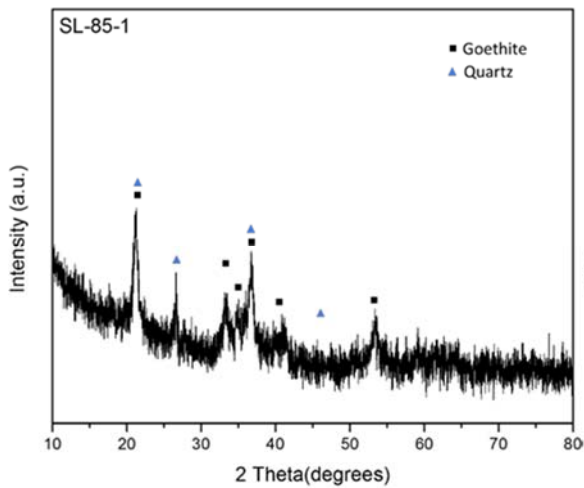


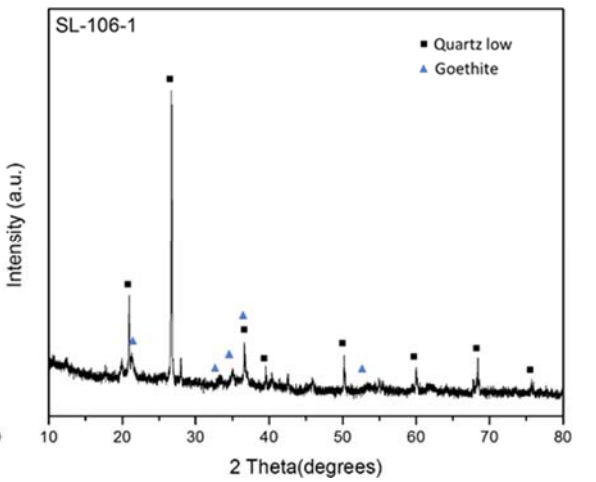
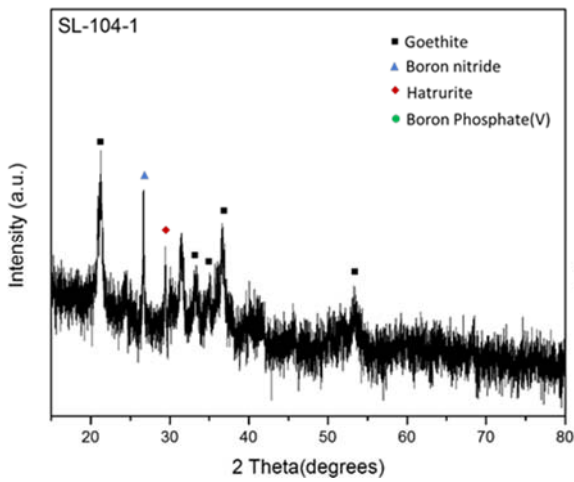
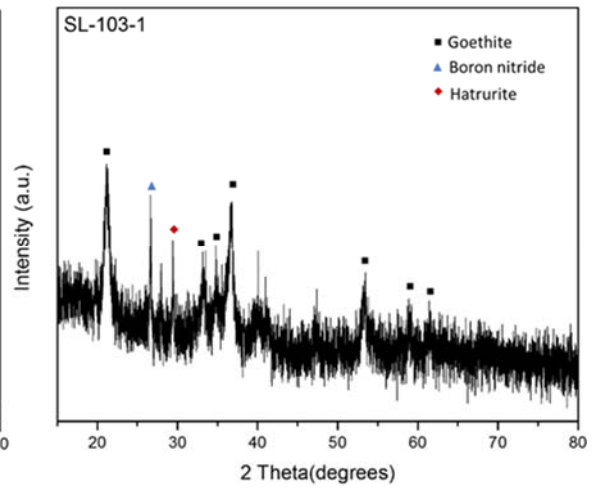
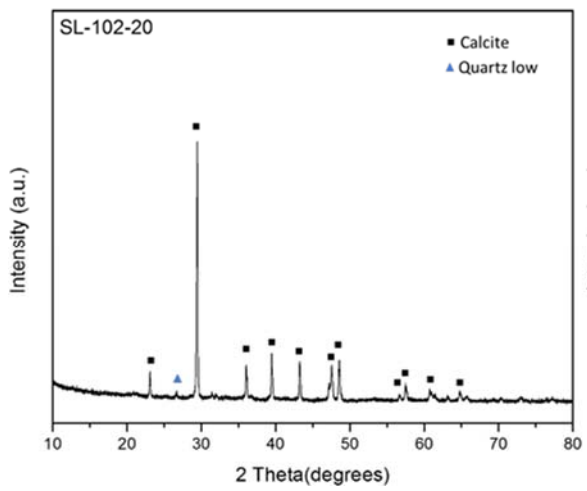
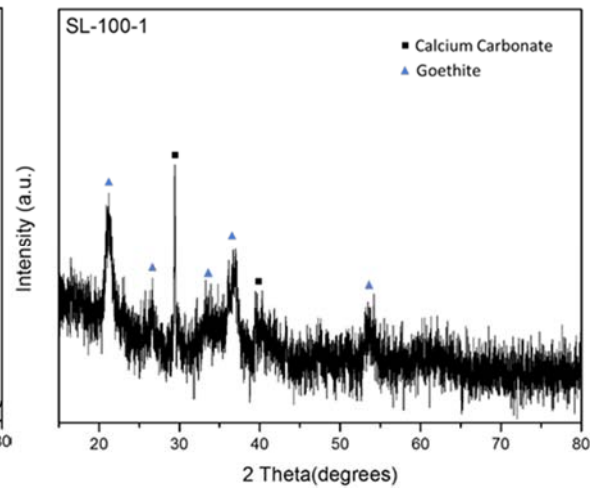
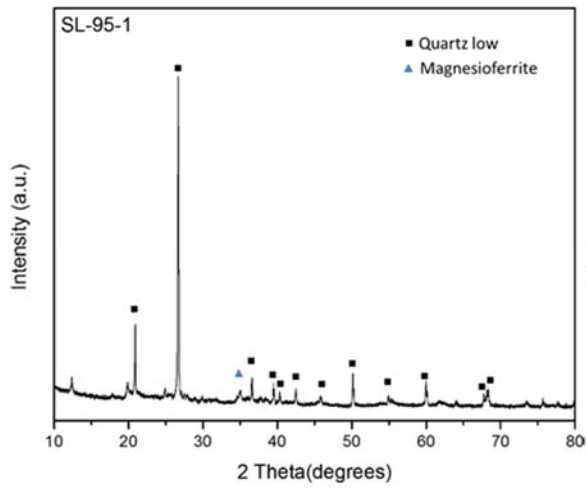


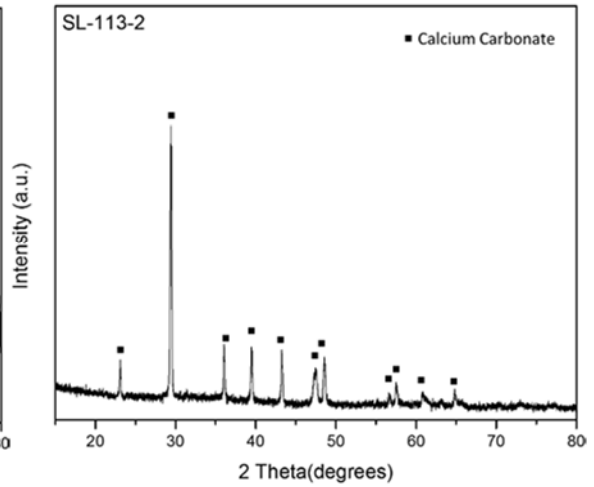
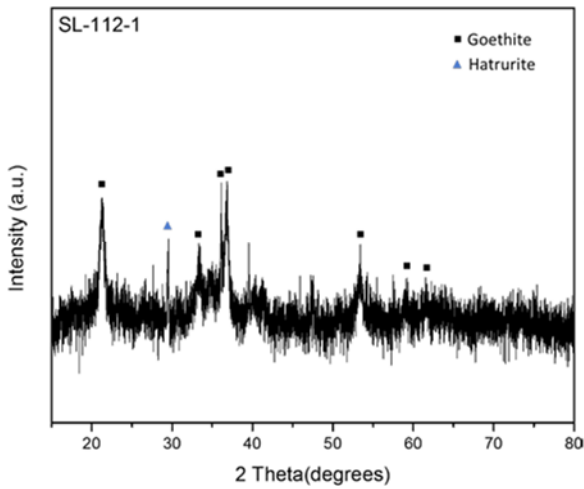
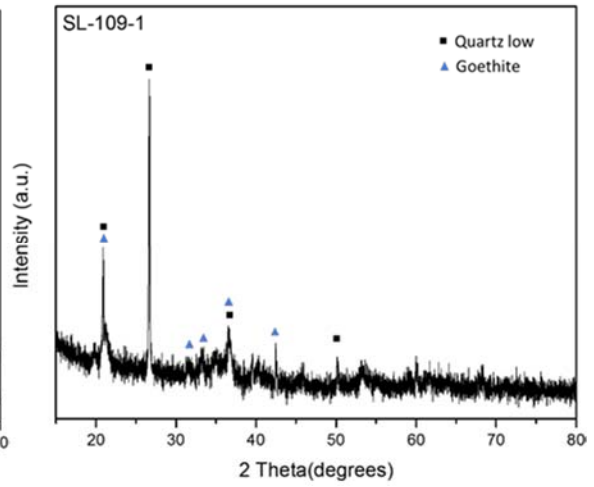
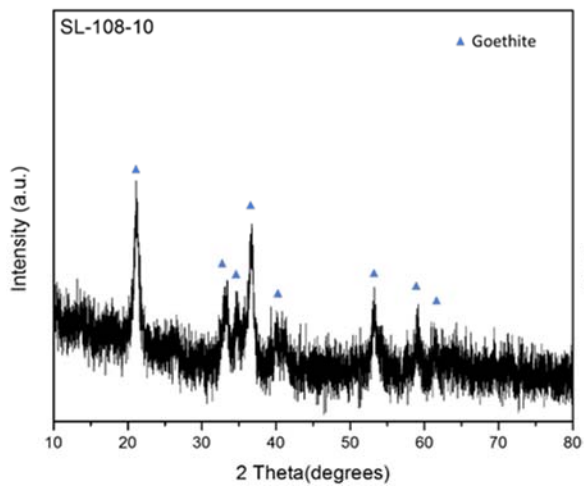
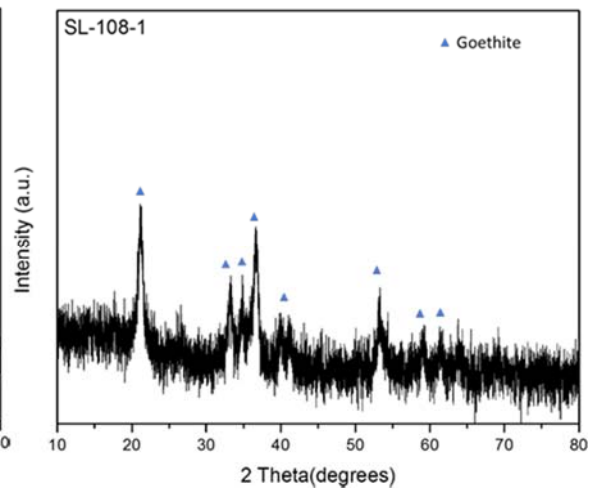
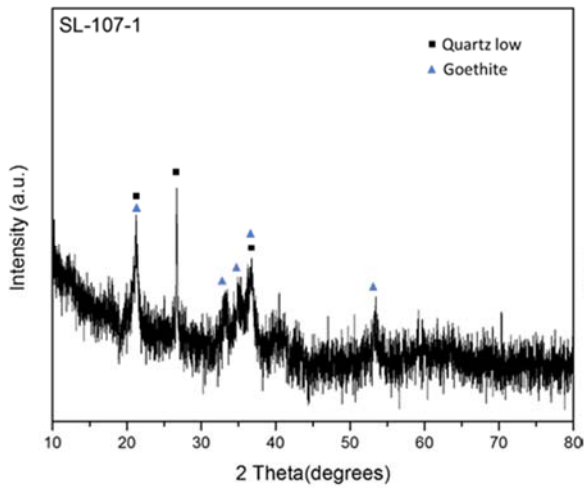


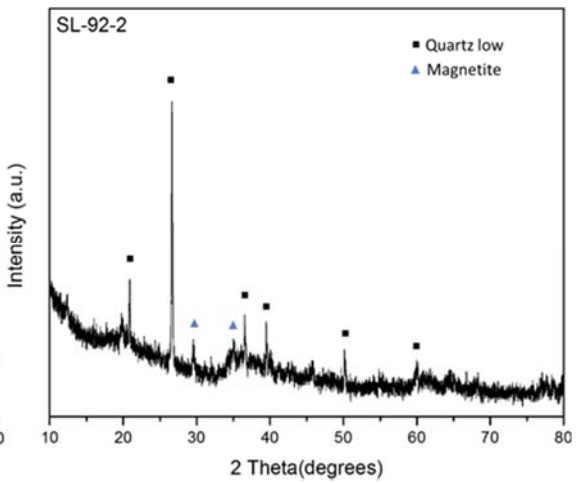
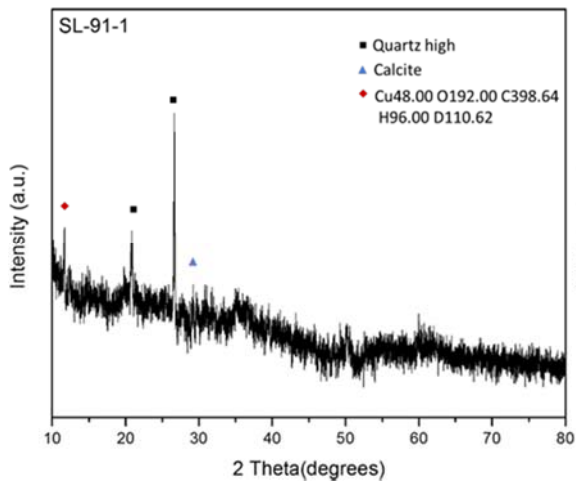
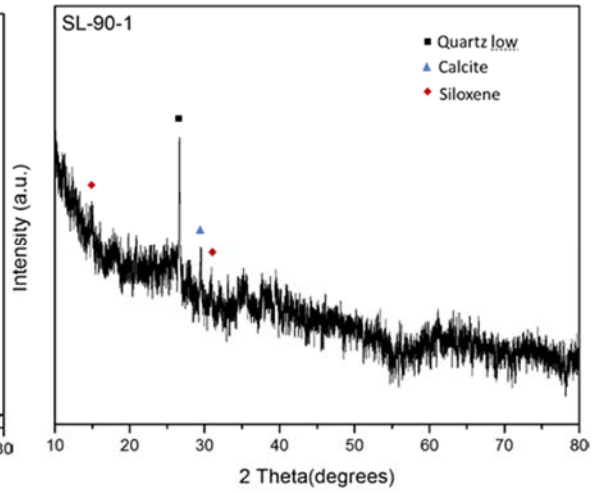
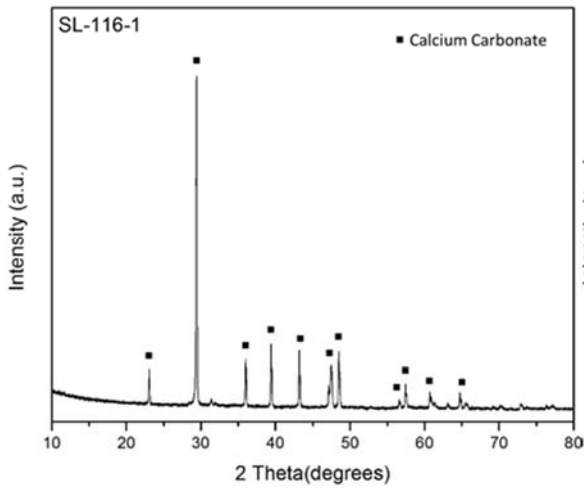
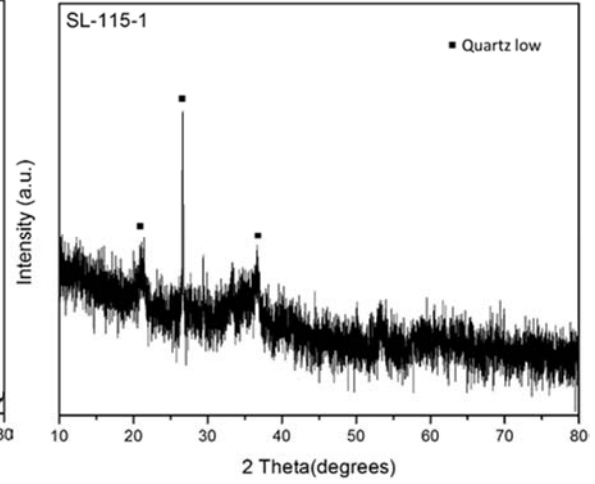
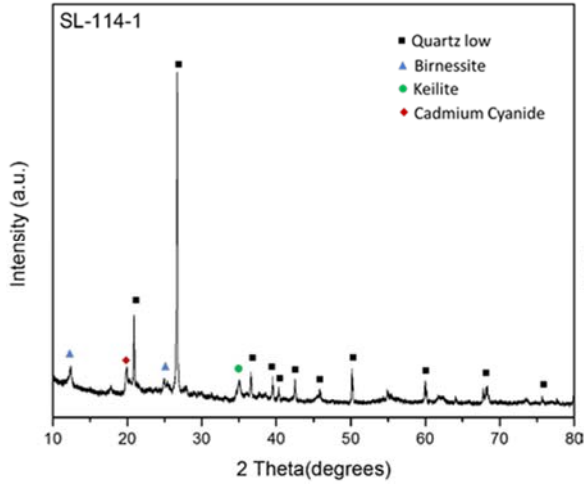


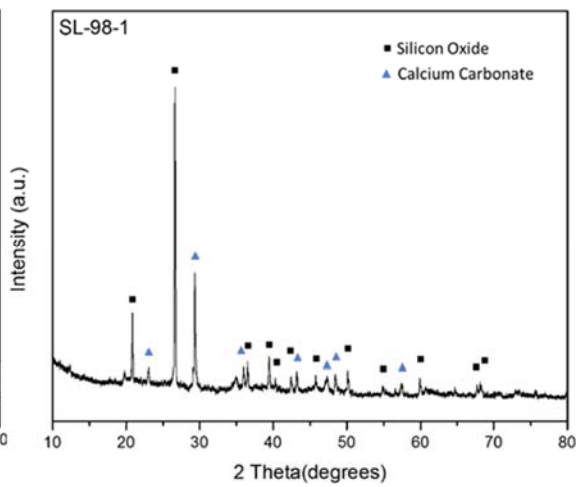
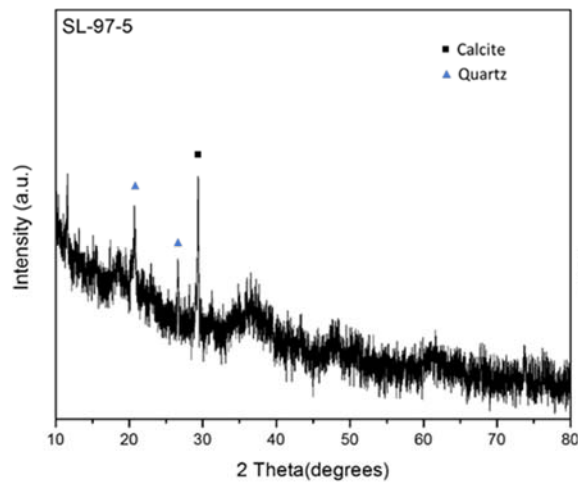
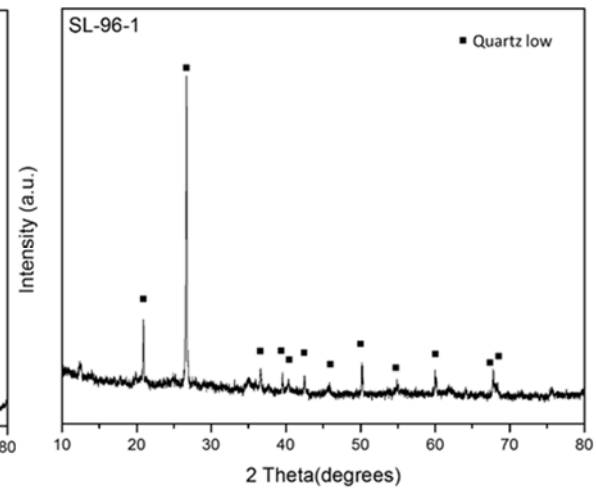
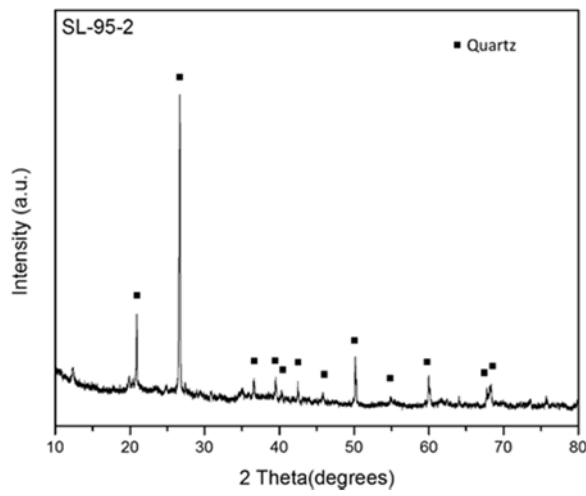
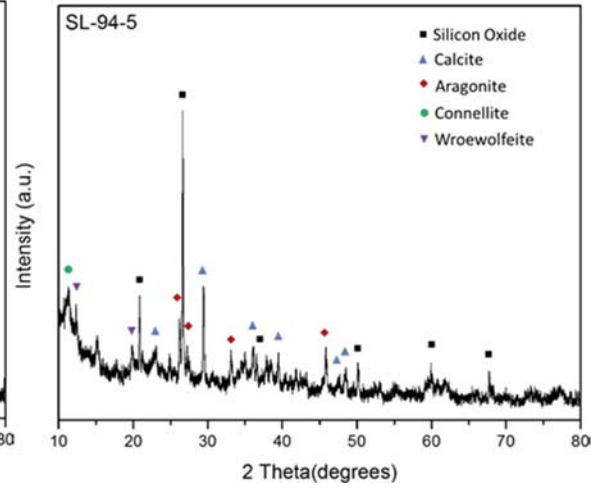
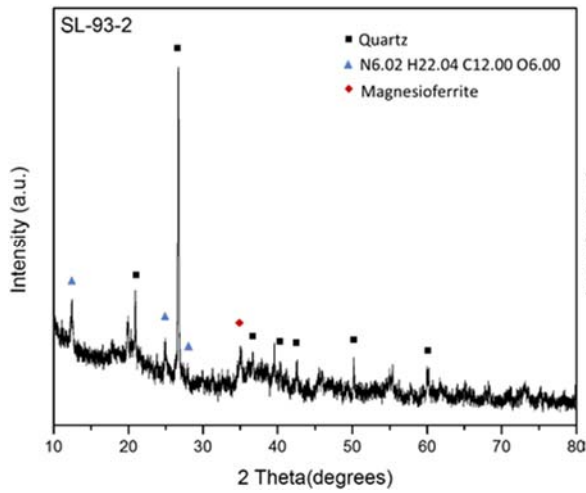


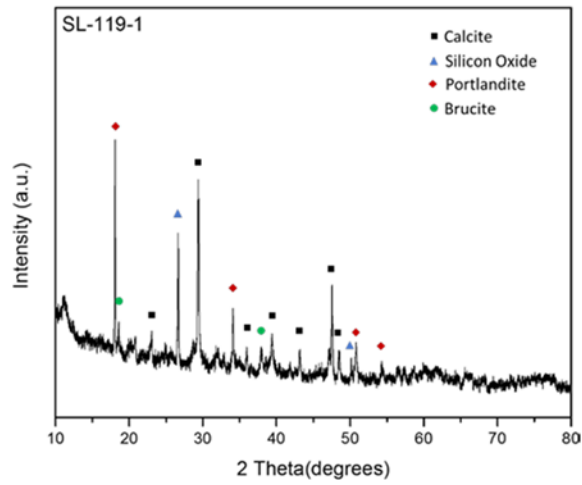
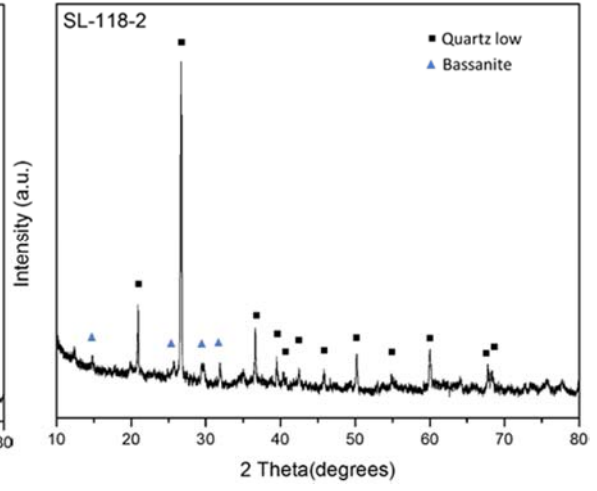
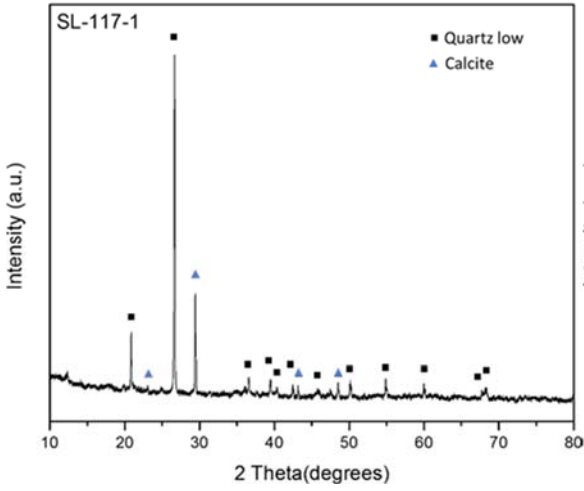
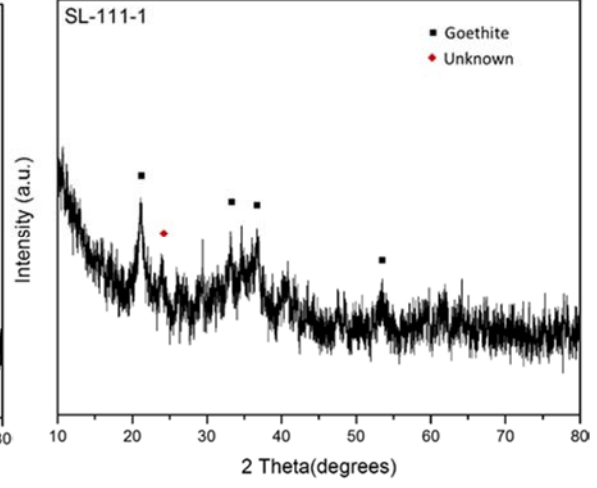
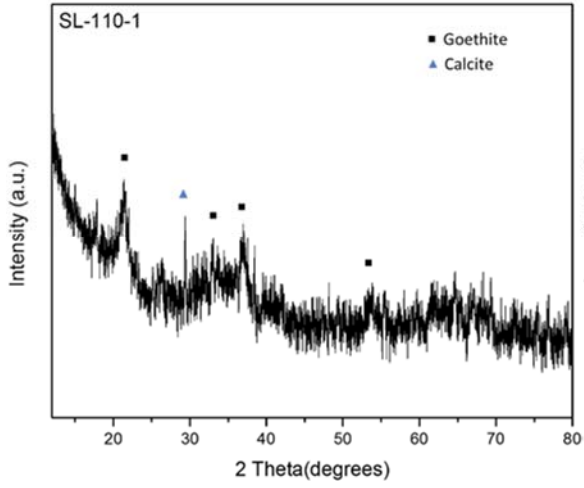




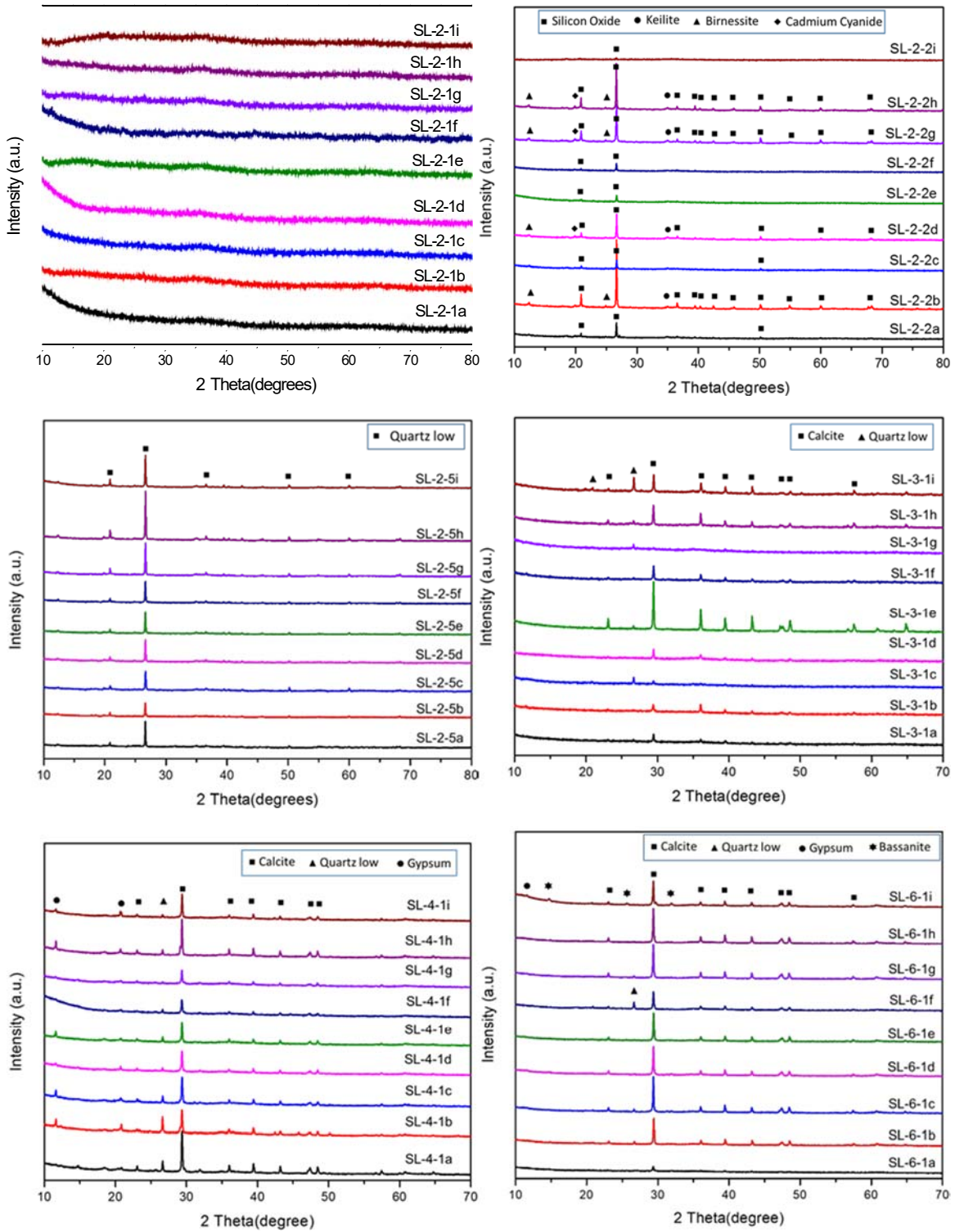


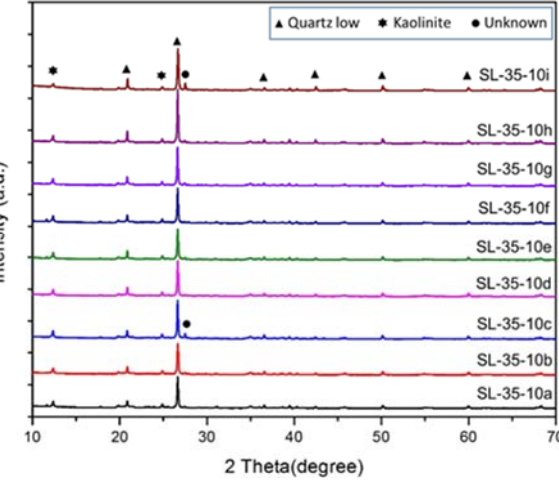
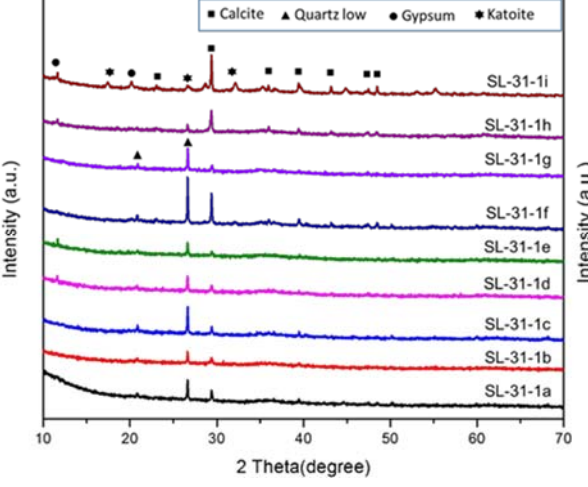
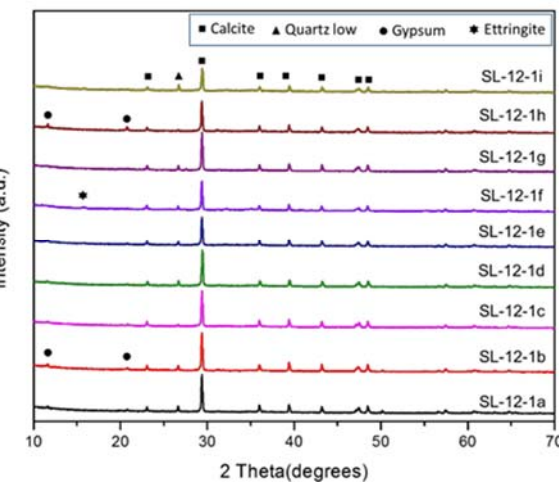
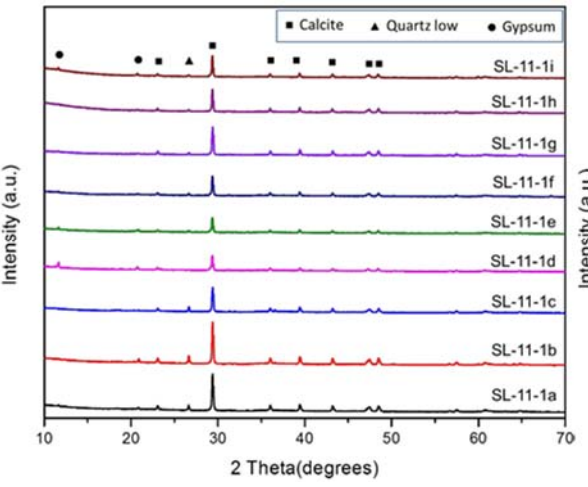
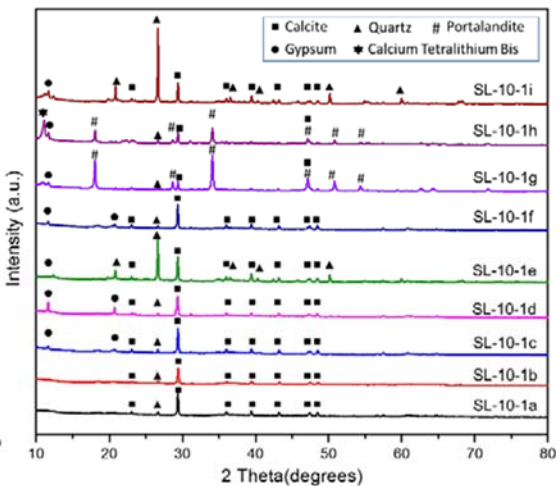
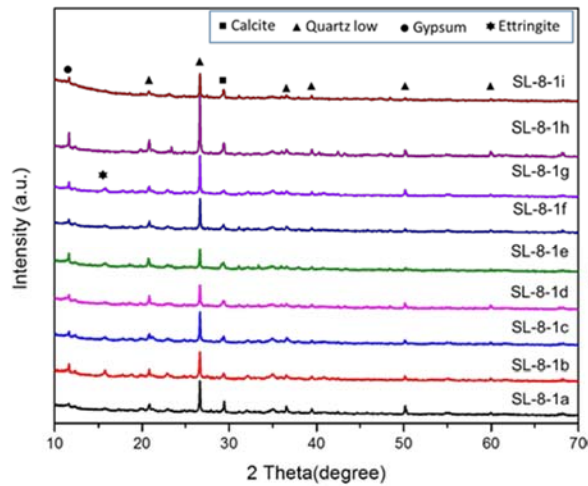


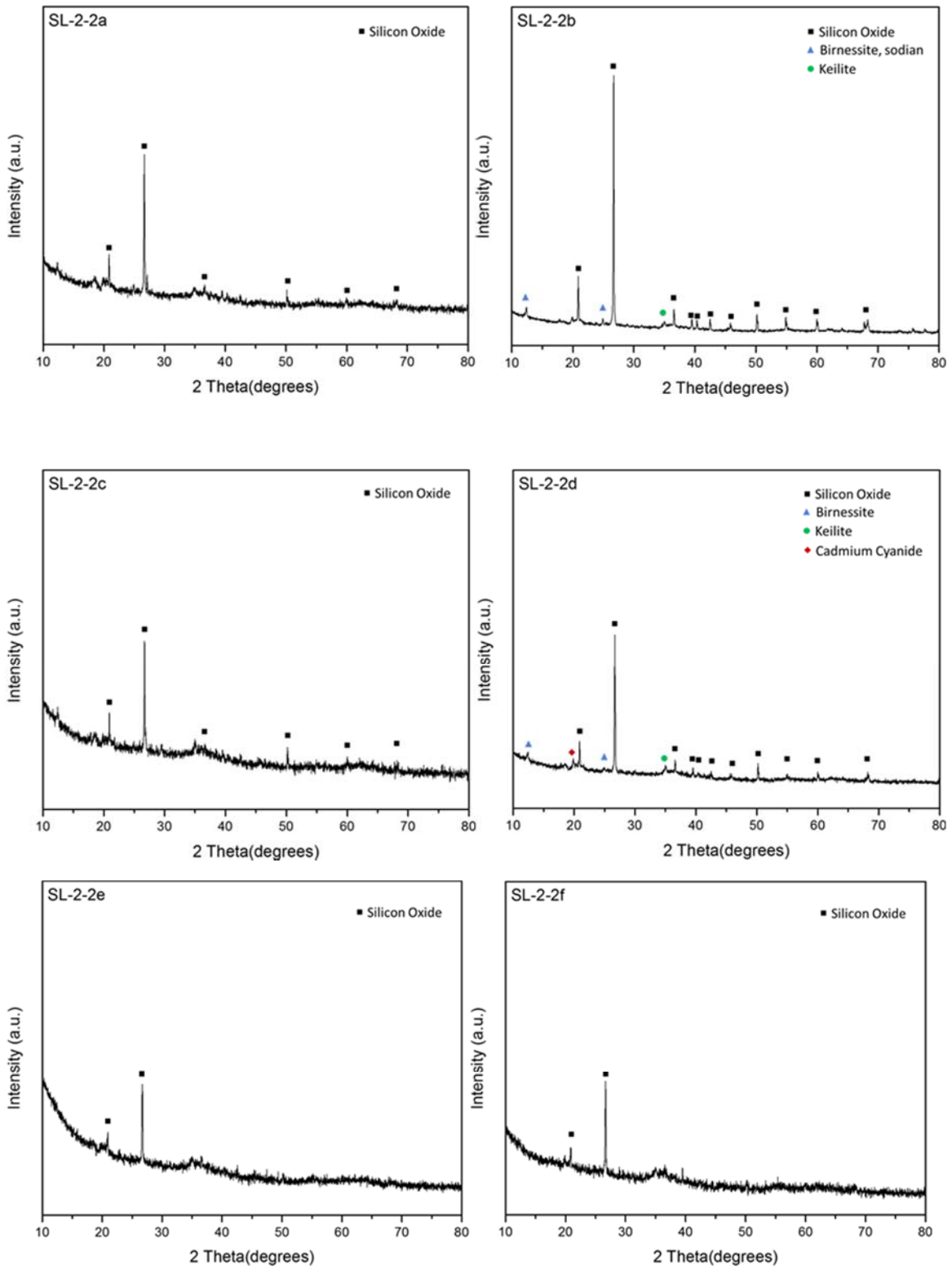


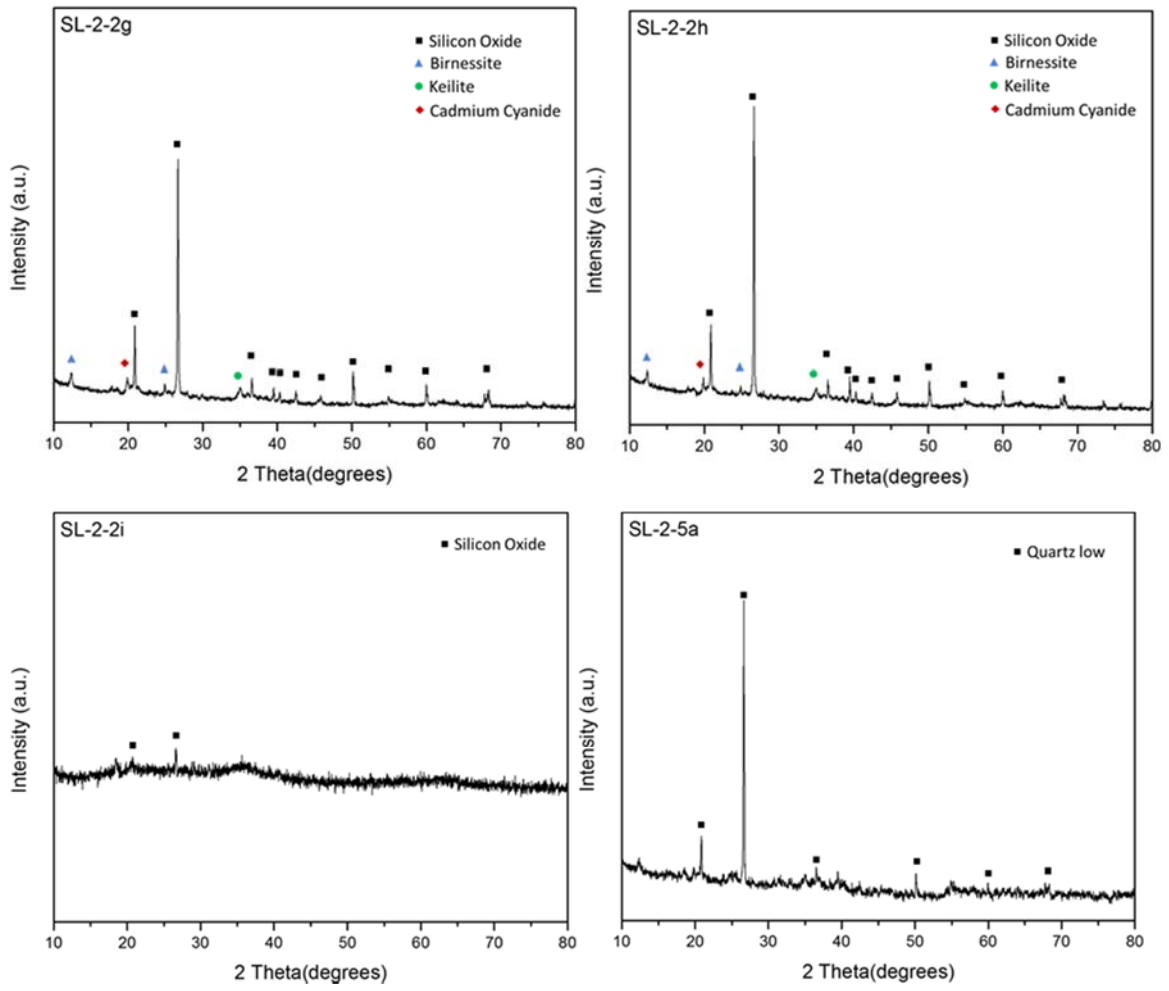


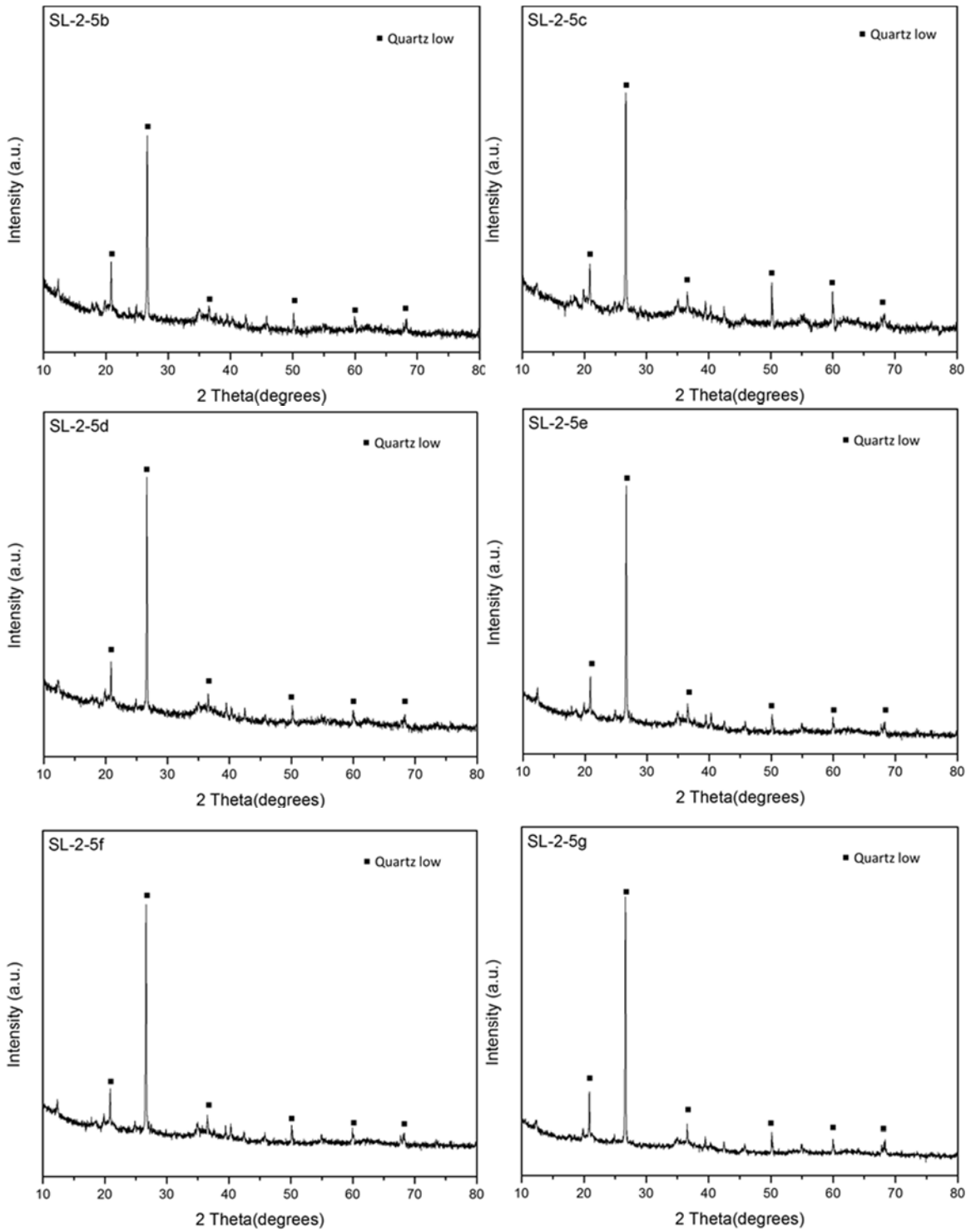
Section A2: XRD spectra of dried sludge samples collected during second pass sampling.

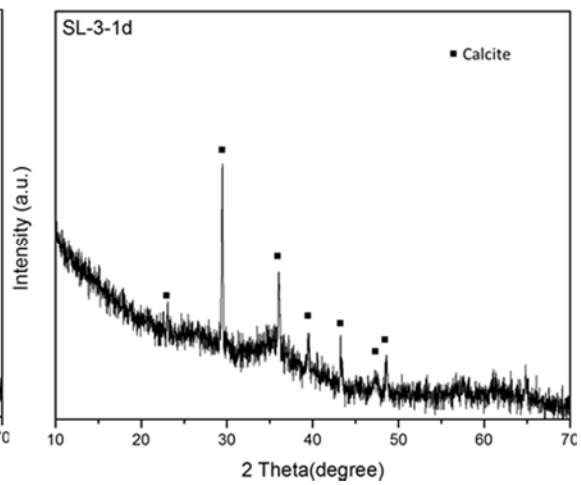
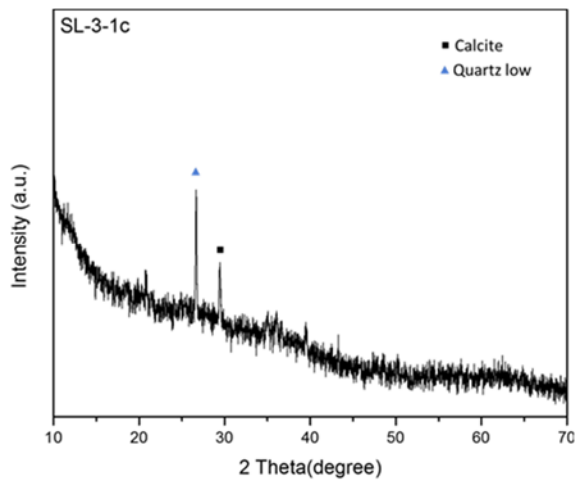
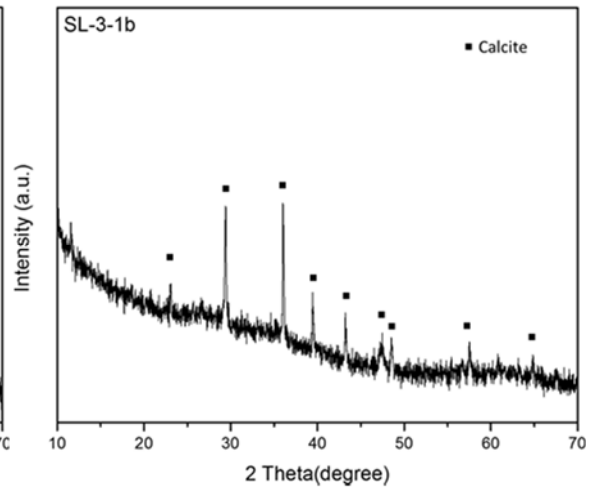
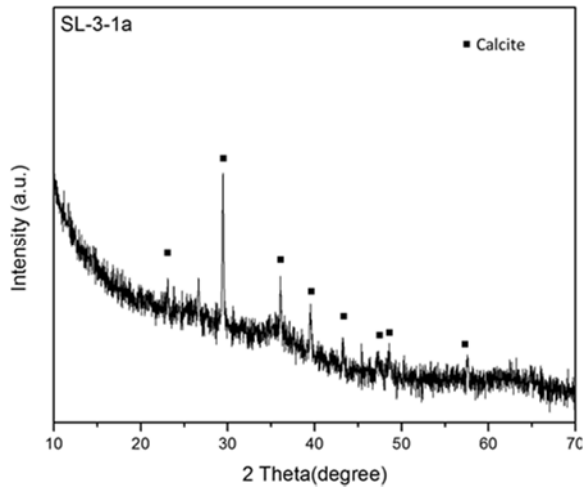
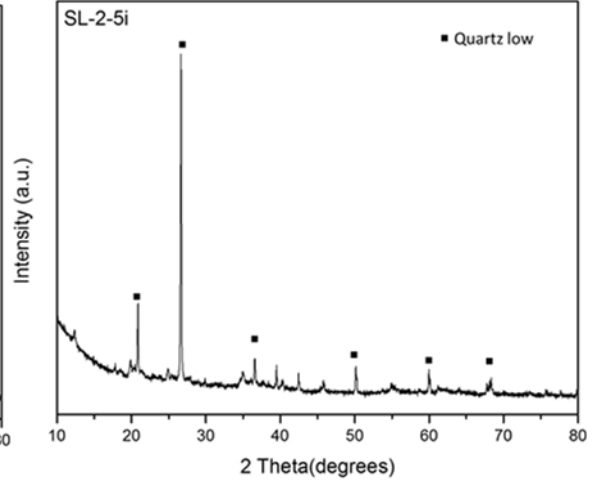
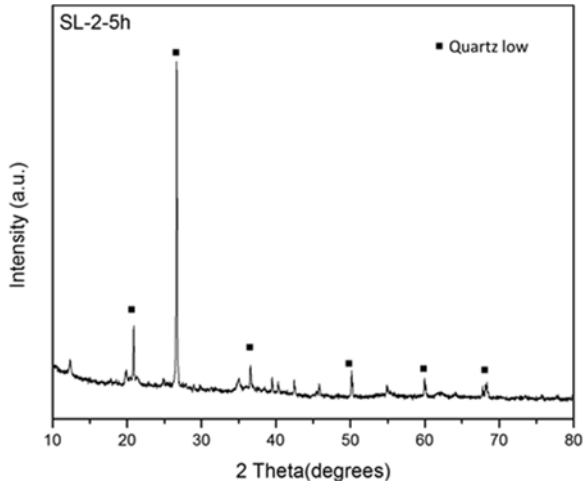


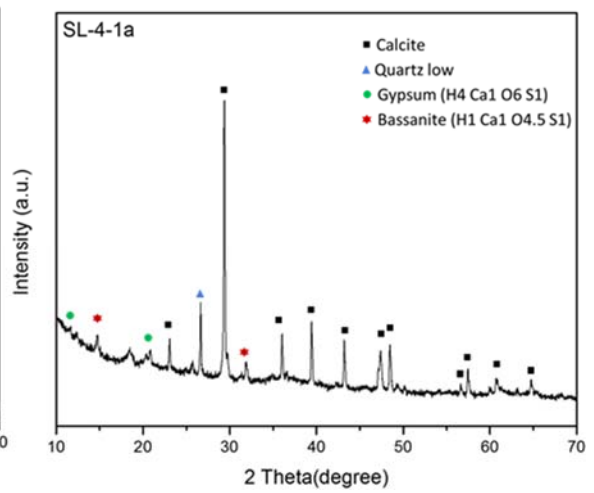
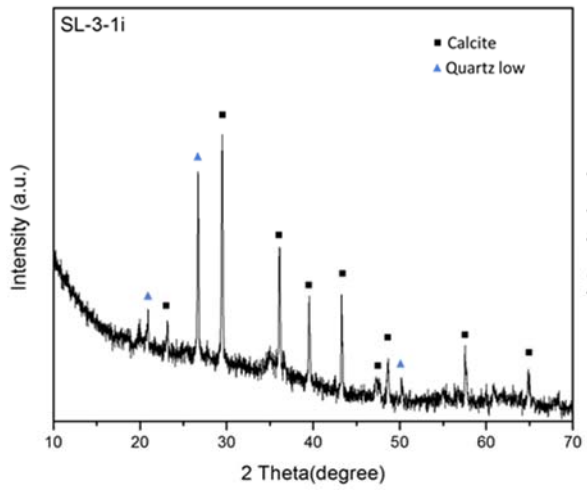
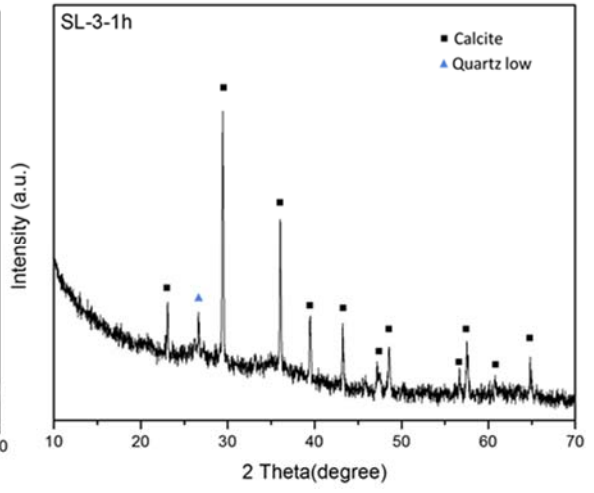
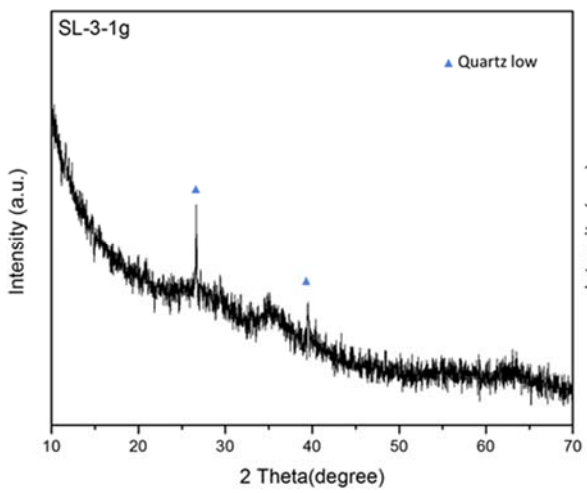
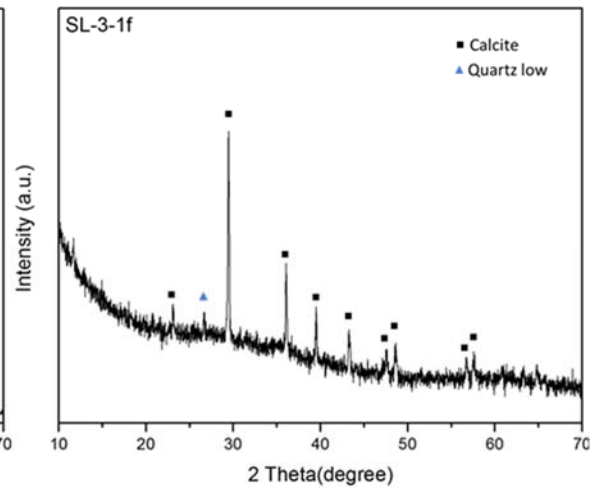
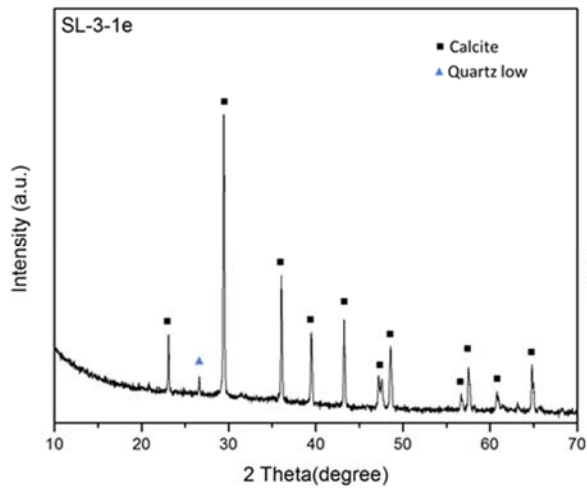


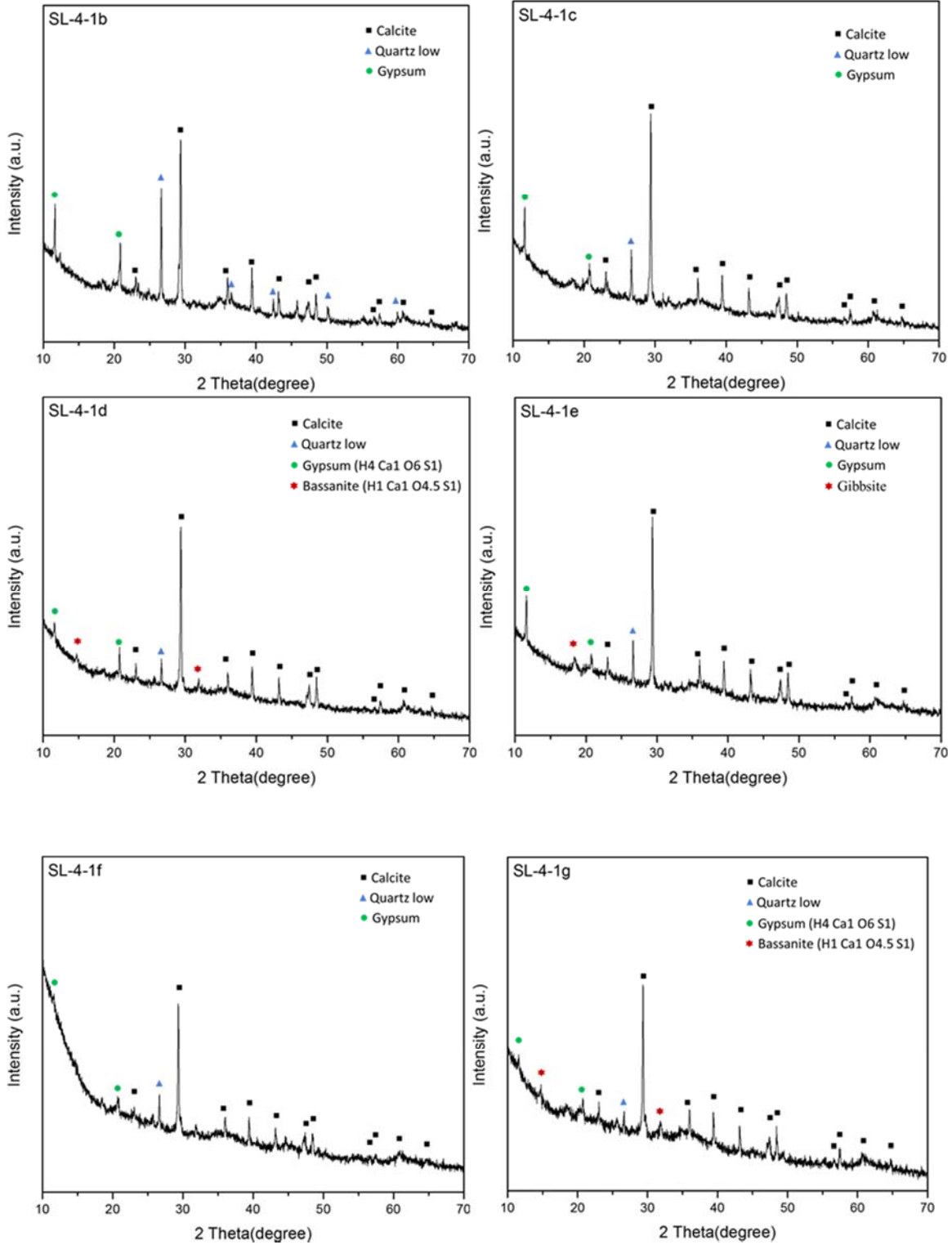


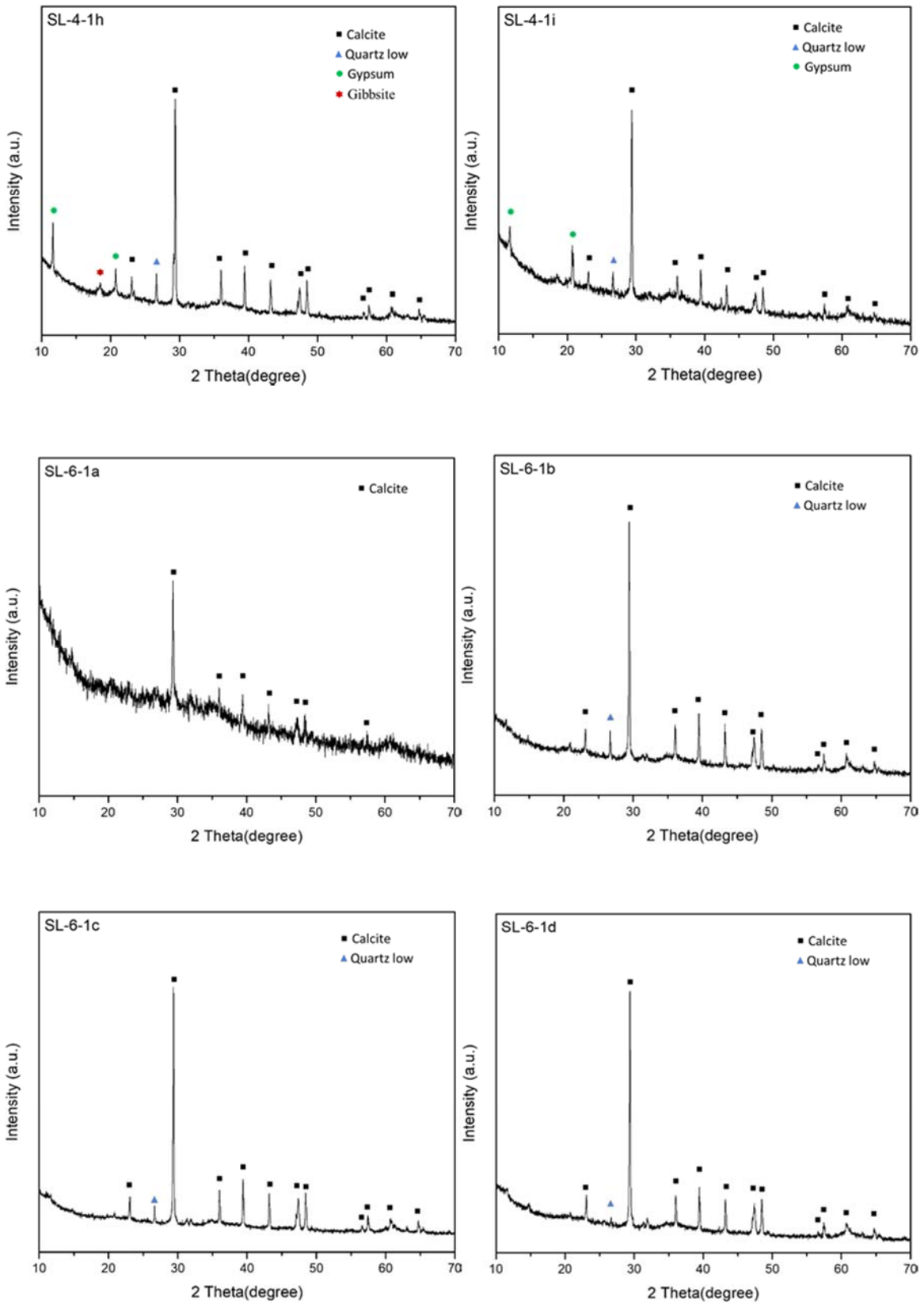


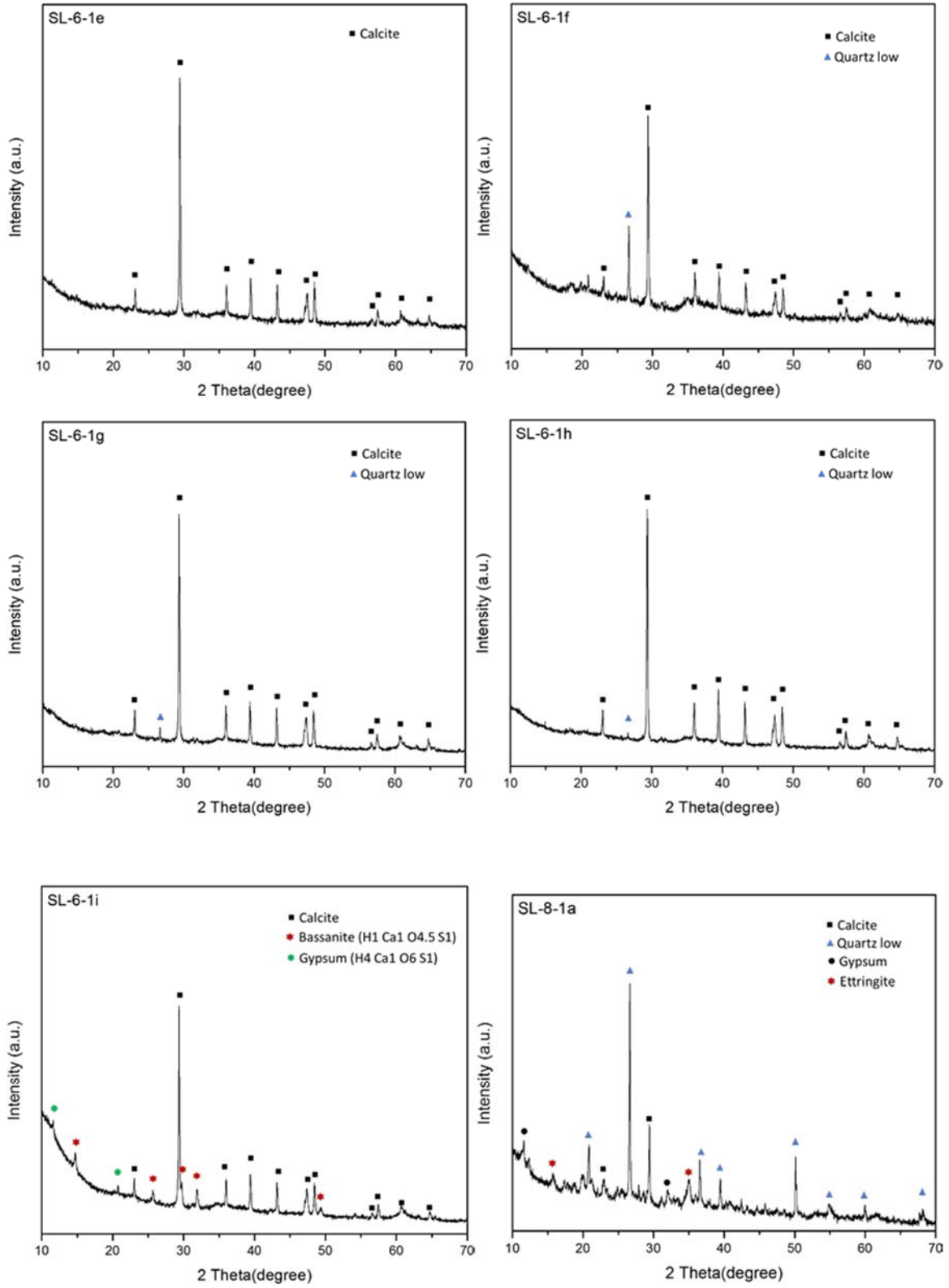


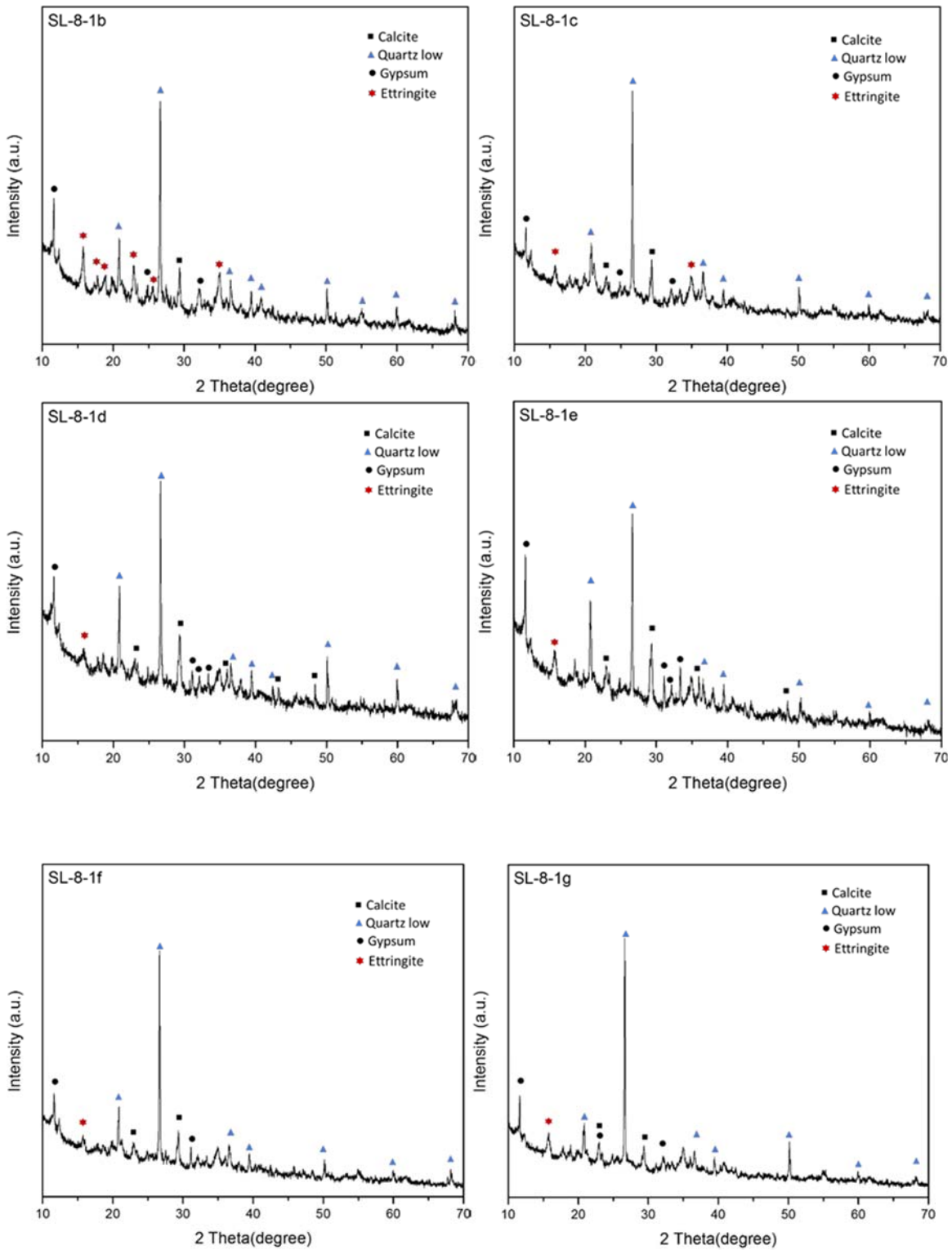


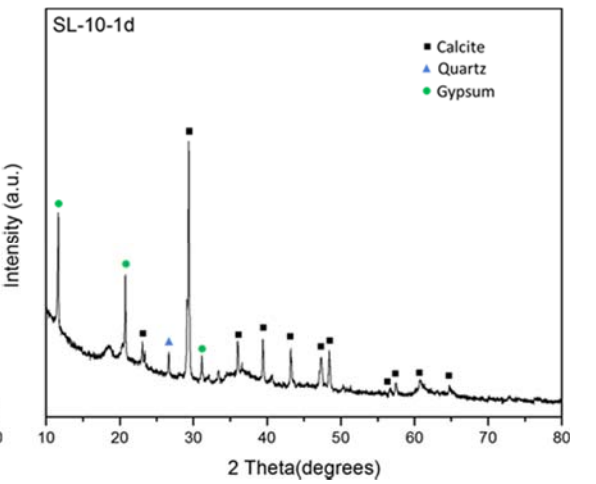
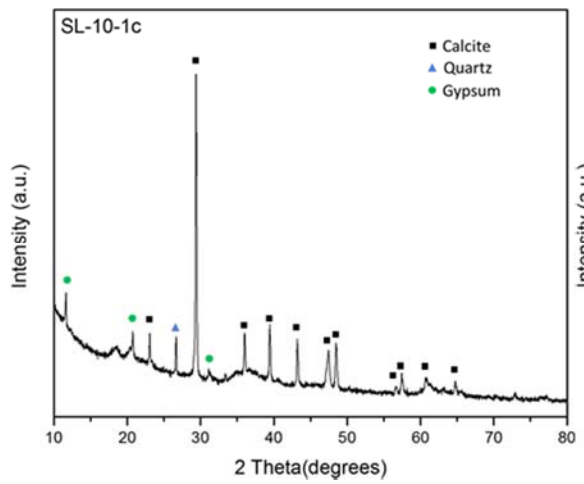
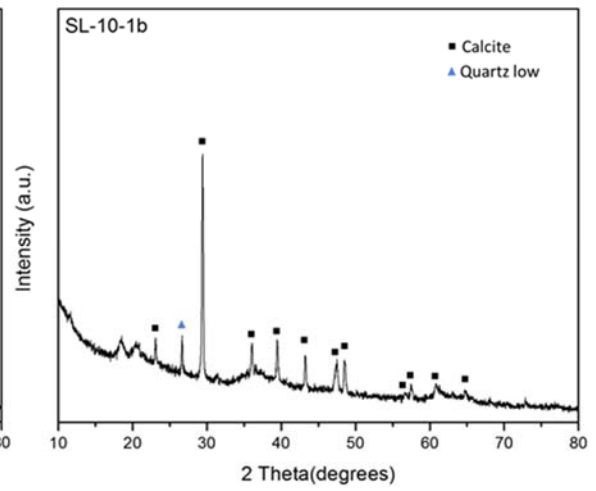
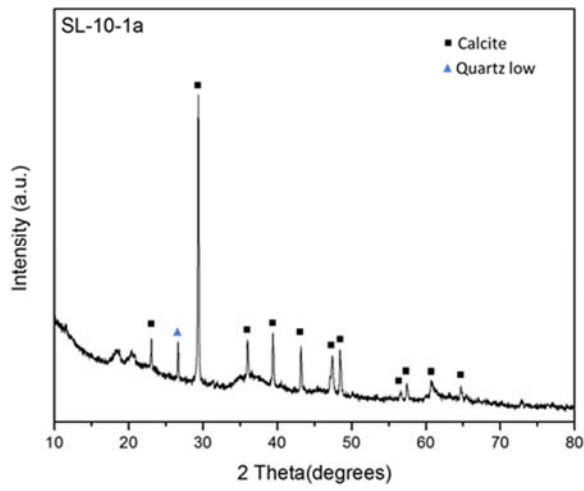
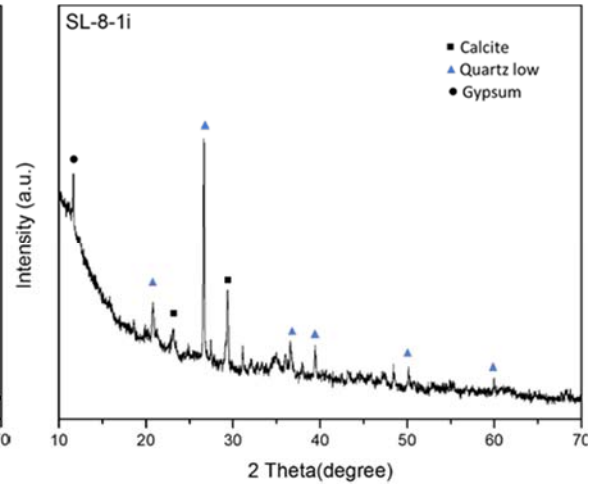
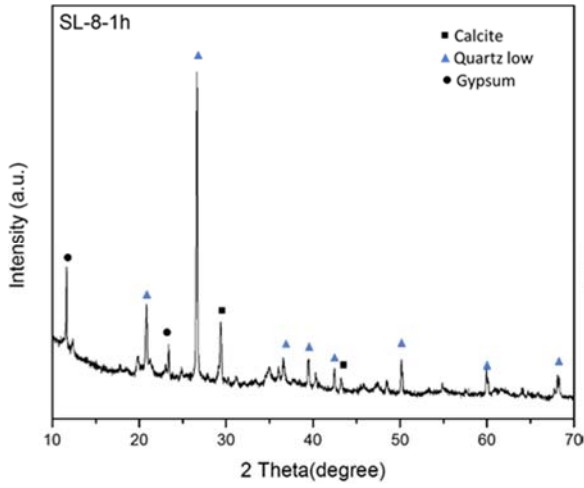


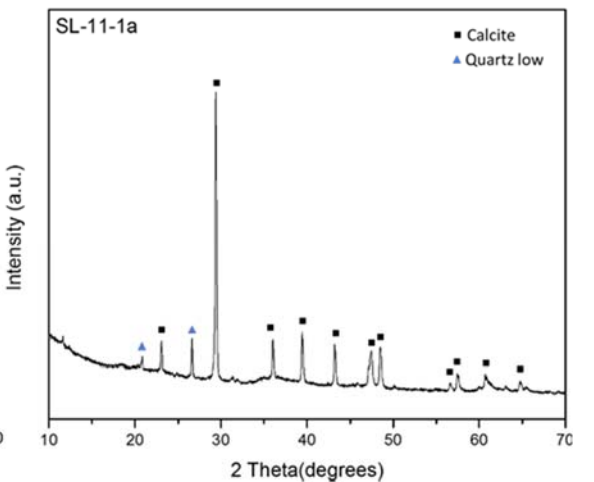
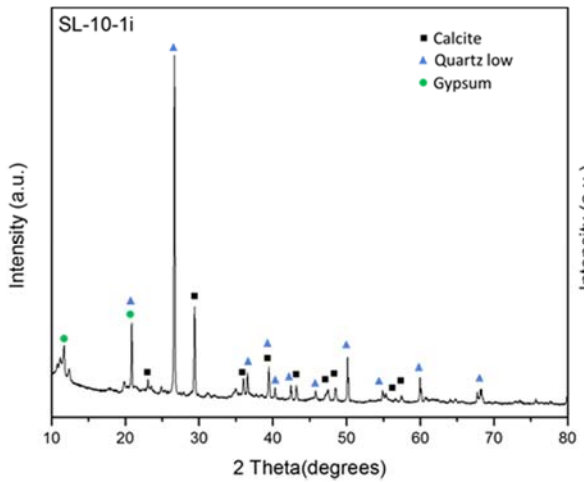
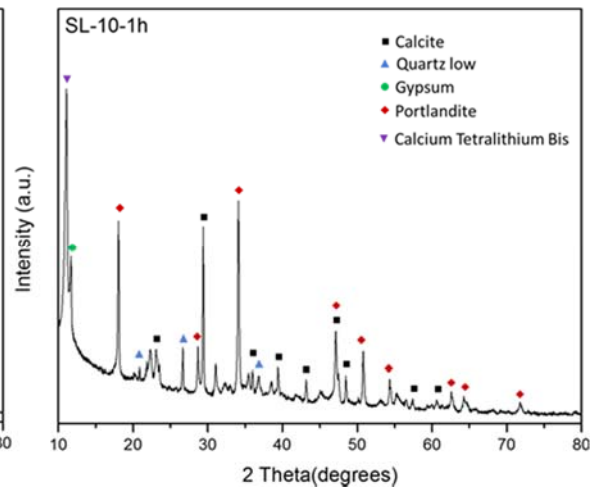
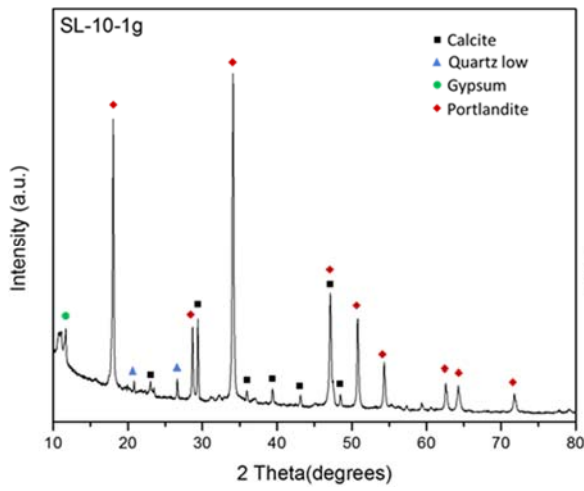
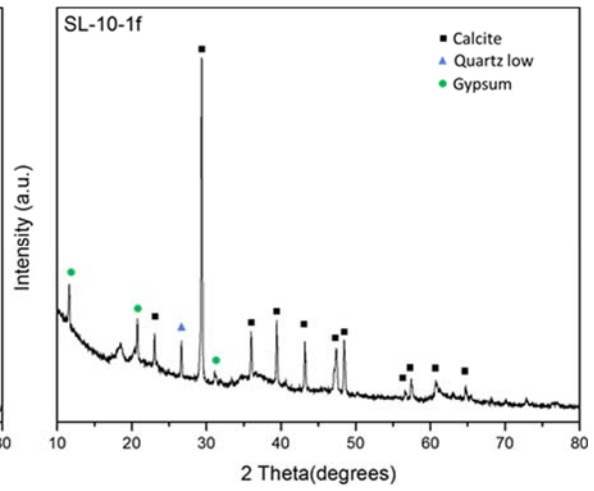
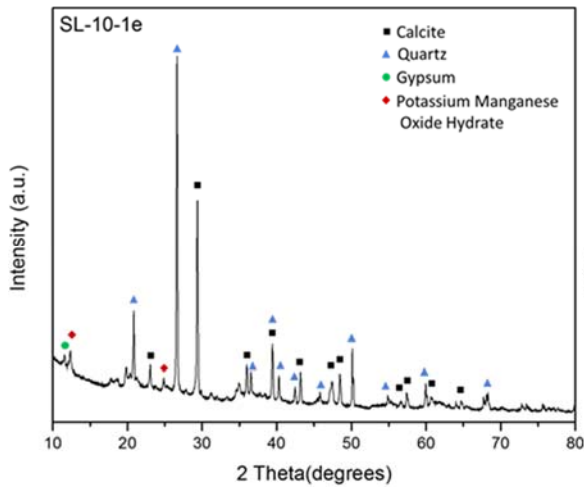


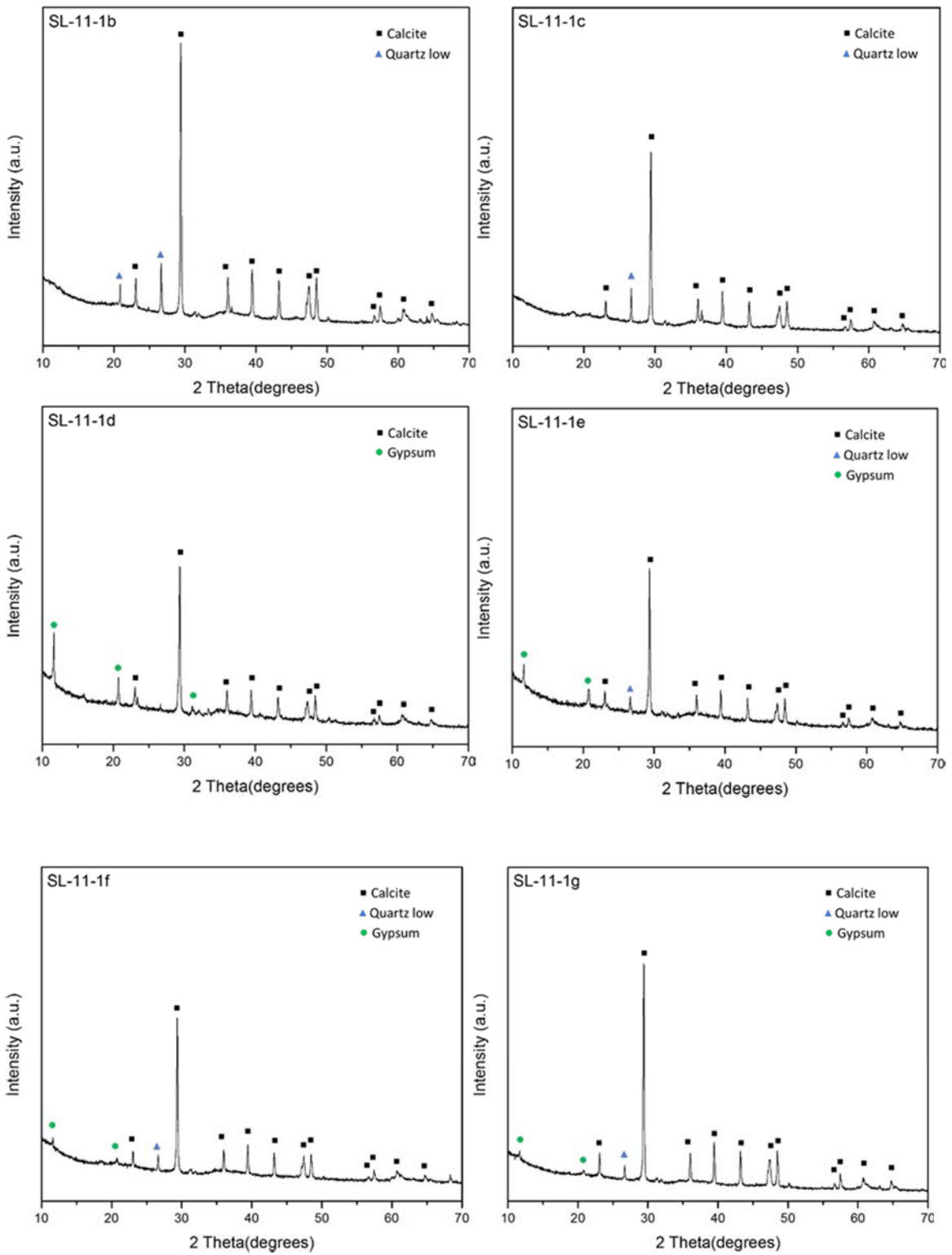


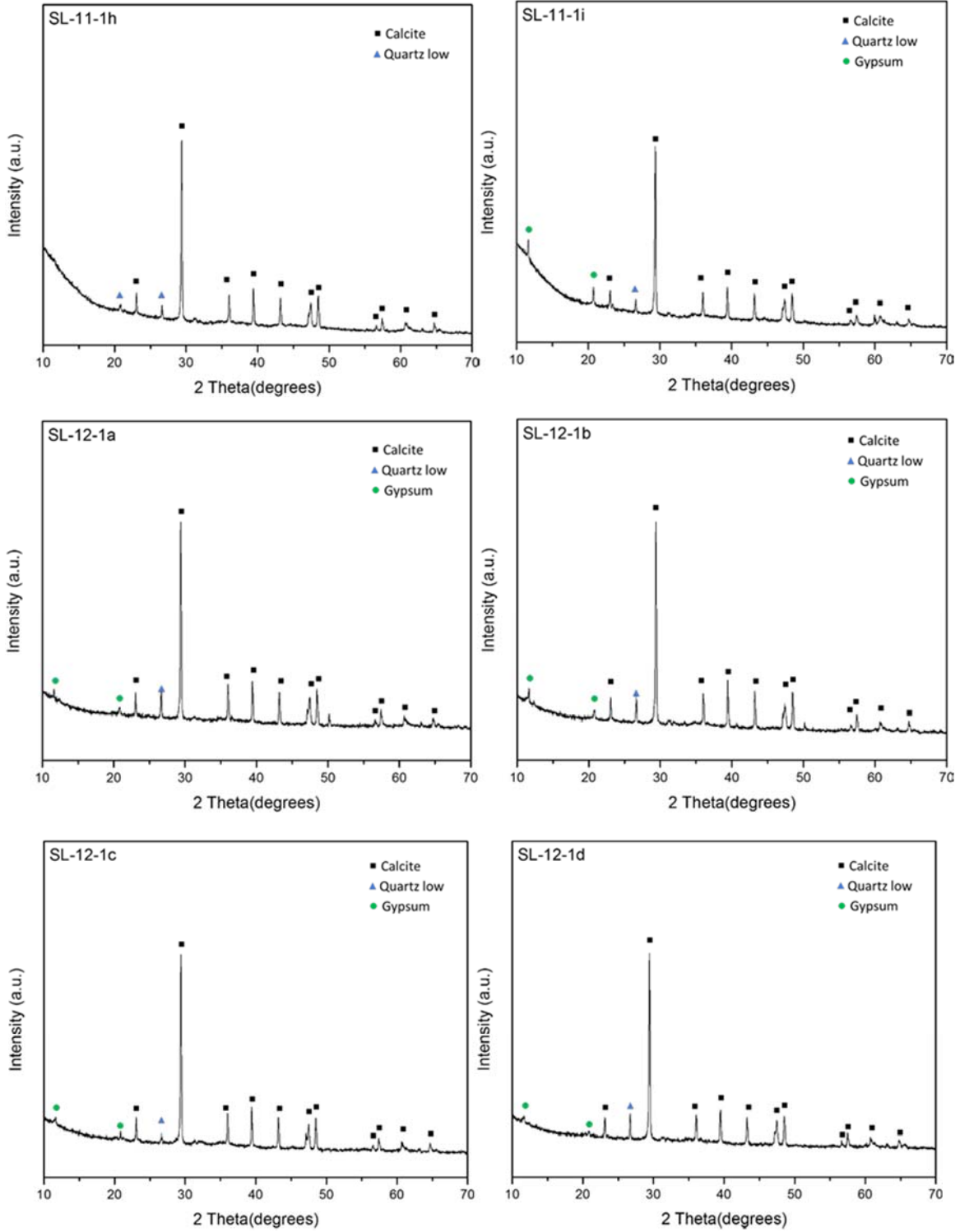


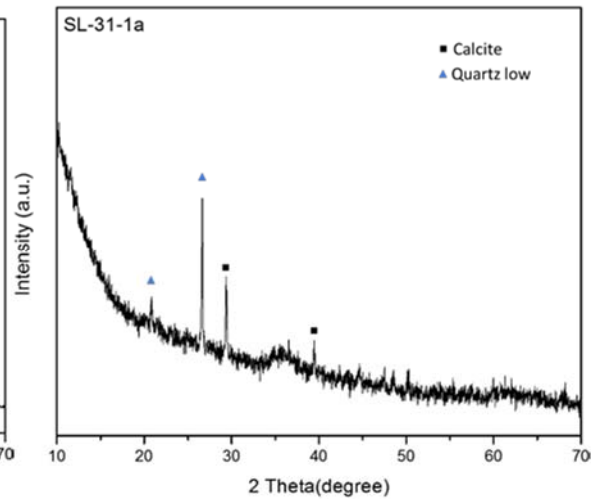
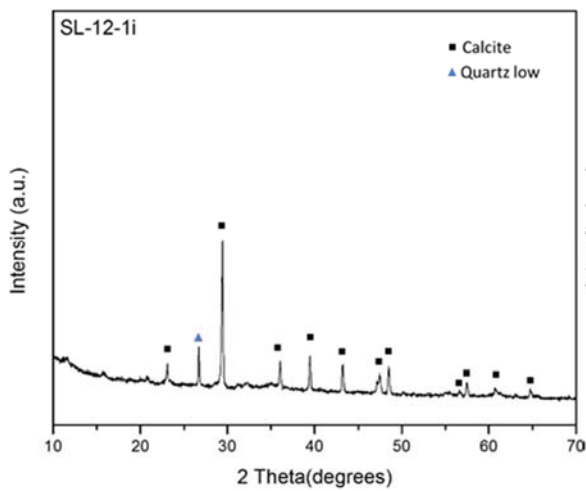
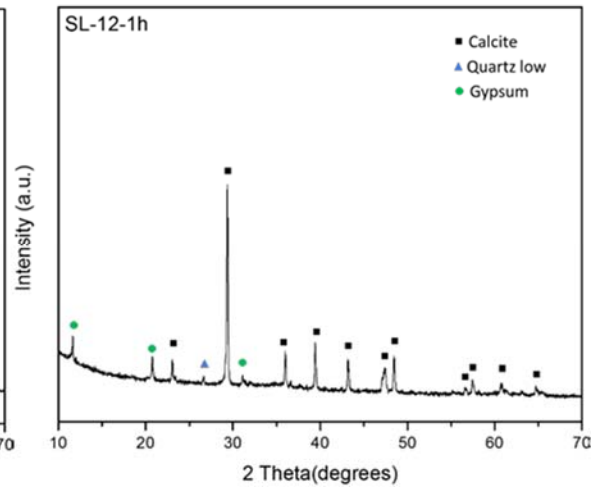
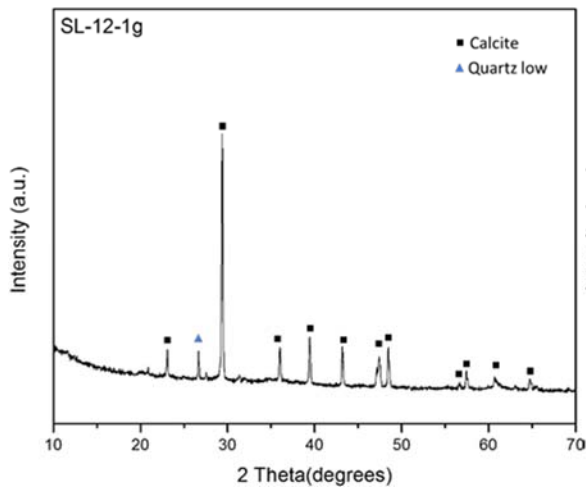
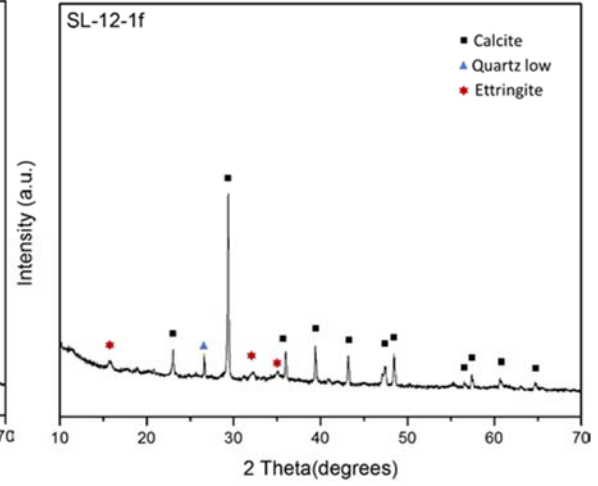
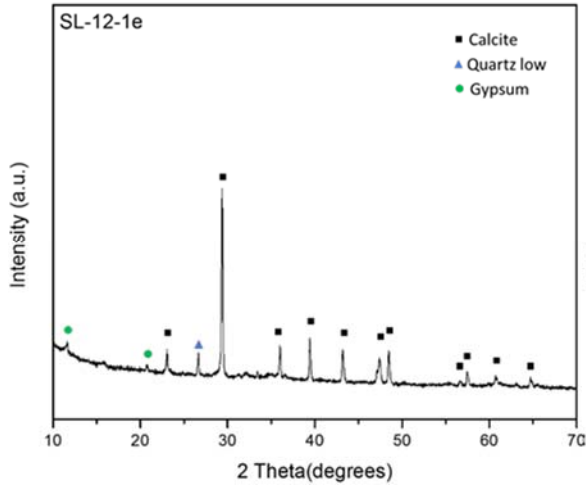


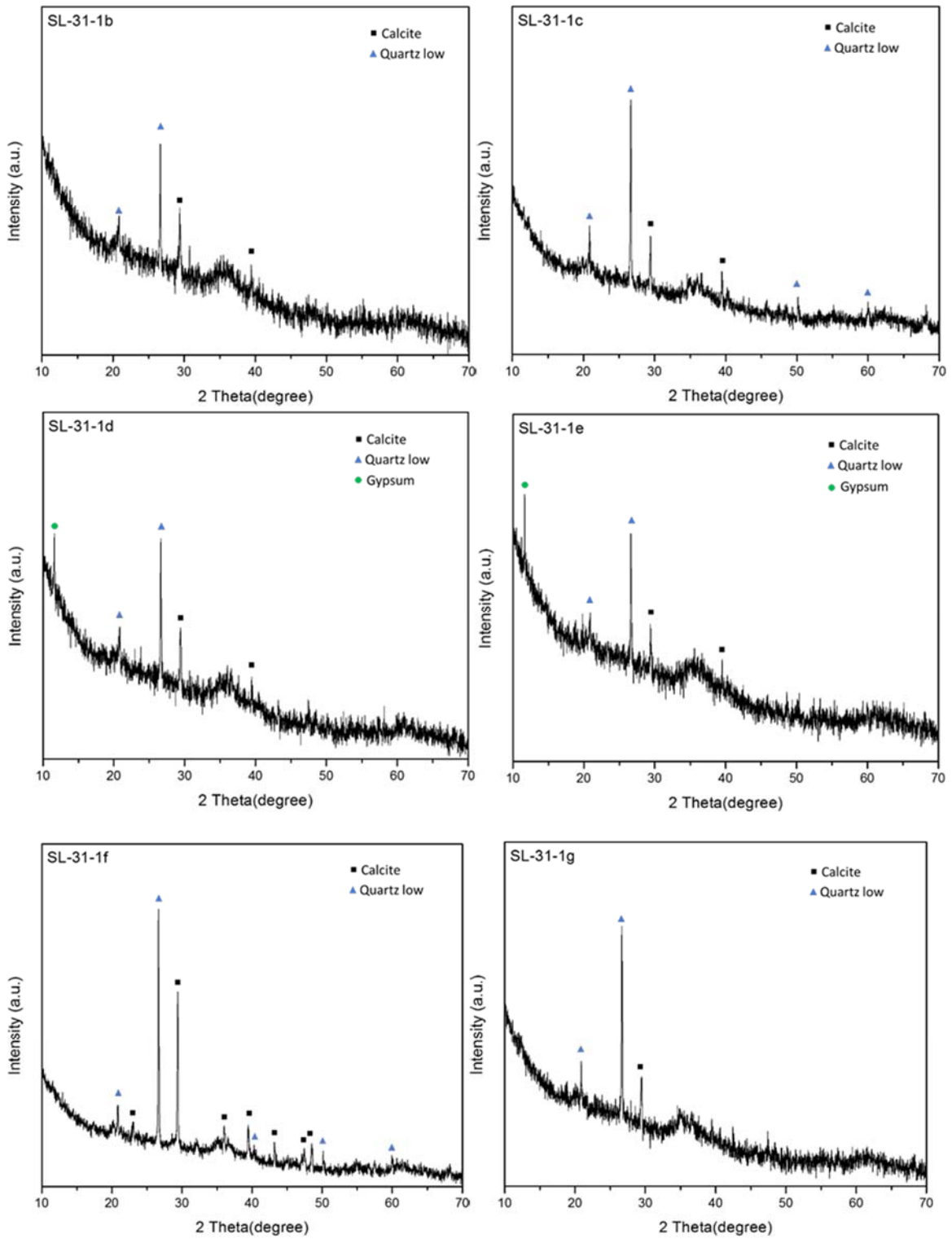


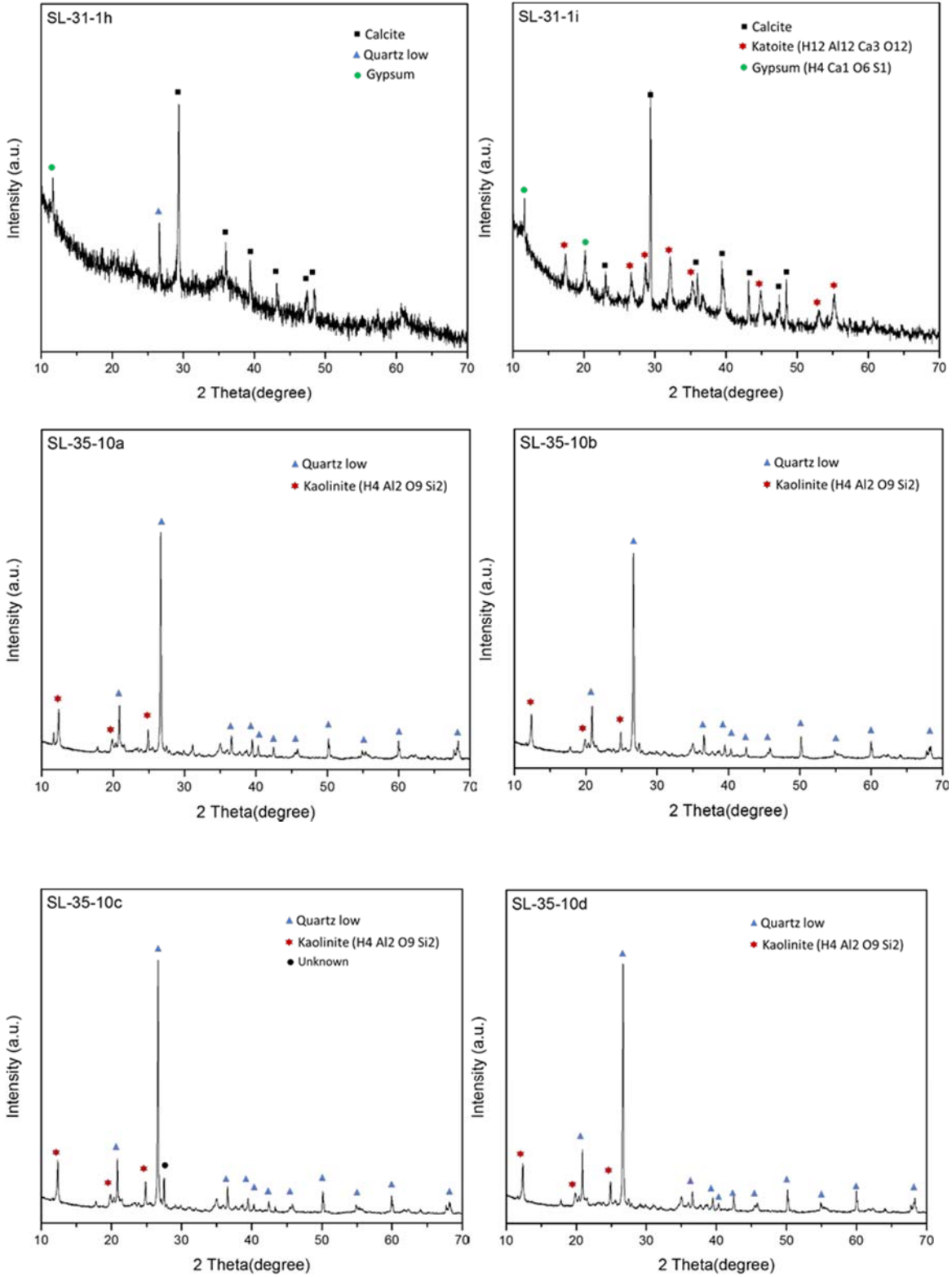


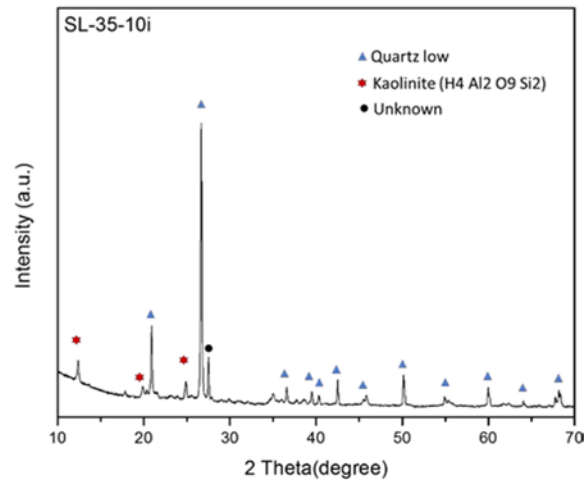
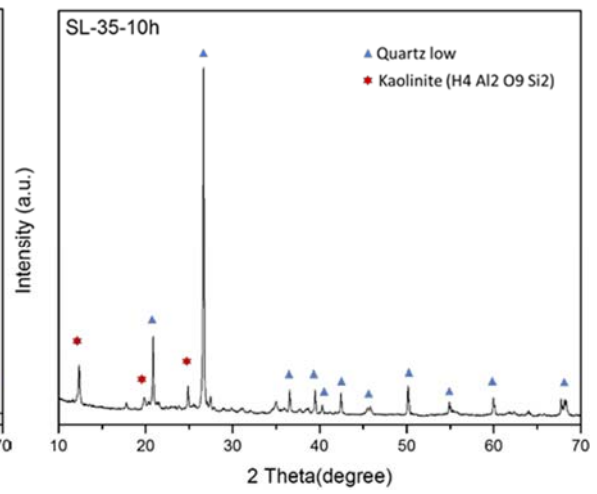
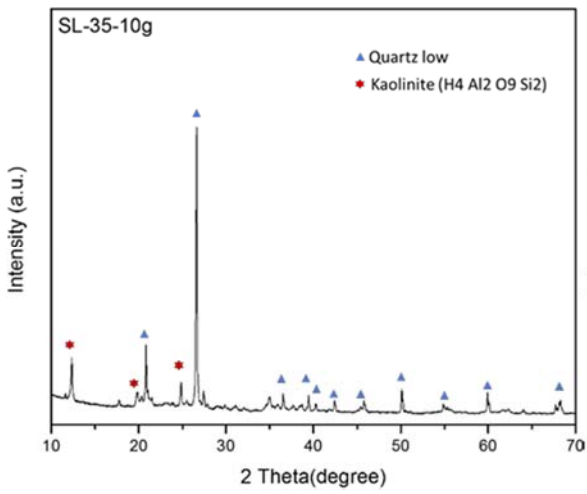
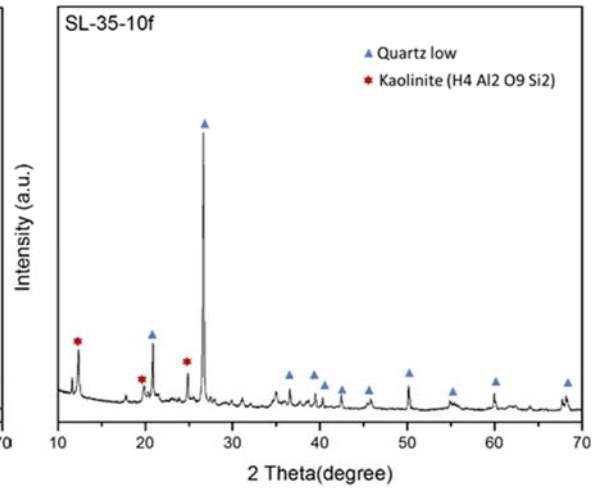
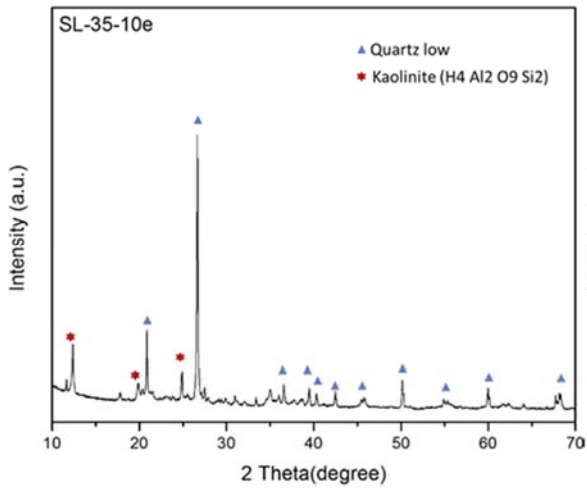












Appendix B: Identified patterns list of corresponding sludge samples.
Section B1: Identified patterns list of corresponding sludge samples shown in Section A1.

Sample ID	Ref. Code	Compound Name	Chemical Formula
SL-18-1	00-033-1161	Silicon Oxide	Si O2
	98-009-2816	Muscovite	H1.714 Al2.577 F0.285 Fe0.14 K0.858 Li0.13 Mg0.01 Na0.147 O11.715 Rb0.022 Si3.193
	96-702-0140	7020139	Ca6.00 C6.00 O18.00
	98-005-9233	Zinc Azide 2.5-hydrate	H5 N6 O2.5 Zn1
SL-20-1	98-042-3568	Calcium Carbonate	C1 Ca1 O3
	98-009-8628	Quartz low	O2 Si1
SL-21-5	96-702-0140	7020139	Ca6.00 C6.00 O18.00
SL-22-5	96-702-0140	7020139	Ca6.00 C6.00 O18.00
SL-23-1	98-016-1623	Gypsum	H4 Ca1 O6 S1
	98-042-3568	Calcium Carbonate	C1 Ca1 O3
	98-016-8354	Silicon Dioxide - Quartz	O2 Si1
SL-24-1	00-005-0586	Calcium Carbonate	Ca C O3
	00-005-0628	Sodium Chloride	Na Cl
SL-24-2	98-015-4750	Strontium Iron(III) Zinc Niobium Oxide (2/0.8/0.2/1/5.9)	Fe0.8 Nb1 O5.9 Sr2 Zn0.2
	98-040-8654	Potassium Hexabismuth Nonaoxide Bromide	Bi6 Br1 K1 O9
	98-026-1866	Cobalt Zinc Oxide (0.02/0.98/1)	Co0.02 O1 Zn0.98
SL-25-1	00-046-1045	Silicon Oxide	Si O2
	96-702-0140	7020139	Ca6.00 C6.00 O18.00
	96-705-2197	7052196	N6.02 H22.04 C12.00 O6.00

	96-222-3166	2-Aminopyridinium diphenylphosphinate monohydrate	P4.00 O12.00 C68.00 H76.00 N8.00
SL-26-2	98-002-0180	Calcite, cadmium	C1 Ca0.67 Cd0.33 O3
	98-002-9210	Quartz low	O2 Si1
	98-005-6090	Aragonite	C1 Ca1 O3
SL-2-2	98-016-8353	Silicon Dioxide - Quartz	O2 Si1
	98-003-1232	Potassium Chloride	Cl1 K1
SL-4-1	98-008-3849	Quartz low	O2 Si1
	98-016-6364	Calcite	C1 Ca1 O3
SL-8-1	98-009-0145	Quartz low	O2 Si1
	98-004-0544	Calcite	C1 Ca1 O3
	98-002-7039	Ettringite	H64 Al2 Ca6 O50 S3
	98-016-1624	Gypsum	H4 Ca1 O6 S1
SL-14-1	98-015-9972	Goethite	H1 Fe1 O2
SL-18-5	96-450-2442	4502441	Ca6.00 C6.00 O18.00
	98-008-3849	Quartz low	O2 Si1
SL-46-5	96-210-0190	2100189	Ca6.00 C6.00 O18.00
	98-016-8354	Silicon Dioxide - Quartz	O2 Si1
SL-47-1	96-901-0408	Goethite	Fe3.88 Co0.12 O8.00
SL-48-5	98-016-6364	Calcite	C1 Ca1 O3
	98-006-2405	Quartz low	O2 Si1
SL-6-1	98-042-3567	Calcium Carbonate	C1 Ca1 O3
	98-017-0539	Zeolite	O2 Si1
SL-10-1	96-900-0967	Calcite	Ca6.00 C6.00 O18.00

	98-002-7221	Gypsum	H4 Ca1 O6 S1
SL-12-1	98-042-3567	Calcium Carbonate	C1 Ca1 O3
	98-016-1623	Gypsum	H4 Ca1 O6 S1
	96-101-1030	Nitratine	Na6.00 N3.00 O18.00
SL-11-1	98-008-6163	Magnesium calcite	C1 Ca0.94 Mg0.06 O3
	98-002-7221	Gypsum	H4 Ca1 O6 S1
	98-006-2407	Quartz low	O2 Si1
SL-13-1	98-020-0725	Quartz low	O2 Si1
	96-900-3724	Bornite	Cu351.99 Fe70.41 S256.00
SL-16-1	--	--	--
SL-31-1	96-900-0575	Calcite	Ca5.40 Mg0.60 C6.00
	98-020-0726	Quartz low	O2 Si1
SL-30-raw	96-900-2160	Goethite	Fe4.00 H4.00 O8.00
SL-35-10	98-020-0723	Quartz low	O2 Si1
	96-150-4407	1504406	N16.00 C88.00 H64.00
	96-900-0368	Eucryptite	Si12.00 Al12.00 Li12.00 O48.00
SL-41-2	98-020-0723	Quartz low	O2 Si1
	96-150-4407	1504406	N16.00 C88.00 H64.00
SL-44-5	96-900-0575	Calcite	Ca5.40 Mg0.60 C6.00 O18.00
	98-006-2409	Quartz low	O2 Si1
SL-45-1	98-006-2406	Quartz low	O2 Si1
	98-003-7195	Huanghoite-(Ce)	C2 Ba1 Ce1 F1 O6
	96-900-1299	Calcite	Ca5.23 Mg0.77 C6.00 O18.00
SL-5-1	98-002-8941	Sylvine, sodian	Cl1 K0.6165 Na0.3835

SL-21-1	96-901-0410	Goethite	Fe3.72 Co0.28 O8.00
SL-33-1	98-016-9890	Aragonite	C1 Ca1 O3
	98-008-3849	Quartz low	O2 Si1
	98-009-4742	Hatnurite	Ca3 O5 Si1
	98-009-6606	Sodium Manganese Oxide Hydrate	H1.088 Mn1 Na0.364 O2.544
SL-35-1	98-007-3468	Portlandite	H2 Ca1 O2
	98-007-7086	Brucite	H2 Mg1 O2
	98-003-9830	Silicon Oxide - Alpha	O2 Si1
	98-016-4935	Calcite	C1 Ca1 O3
SL-43-1	98-015-8616	Berlinite	Al1 O4 P1
	96-432-1789	4321788	W0.06 Cu0.06 F1.64 O0.66 N1.26 C9.36
	98-007-5379	Copper Cobalt Diphosphate(V)	Co1 Cu1 O7 P2
SL-43-5	98-006-2406	Quartz low	O2 Si1
	98-005-5568	Bismuth Lanthanum Strontium Oxide	Bi1 La0.84 O5.724 Sr2.16
	98-003-7195	Huanghoite-(Ce)	C2 Ba1 Ce1 F1 O6
SL-46-1	98-001-0405	Calcite, magnesian	C1 Ca0.9 Mg0.1 O3
	98-006-2408	Quartz low	O2 Si1
	98-003-3690	Lithiophorite	H42 Al14 Li6 Mn21 O84
SL-48-1	98-020-0726	Quartz low	O2 Si1
	98-006-8175	Hiortdahlite II	Ca9.48 F5 Na2.76 O31 Si8 Y1.76 Zr2
	98-000-9860	Iron Carbide	C0.63 Fe4
SL-49-1	96-900-0575	Calcite	Ca5.40 Mg0.60 C6.00 O18.00
	98-024-0999	Boron Nitride	B1 N1

SL-51-5	98-020-0722	Quartz low	O2 Si1
	98-003-3690	Lithiophorite	H42 Al14 Li6 Mn21 O84
SL-54-5	96-900-0575	Calcite	Ca5.40 Mg0.60 C6.00 O18.00
	98-020-0725	Quartz low	O2 Si1
	96-220-4392	Di(ethylenediamineK2N,N'^^)(thiosulfato\KS) copper(II)	Cu4.00 N16.00 H64.00 O12.00 S8.00 C16.00
SL-56-1	96-900-0575	Calcite	Ca5.40 Mg0.60 C6.00 O18.00
SL-57-2	98-020-0725	Quartz low	O2 Si1
	98-016-2614	Cristobalite alpha	O2 Si1
	98-020-2603	Potassium Beryllium Phosphate	Be1 K1 O4 P1
	96-200-2922	(1,4-diaminobenzene).(2,6-dihydroxynaphthalene)	O4.00 H32.00 C32.00 N4.00
SL-58-5	98-009-8628	Quartz low	O2 Si1
	96-900-0575	Calcite	Ca5.40 Mg0.60 C6.00 O18.00
	98-008-2444	Magnetite	Fe2.937 O4
SL-2-5	98-006-2405	Quartz low	O2 Si1
	96-705-2197	7052196	N6.02 H22.04 C12.00 O6.00
SL-9-1	96-101-1160	Quartz low	Si6.00 O6.00
	98-007-9674	Calcite	C1 Ca1 O3
SL-15-1	00-046-1045	Silicon Oxide	Si O2
	96-901-2818	Friedelite	Mn32.00 Si24.00 O96.00 Cl4.00
SL-30-1	98-001-0405	Calcite, magnesian	C1 Ca0.9 Mg0.1 O3
	98-006-2405	Quartz low	O2 Si1
SL-37-1	98-006-9060	Bassanite	H1 Ca1 O4.5 S1
	98-002-8275	Brucite	H2 Mg1 O2

	98-016-9914	Calcite	C1 Ca1 O3
	98-024-5581	Portlandite	D2 Ca1 O2
	00-046-1045	Silicon Oxide	Si O2
SL-50-1	96-900-9667	Quartz	Si3.00 O6.00
	98-015-8445	Magnesioferrite	Fe2 Mg1 O4
SL-64-2	98-015-8962	Quartz low	O2 Si1
	98-020-0725	Tychite	C4 Mg2 Na6 O16 S1
SL-66-1	98-009-0145	Quartz low	O2 Si1
	98-020-0413	Bayerite	D3 Al1 O3
	98-009-4742	Hatrumite	Ca3 O5 Si1
	98-009-7199	Birnessite (Na-rich)	H3 Mn2 Na0.58 O5.5
SL-67-1	98-009-0145	Quartz low	O2 Si1
SL-72-P	98-016-1623	Gypsum	H4 Ca1 O6 S1
	98-004-0112	Calcite	C1 Ca1 O3
	98-002-7826	Quartz low	O2 Si1
SL-73-p	98-015-9970	Goethite	H1 Fe1 O2
SL-78-1	98-001-6332	Quartz low	O2 Si1
	96-900-3078	Goethite	Fe4.00 O8.00
SL-79-1	98-010-0341	Quartz low	O2 Si1
	98-004-0107	Calcite	C1 Ca1 O3
	98-008-5570	Richetite	H106 Fe0.47 Mg0.83 O173 Pb8.74 U36
	98-024-0832	Magnesioferrite	Fe2 Mg1 O4
SL-80-1	98-004-0112	Calcite	C1 Ca1 O3

	98-006-2404	Quartz low	O2 Si1
	98-018-5049	Dolomite	C2 Ca1 Mg1 O6
	98-015-2289	Birnessite	H0.8 K0.296 Mn0.926 O2.4
	96-210-2324	2102323	C96.00 H192.00
	98-015-8443	Magnesioferrite	Fe2 Mg1 O4
SL-80-2	98-004-0544	Calcite	C1 Ca1 O3
	98-008-3849	Quartz low	O2 Si1
	98-017-1518	Dolomite	C2 Ca1 Mg1 O6
	98-015-8443	Magnesioferrite	Fe2 Mg1 O4
	98-015-2289	Birnessite	H0.8 K0.296 Mn0.926 O2.4
	96-210-2324	2102323	C96.00 H192.00
SL-81-2	98-008-3849	Quartz low	O2 Si1
SL-82-1	96-101-1160	Quartz low	Si6.00 O6.00
	98-016-4813	Magnetite	Fe3 O4
	98-015-6189	Birnessite, barian	H1.776 Ba0.29 Mn2 O4.888
SL-83-1	96-901-0407	Goethite	Fe4.00 O8.00
	98-016-8355	Silicon Dioxide - Quartz	O2 Si1
SL-85-1	96-901-1413	Goethite	Fe4.00 O8.00
	98-006-2404	Quartz low	O2 Si1
SL-86-1	98-003-9830	Silicon Oxide - Alpha	O2 Si1
	98-024-0372	Dimethyltindiaquadimolybdate Hydrate	C2 H12 Mo2 O10 Sn1
SL-87-1	98-004-0107	Calcite	C1 Ca1 O3
	98-015-7995	Aragonite	C1 Ca1 O3

	00-033-1161	Silicon Oxide	Si O2
SL-87-5	98-004-0107	Calcite	C1 Ca1 O3
	98-015-4289	Quartz	O2 Si1
	98-016-9892	Aragonite	C1 Ca1 O3
SL-88-1	98-016-6364	Calcite	C1 Ca1 O3
	98-006-2405	Quartz low	O2 Si1
SL-91-2	00-033-1161	Silicon Oxide	Si O2
	98-015-8444	Magnesioferrite	Fe2 Mg1 O4
SL-95-1	98-006-2405	Quartz low	O2 Si1
	98-015-8445	Magnesioferrite	Fe2 Mg1 O4
SL-100-1	98-042-3567	Calcium Carbonate	C1 Ca1 O3
	96-900-2159	Goethite	Fe4.00 H4.00 O8.00
SL-102-20	98-002-7826	Quartz low	O2 Si1
	98-001-6710	Calcite	C1 Ca1 O3
SL-103-1	98-018-4786	Goethite	H1 Fe1 O2
	96-101-0603	Boron nitride	B2.00 N2.00
	98-009-4742	Hatrumite	Ca3 O5 Si1
SL-104-1	98-018-4786	Goethite	H1 Fe1 O2
	96-101-0603	Boron nitride	B2.00 N2.00
	98-009-4742	Hatrumite	Ca3 O5 Si1
	98-015-0374	Boron Phosphate(V)	B1 O4 P1
SL-106-1	98-009-3974	Quartz low	O2 Si1
	98-015-9962	Goethite	H1 Fe1 O2

SL-107-1	98-008-3849	Quartz low	O2 Si1
	98-007-1810	Goethite	H1 Fe1 O2
SL-108-1	98-007-7327	Goethite	H1 Fe1 O2
SL-108-10	98-007-7327	Goethite	H1 Fe1 O2
SL-109-1	98-003-7156	Goethite	H1 Fe1 O2
	98-020-0721	Quartz low	O2 Si1
SL-112-1	98-024-5057	Goethite	H1 Fe1 O2
	98-009-4742	Hatrurite	Ca3 O5 Si1
SL-113-2	98-042-3568	Calcium Carbonate	C1 Ca1 O3
SL-114-1	98-004-1412	Quartz low	O2 Si1
	96-900-4709	Keilite	Fe2.23 Mg1.28 Mn0.19 Ca0.15 Cr0.12 Zn0.01 Ti0.00 S4.00
	98-015-2288	Birnessite	H0.84 K0.296 Mn0.926 O2.42
	98-041-3106	Cadmium Cyanide	C2 Cd1 N2
SL-115-1	98-009-0145	Quartz low	O2 Si1
SL-116-1	98-042-3568	Calcium Carbonate	C1 Ca1 O3
SL-90-1	98-002-7833	Quartz low	O2 Si1
	98-016-9925	Calcite	C1 Ca1 O3
	98-004-1479	Siloxene	H2 O1 Si2
SL-91-1	98-004-2498	Quartz high	O2 Si1
	98-016-9925	Calcite	C1 Ca1 O3
	96-410-4960	4104959	Cu48.00 O192.00 C398.64 H96.00 D110.62
SL-92-2	98-006-2404	Quartz low	O2 Si1
	98-008-5807	Magnetite	Fe3 O4

SL-93-2	96-900-5018	Quartz	Si6.00 O6.00
	96-705-2197	7052196	N6.02 H22.04 C12.00 O6.00
	98-015-8442	Magnesioferrite	Fe2 Mg1 O4
SL-94-5	00-033-1161	Silicon Oxide	Si O2
	98-001-8166	Calcite	C1 Ca1 O3
	98-003-2100	Aragonite	C1 Ca1 O3
	98-004-0091	Wroewolfeite	H10 Cu4 O12 S1
	96-900-9998	Connellite	Cu15.00 Cl1.65 O56.97 N0.04 S0.11
SL-95-2	96-500-0036	Quartz	Si3.00 O6.00
SL-96-1	96-500-0036	Quartz	Si3.00 O6.00
SL-97-5	98-004-0107	Calcite	C1 Ca1 O3
	98-015-6196	Quartz	O2 Si1
SL-98-1	98-042-3567	Calcium Carbonate	C1 Ca1 O3
	00-046-1045	Silicon Oxide	Si O2
SL-110-1	98-007-7327	Goethite	H1 Fe1 O2
	98-004-0107	Calcite	C1 Ca1 O3
SL-111-1	98-015-9972	Goethite	H1 Fe1 O2
	---	Unknown	---
SL-117-1	98-008-3849	Quartz low	O2 Si1
	96-900-7690	Calcite	Ca6.00 C6.00 O18.00
SL-118-2	96-101-1160	Quartz low	Si6.00 O6.00
	98-006-9060	Bassanite	H1 Ca1 O4.5 S1
SL-119-1	96-900-0096	Calcite	Ca6.00 C6.00 O18.00
	98-007-9198	Brucite	H2 Mg1 O2

	98-003-9830	Silicon Oxide - Alpha	O2 Si1
	98-020-2224	Portlandite	H2 Ca1 O2

Section B2: Identified patterns list of corresponding sludge samples shown in Section A2.

Sample ID	Ref. Code	Compound Name	Chemical Formula
SL-2-2a	98-002-9122	Quartz low	Si O2
SL-2-2b	00-046-1045	Silicon Oxide	Si O2
	98-015-6187	Birnessite, sodian	H2.76 Mn2 Na0.58 O5.38
	96-901-0154	Keilite	Fe1.75Mn1.42Mg0.64 Ca0.07 Cr0.08 Zn0.00 S4.00
SL-2-2c	98-004-2498	Quartz high	O2 Si1
SL-2-2d	00-046-1045	Silicon Dioxide	Si O2
	98-018-0735	Birnessite, sodian	H1 D2 Mn2 Na0.6 O5.5
	98-041-3106	Cadmium Cyanide	C2 Cd1 N2
	96-900-4709	Keilite	Fe2.23Mg1.28Mn0.19 Ca0.15Cr0.12 Zn0.01 Ti0.00 S4.00
SL-2-2e	98-006-2405	Quartz low	Si O2
SL-2-2f	98-006-2405	Quartz low	Si O2
SL-2-2g	98-016-8355	Silicon Dioxide - Quartz	O2 Si1
	98-015-2288	Birnessite	H0.84 K0.296 Mn0.926 O2.42
	98-041-3106	Cadmium Cyanide	C2 Cd1 N2
	96-900-4709	Keilite	Fe2.23Mg1.28Mn0.19 Ca0.15Cr0.12 Zn0.01 Ti0.00 S4.00
SL-2-2h	00-046-1045	Silicon Dioxide	Si O2
	98-018-0735	Birnessite, sodian	H1 D2 Mn2 Na0.6 O5.5
	98-041-3106	Cadmium Cyanide	C2 Cd1 N2
	96-900-4709	Keilite	Fe2.23Mg1.28Mn0.19 Ca0.15 Cr0.12 Zn0.01 Ti0.00 S4.00
	98-015-2288	Birnessite	H0.84 K0.296 Mn0.926 O2.42
SL-2-2i	98-004-2498	Quartz high	Si O2
SL-2-5a,b, c,d,e,f,g,h,i	98-008-3849	Quartz low	Si O2
SL-3-1a, b, d, g	98-003-7241	Calcite	C1 Ca1 O3
SL-3-1c, e, f, h, i	98-003-7241	Calcite	C1 Ca1 O3
	98-008-3849	Quartz low	O2 Si1

SL-4-1b, c, f, i	98-004-0112	Calcite	C1 Ca1 O3
	98-004-0009	Quartz low	O2 Si1
	98-002-7221	Gypsum	H4 Ca1 O6 S1
SL-4-1a, d, g	98-004-0112	Calcite	C1 Ca1 O3
	98-004-0009	Quartz low	O2 Si1
	98-002-7221	Gypsum	H4 Ca1 O6 S1
	98-007-3263	Bassanite	H1 Ca1 O4.5 S1
SL-4-1e, h	98-004-0112	Calcite	C1 Ca1 O3
	98-004-0009	Quartz low	O2 Si1
	98-002-7221	Gypsum	H4 Ca1 O6 S1
	98-003-6233	Gibbsite	H3 Al1 O3
SL-6-1a,e	98-016-4935	Calcite	C1 Ca1 O3
SL-6-1b,c,d,f,g,h	98-004-0112	Calcite	C1 Ca1 O3
	98-004-0009	Quartz low	O2 Si1
SL-6-1i	98-004-0112	Calcite	C1 Ca1 O3
	98-007-9528	Bassanite	H1 Ca1 O4.5 S1
	98-003-6186	Gypsum	H4 Ca1 O6 S1
SL-8-1a,b,c,d,e,f,g	98-020-0721	Quartz low	O2 Si1
	98-015-5395	Ettringite	H64 Al2 Ca6 O50 S3
	98-002-7221	Gypsum	H4 Ca1 O6 S1
	98-015-8258	Calcite	C1 Ca1 O3
SL-8-1h,i	98-020-0721	Quartz low	O2 Si1
	98-015-8258	Calcite	C1 Ca1 O3
	98-002-7221	Gypsum	H4 Ca1 O6 S1
SL-10-1a	96-900-9668	Calcite	Ca6.00 C6.00 O18.00
	98-001-6331	Quartz low	Si O2
SL-10-1b	98-016-6364	Calcite	C1 Ca1 O3
	98-002-7833	Quartz low	Si O2
SL-10-1c	98-016-6364	Calcite	C1 Ca1 O3
	96-900-9667	Quartz	Si3.00 O6.00
	96-900-6647	Gypsum (deuterated)	Ca8.00 S8.00 O24.00 D16.00
SL-10-1d	98-016-9913	Calcite	C1 Ca1 O3
	96-900-6647	Gypsum (deuterated)	Ca8.00 S8.00 O24.00 D16.00
	98-015-6198	Quartz	O2 Si1
SL-10-1e	98-015-6198	Quartz	O2 Si1
	98-004-0112	Calcite	C1 Ca1 O3
	98-008-1367	Potassium Manganese Oxide Hydrate	H1.08 K0.27 Mn1 O2.54
	98-040-9581	Gypsum	H4 Ca1 O6 S1
SL-10-1f	98-016-9913	Calcite	C1 Ca1 O3
	98-008-3849	Quartz low	O2 Si1
	98-040-9581	Gypsum	H4 Ca1 O6 S1

SL-10-1g	98-007-9674	Calcite	C1 Ca1 O3
	96-101-1075	Gypsum	S4.00 Ca4.00 O24.00 H0.00
	98-020-2220	Portlandite	H2 Ca1 O2
	98-009-3094	Quartz low	O2 Si1
SL-10-1h	98-015-8257	Calcite	C1 Ca1 O3
	98-020-2220	Portlandite	H2 Ca1 O2
	98-016-2610	Quartz low	O2 Si1
	96-101-1075	Gypsum	S4.00 Ca4.00 O24.00 H0.00
	98-025-0215	Calcium Tetralithium Bis (dihydroxooctaoxopentaborate)	H4 B10 Ca1 Li4 O20
SL-10-1i	98-008-3849	Quartz low	Si O2
	96-900-9668	Calcite	Ca6.00 C6.00 O18.00
	98-040-9581	Gypsum	H4 Ca1 O6 S1
SL-11-1a,b,c,h SL-12-1g,i	98-008-0869	Calcite	C1 Ca1 O3
	98-009-0145	Quartz low	O2 Si1
SL-11-1e, f, g, i SL-12-1a, b,c,d,e,h	98-008-0869	Calcite	C1 Ca1 O3
	98-009-0145	Quartz low	O2 Si1
	98-016-1623	Gypsum	H4 Ca1 O6 S1
SL-11-1d	98-008-0869	Calcite	C1 Ca1 O3
	98-016-1623	Gypsum	H4 Ca1 O6 S1
SL-12-1f	98-008-0869	Calcite	C1 Ca1 O3
	98-002-7039	Ettringite	H64 Al2 Ca6 O50 S3
SL-31- 1a,b,c,f,g	98-004-0112	Calcite	C1 Ca1 O3
	98-006-7117	Quartz low	O2 Si1
SL-31-1d,e,h	98-004-0112	Calcite	C1 Ca1 O3
	98-006-7117	Quartz low	O2 Si1
	98-008-1652	Gypsum	H4 Ca1 O6 S1
SL-31-1i	98-007-9674	Calcite	C1 Ca1 O3
	98-008-1652	Gypsum	H4 Ca1 O6 S1
	98-009-4631	Katoite	H12 Al12 Ca3 O12
SL-35-10a, b,d,e,f,g,h	98-008-3849	Quartz low	O2 Si1
	98-006-8698	Kaolinite 1A	H4 Al2 O9 Si2
SL-35-10c,i	98-008-3849	Quartz low	O2 Si1
	98-006-8698	Kaolinite 1A	H4 Al2 O9 Si2
	--	Unknown	--

Appendix C: Sample Site Information

										SM	surface mine
										REF	refuse
										UG	underground mine
										f	flooded
type	site code		Field notes, site name and location	state	county	seam	basin	source	treatment	chemical	
raw AMD/sludge	AQ/SL	1	WVDEP OSR Royal Scot Buc Lilly, Lat. 38.012191, Long. -80.604779	WV	Greenbrier	Poca 3-6, BECKLEY, Firecreek, SEWELL, LITTLE RALEIGH	CAPP	REF	Active	NaOH	
raw AMD/sludge	AQ/SL	1	WVDEP OSR Royal Scot Buc Lilly, Lat. 38.012191, Long. -80.604779	WV	Greenbrier	Poca 3-6, BECKLEY, Firecreek, SEWELL, LITTLE RALEIGH	CAPP	REF	Active	NaOH	
raw AMD/sludge	AQ/SL	2	WVDEP OSR Omega, Lat. 39.533042, Long. -79.939871	WV	Monongalia	Upper Freeport	NAPP	UG f	Active	Ca(OH)2	
raw AMD/sludge	AQ/SL	2	WVDEP OSR Omega, Lat. 39.533042, Long. -79.939871	WV	Monongalia	Upper Freeport	NAPP	UG f	Active	Ca(OH)2	
raw AMD/sludge	AQ/SL	3	WVDEP OSR T&T #2, Lat. 39.544341, Long. -79.632630	WV	Preston	Upper Freeport	NAPP	UG f	Active	Ammonia	
raw AMD/sludge	AQ/SL	4	1 WVDEP OSR VIKING, Lat. 39.564822, Long. -79.643319	WV	Preston	Upper Freeport	NAPP	UG f	Active	CaO	
raw AMD/sludge	AQ/SL	4	WVDEP OSR VIKING, Lat. 39.564822, Long. -79.643319	WV	Preston	Upper Freeport	NAPP	UG f	Active	CaO	
raw AMD/sludge	AQ/SL	5	WVDEP OSR LOBO CAPITAL, Lat. 39.585699, Long. -79.639462	WV	Preston	Upper Freeport	NAPP	UG f	Active	NaOH	
raw AMD/sludge	AQ/SL	6	1 WVDEP OSR FREEPORT MINING, Lat. 39.640666, Long. 79.734928	WV	Preston	Upper Freeport	NAPP	SM UG f	Active	Ca(OH)2	
raw AMD/sludge	AQ/SL	6	WVDEP OSR FREEPORT MINING, Lat. 39.640666, Long. 79.734928	WV	Preston	Upper Freeport	NAPP	SM UG f	Active	Ca(OH)2	
raw AMD/sludge	AQ/SL	7	WVDEP OSR FREEPORT MINING, Lat. 39.640600, Long. 79.734900	WV	Preston	Upper Freeport	NAPP	SM UG f	Active	Ca(OH)2	
raw AMD/sludge	AQ/SL	8	1 WVDEP OSR EDWARD E THOMPSON S-1041-89, Lat. 39.701441, Long. -79.863569	WV	Monongalia	Pittsburgh	NAPP	SM UG f	Active	NaOH	

									SM	surface mine
									REF	refuse
									UG	underground mine
									f	flooded
type	site code		Field notes, site name and location	state	county	seam	basin	source	treatment	chemical
raw AMD/sludge	AQ/SL	8	WVDEP OSR EDWARD E THOMPSON S-1041-89, Lat. 39.701441, Long. -79.863569	WV	Monongalia	Pittsburgh	NAPP	SM UG f	Active	NaOH
raw AMD/sludge	AQ/SL	9 1	WVDEP OSR FARKAS COAL, Lat. 39.719638, Long. -79.874829	WV	Monongalia	Upper Freeport	NAPP	SM	Active	NaOH
raw AMD/sludge	AQ/SL	9	WVDEP OSR FARKAS COAL, Lat. 39.719638, Long. -79.874829	WV	Monongalia	Upper Freeport	NAPP	SM	Active	NaOH
raw AMD/sludge	AQ/SL	10 A	WVDEP OSR ED E DEVELOPMENT, Lat. 39.484679, Long. -79.899918	WV	Monongalia	M,L Kittanning	NAPP	SM	Active	Ca(OH)2
raw AMD/sludge	AQ/SL	10 B	WVDEP OSR ED E DEVELOPMENT, Lat. 39.484679, Long. -79.899918	WV	Monongalia	M,L Kittanning	NAPP	SM	Active	Ca(OH)2
raw AMD/sludge	AQ/SL	10	WVDEP OSR ED E DEVELOPMENT, Lat. 39.484679, Long. -79.899918	WV	Monongalia	M,L Kittanning	NAPP	SM	Active	Ca(OH)2
raw AMD/sludge	AQ/SL	11	WVDEP OSR S. KELLY INDUSTRIES, Lat. 39.515335, Long. -79.949859	WV	Monongalia	Upper Freeport	NAPP	SM	Active	Ca(OH)2
raw AMD/sludge	AQ/SL	11	WVDEP OSR S. KELLY INDUSTRIES, Lat. 39.515335, Long. -79.949859	WV	Monongalia	Upper Freeport	NAPP	SM	Active	Ca(OH)2
raw AMD/sludge	AQ/SL	12	WVDEP OSR Z & F DEVELOPMENT, Lat. 39.555629, Long. -80.031582	WV	Monongalia	Upper Freeport	NAPP	SM, UG f	Active	Ca(OH)2
raw AMD/sludge	AQ/SL	12	WVDEP OSR Z & F DEVELOPMENT, Lat. 39.555629, Long. -80.031582	WV	Monongalia	Upper Freeport	CAPP	UG f	none	
raw AMD/sludge	AQ/SL	13	Location restricted under access NDA	WV	Kanawha	#2 Gas	CAPP	UG f	none	

								SM	surface mine	
								REF	refuse	
								UG	underground mine	
								f	flooded	
type	site code		Field notes, site name and location	state	county	seam	basin	source	treatment	chemical
raw AMD/sludge	AQ/SL	14	Location restricted under access NDA	WV	Kanawha	Unknown	CAPP	ref	none	
raw AMD/sludge	AQ/SL	15	Location restricted under access NDA	WV	Kanawha	Powellton	CAPP	UG f	Passive	Ammonia
raw AMD/sludge	AQ/SL	16	Location restricted under access NDA	WV	Kanawha	Eagle	CAPP	UG f	Passive	Ammonia
raw AMD/sludge	AQ/SL	17	Location restricted under access NDA	WV	Kanawha	5 Block	CAPP	SM	Passive	Ammonia
raw AMD/sludge	AQ/SL	18	1 Location restricted under access NDA	WV	Kanawha	Coalburg	CAPP	UG f	none	Ca(OH)2
raw AMD/sludge	AQ/SL	18	Location restricted under access NDA	WV	Kanawha	Coalburg	CAPP	UG f	none	Ca(OH)2
raw AMD/sludge	AQ/SL	19	Location restricted under access NDA	WV	Kanawha	Coalburg	CAPP	ref	none	Ca(OH)2
raw AMD/sludge	AQ/SL	20	Location restricted under access NDA	PA	Cambria	Freeport	NAPP	UG f	Active	CaO - soon to be peroxide
raw AMD/sludge	AQ/SL	21	1 PADEP - Lancashire #15 or Barnes & Tucker Mine Operated by Denny Lloyd, Lat. 40.628946, Long. - 78.770555	PA	Cambria	Kittanning B	NAPP	UG f	Active	peroxide
raw AMD/sludge	AQ/SL	21	PADEP - Lancashire #15 or Barnes & Tucker Mine Operated by Denny Lloyd, Lat. 40.628946, Long. - 78.770555	PA	Cambria	Kittanning B	NAPP	UG f	Active	peroxide
raw AMD/sludge	AQ/SL	22	Location restricted under access NDA	PA	Indiana	Kittanning B	NAPP	UG f	Active	Ca(OH)2
raw AMD/sludge	AQ/SL	23	Location restricted under access NDA	PA	Westmoreland	Freeport	NAPP	ref	Active	Ca(OH)2
raw AMD/sludge	AQ/SL	24	Location restricted under access NDA	PA	Greene	Pittsburgh	NAPP	UG f	Active	peroxide

									SM	surface mine
									REF	refuse
									UG	underground mine
									f	flooded
type	site code		Field notes, site name and location	state	county	seam	basin	source	treatment	chemical
raw AMD/sludge	AQ/SL	25	Location restricted under access NDA	PA	Greene	Pittsburgh	NAPP	ref	Active	Ca(OH)2
raw AMD/sludge	AQ/SL	26	2 Location restricted under access NDA	PA	Fayette	Refractory Clay	NAPP	SM	Active	soda ash, Ca(OH)2, NaOH
raw AMD/sludge	AQ/SL	26	Location restricted under access NDA	PA	Fayette	Refractory Clay	NAPP	SM	Active	soda ash, Ca(OH)2, NaOH
raw AMD/sludge	AQ/SL	27	Location restricted under access NDA	PA	Greene	Pittsburgh	NAPP	UG f	Active	Ca(OH)2
raw AMD/sludge	AQ/SL	28	Location restricted under access NDA	WV	Monongalia	Pittsburgh	NAPP	UG	none	none
raw AMD/sludge	AQ/SL	29	Location restricted under access NDA	WV	Monongalia	Pittsburgh	NAPP	UG	none	none
raw AMD/sludge	AQ/SL	30	Location restricted under access NDA	WV	Monongalia	Pittsburgh	NAPP	UG f	Active	Ca(OH)2
raw AMD/sludge	AQ/SL	31	1 WVDEP OSR Borgman, Lat. 39.446413, Long. -79.732635	WV	Preston	0	NAPP	UG	Active	0
raw AMD/sludge	AQ/SL	31	WVDEP OSR Borgman, Lat. 39.446413, Long. -79.732635	WV	Preston		NAPP	UG	Active	
raw AMD/sludge	AQ/SL	32	1 Location restricted under access NDA	WV	Clay	Coalburg	NAPP	SM	Active	NaOH
raw AMD/sludge	AQ/SL	32	Location restricted under access NDA	WV	Clay	Coalburg	NAPP	SM	Active	NaOH
raw AMD/sludge	AQ/SL	33	1 Location restricted under access NDA	WV	Clay	Coalburg	NAPP	SM	Active	NaOH, now CaO, KMnO4, floccs
raw AMD/sludge	AQ/SL	33	Location restricted under access NDA	WV	Clay	Coalburg	NAPP	SM	Active	NaOH, now CaO, KMnO4, floccs
raw AMD/sludge	AQ/SL	34	Location restricted under access NDA	WV	Clay	Coalburg	NAPP	SM	Active	CaO
raw AMD/sludge	AQ/SL	35	1 Location restricted under access NDA	WV	Nicholas	Coalburg	NAPP	SM	Active	CaO and NaOH, Flocc, KMnO4

										SM	surface mine
										REF	refuse
										UG	underground mine
										f	flooded
type	site code			Field notes, site name and location	state	county	seam	basin	source	treatment	chemical
raw AMD/sludge	AQ/SL	35	1	Location restricted under access NDA	WV	Nicholas	Coalburg	NAPP	SM	Active	CaO and NaOH, Floc, KMnO4
raw AMD/sludge	AQ/SL	35		Location restricted under access NDA	WV	Nicholas	Coalburg	NAPP	SM	Active	CaO and NaOH, Floc, KMnO4
raw AMD/sludge	AQ/SL	36		Location restricted under access NDA	WV	Nicholas	Clarion	NAPP	SM	Active	CaO
raw AMD/sludge	AQ/SL	37		Location restricted under access NDA	WV	Nicholas	Clarion	NAPP	SM	Active	CaO
raw AMD/sludge	AQ/SL	38		Location restricted under access NDA	WV	Nicholas	Clarion	NAPP	SM	Active	NaOH
raw AMD/sludge	AQ/SL	39	1	Location restricted under access NDA	WV	Nicholas	Clarion, 5Block, M Kittanning	NAPP	SM	Active	NaOH
raw AMD/sludge	AQ/SL	39		Location restricted under access NDA	WV	Nicholas	Clarion, 5Block, M Kittanning	NAPP	SM	Active	NaOH
raw AMD/sludge	AQ/SL	40	1	Location restricted under access NDA	WV	Nicholas	Clarion, 5Block, M Kittanning	NAPP	SM	Active	NaOH
raw AMD/sludge	AQ/SL	40		Location restricted under access NDA	WV	Nicholas	Clarion, 5Block, M Kittanning	NAPP	SM	Active	NaOH
raw AMD/sludge	AQ/SL	41		Location restricted under access NDA	WV	Nicholas	Clarion, 5Block, M Kittanning	NAPP	SM	Active	NaOH
raw AMD/sludge	AQ/SL	42		Location restricted under access NDA	WV	Nicholas	Clarion, 5Block, M Kittanning	NAPP	SM	Active	NaOH, KMnO4
raw AMD/sludge	AQ/SL	43		Location restricted under access NDA	WV	Nicholas	Eagle	NAPP	ref	Active	H2O2
raw AMD/sludge	AQ/SL	44		WVDEP OSR Star Refuse, Lat. 37.821227, Long. -81.203864	WV	Raleigh	Refuse	CAPP	ref	Active	CaO
raw AMD/sludge	AQ/SL	45		WVDEP OSR Brady Cline, Lat. 38.417910, Long. -80.799495	WV	Nicholas	Lower Kittanning	NAPP	UGf	Active	CaO
raw AMD/sludge	AQ/SL	46		WVDEP OSR Falcon Land Co., Lat. 38.170280, Long. -80.599632	WV	Nicholas	Refuse	NAPP	ref	Active	CaO

								SM	surface mine		
								REF	refuse		
								UG	underground mine		
								f	flooded		
type	site code		Field notes, site name and location	state	county	seam	basin	source	treatment	chemical	
raw AMD/sludge	AQ/SL	47	Location restricted under access NDA	WV	Fayette	Refuse	CAPP	ref	Passive	OLC, Ca(OH)2stone Beds, SAPS?	
raw AMD/sludge	AQ/SL	48 1	WVDEP OSR WOCAP, Lat. 39.458535, Long. -79.728208	WV	Preston	Upper Freeport	NAPP	SM, UG nf	Active	CaO	
raw AMD/sludge	AQ/SL	48 1	WVDEP OSR WOCAP, Lat. 39.458535, Long. -79.728208	WV	Preston	Upper Freeport	NAPP	SM, UG nf	Active	CaO	
raw AMD/sludge	AQ/SL	48	WVDEP OSR WOCAP, Lat. 39.458535, Long. -79.728208	WV	Preston	Upper Freeport	NAPP	SM, UG nf	Active	CaO	
raw AMD/sludge	AQ/SL	49 1	WVDEP OSR Preston Energy, Lat. 39.429154, Long. -79.769337	WV	Preston	Upper Freeport	NAPP	SM	Active	CaO	
raw AMD/sludge	AQ/SL	49	WVDEP OSR Preston Energy, Lat. 39.429154, Long. -79.769337	WV	Preston	Upper Freeport	NAPP	SM	Active	CaO	
raw AMD/sludge	AQ/SL	50	WVDEP OSR Mangus, Lat. 39.370101, Long. -79.855909	WV	Preston	Unknown	NAPP	SM - MAYBE UG nf	Active	NaOH	
raw AMD/sludge	AQ/SL	50	WVDEP OSR Mangus, Lat. 39.370101, Long. -79.855909	WV	Preston	Unknown	NAPP	SM - MAYBE UG nf	Active	NaOH	
raw AMD/sludge	AQ/SL	51 1	WVDEP OSR F&M, Lat. 39.303126, Long. -79.773553	WV	Preston	Lower Kittanning	NAPP	SM	Active	Ammonia, CaO, NaOH	
raw AMD/sludge	AQ/SL	51 5	WVDEP OSR F&M, Lat. 39.303126, Long. -79.773553	WV	Preston	Lower Kittanning	NAPP	SM	Active	Ammonia, CaO, NaOH	
raw AMD/sludge	AQ/SL	51	WVDEP OSR F&M, Lat. 39.303126, Long. -79.773553	WV	Preston	Lower Kittanning	NAPP	SM	Active	Ammonia, CaO, NaOH	
raw AMD/sludge	AQ/SL	52	WVDEP OSR F&M, Lat. 39.316762, Long. -79.766314	WV	Preston	Lower Kittanning	NAPP	SM	Active	Ammonia, CaO, NaOH	
raw AMD/sludge	AQ/SL	53 1	WVDEP OSR Daugherty, Lat. 39.561261, Long. -79.738453	WV	Preston	Upper Freeport	NAPP	SM	Active	CaO	

									SM	surface mine
									REF	refuse
									UG	underground mine
									f	flooded
type	site code		Field notes, site name and location	state	county	seam	basin	source	treatment	chemical
raw AMD/sludge	AQ/SL	53	WVDEP OSR Daugherty, Lat. 39.561261, Long. -79.738453	WV	Preston	Upper Freeport	NAPP	SM	Active	CaO
raw AMD/sludge	AQ/SL	54	WVDEP OSR Daugherty, Lat. 39.568147, Long. -79.746906	WV	Preston	Upper Freeport	NAPP	SM	Active	CaO
raw AMD/sludge	AQ/SL	54	WVDEP OSR Daugherty, Lat. 39.568147, Long. -79.746906	WV	Preston	Upper Freeport	NAPP	SM	Active	CaO
raw AMD/sludge	AQ/SL	55	Location restricted under access NDA	WV	Preston	Refuse	NAPP	ref	Active	CaO
raw AMD/sludge	AQ/SL	56	Location restricted under access NDA	WV	Tucker	Freeport - Upper & Lower	NAPP	UG f	Active	Ca(OH)2
raw AMD/sludge	AQ/SL	57	Location restricted under access NDA	WV	Monongalia	Freeport	NAPP	SM	Active	NaOH
raw AMD/sludge	AQ/SL	57	Location restricted under access NDA	WV	Monongalia	Freeport	NAPP	SM	Active	NaOH
raw AMD/sludge	AQ/SL	57	Location restricted under access NDA	WV	Monongalia	Freeport	NAPP	SM	Active	NaOH
raw AMD/sludge	AQ/SL	58	Location restricted under access NDA	WV	Monongalia	Freeport	NAPP	SM	Active	NaOH
raw AMD/sludge	AQ/SL	58	Location restricted under access NDA	WV	Monongalia	Freeport	NAPP	SM	Active	NaOH
raw AMD/sludge	AQ/SL	59	PADEP Pearce Site, Lat. 40.975194, Long. -78.318800	PA	Clearfield	Lower Kittanning	NAPP	SM	Passive	none
raw AMD/sludge	AQ/SL	59	PADEP Pearce Site, Lat. 40.975194, Long. -78.318800	PA	Clearfield	Lower Kittanning	NAPP	SM	Passive	none
raw AMD/sludge	AQ/SL	60	PADEP Pearce Site, Lat. 40.974971, Long. -78.318778	PA	Clearfield	Lower Kittanning	NAPP	SM	Passive	none
raw AMD/sludge	AQ/SL	61	PADEP Pearce Site, Lat. 40.975115, Long. -78.318799	PA	Clearfield	Lower Kittanning	NAPP	SM	Passive	none

									SM	surface mine
									REF	refuse
									UG	underground mine
									f	flooded
type	site code		Field notes, site name and location	state	county	seam	basin	source	treatment	chemical
raw AMD/sludge	AQ/SL	62	WVDEP OSR Royal Scot Mine #59, Lat. 38.041936, Long. - 80.621586	WV	Greenbrier	Poca 6	CAPP	UG f	Active	CaO
raw AMD/sludge	AQ/SL	63	Location restricted under access NDA	OH	Athens	Refuse	CAPP	REF	Active	NaOH
raw AMD/sludge	AQ/SL	64	Location restricted under access NDA	OH	Harrison	Refuse	CAPP	ref	Active	NaOH
raw AMD/sludge	AQ/SL	65	1 WVDEP OSR BUFFALO COAL A-34, Lat. 39.207733, Long. - 79.297947	WV	Grant	Upper Freeport	NAPP	SM	Active	Ca(OH) ₂ , NaOH backup. once Was Ammonia
raw AMD/sludge	AQ/SL	65	WVDEP OSR BUFFALO COAL A-34, Lat. 39.207733, Long. - 79.297947	WV	Grant	Upper Freeport	NAPP	SM	Active	Ca(OH) ₂ , NaOH backup. once Was Ammonia
raw AMD/sludge	AQ/SL	66	1 WVDEP OSR BUFFALO COAL DOZER PIT SITE, Lat. 39.157241, Long. -79.289342	WV	Grant	Upper Freeport	NAPP	SM	Active	Ca(OH) ₂ , NaOH backup.
raw AMD/sludge	AQ/SL	66	WVDEP OSR BUFFALO COAL DOZER PIT SITE, Lat. 39.157241, Long. -79.289342	WV	Grant	Upper Freeport	NAPP	SM	Active	Ca(OH) ₂ , NaOH backup.
raw AMD/sludge	AQ/SL	67	1 WVDEP OSR BUFFALO COAL EASTER EGG SITE, Lat. 39.110877, Long. -79.298580	WV	Tucker	Upper Freeport	NAPP	SM	Active	NaOH, once Ammonia
raw AMD/sludge	AQ/SL	67	WVDEP OSR BUFFALO COAL EASTER EGG SITE, Lat. 39.110877, Long. -79.298580	WV	Tucker	Upper Freeport	NAPP	SM	Active	NaOH, once Ammonia
raw AMD/sludge	AQ/SL	68	1 WVDEP OSR CHESTNUT RIDGE, Lat. 39.377473, Long. - 79.176819	WV	Mineral	Little Clarksburg	NAPP	SM	Active	Ca(OH) ₂
raw AMD/sludge	AQ/SL	68	WVDEP OSR CHESTNUT RIDGE, Lat. 39.377473, Long. - 79.176819	WV	Mineral	Little Clarksburg	NAPP	SM	Active	Ca(OH) ₂

									SM	surface mine	
									REF	refuse	
									UG	underground mine	
									f	flooded	
type	site code			Field notes, site name and location	state	county	seam	basin	source	treatment	chemical
raw AMD/sludge	AQ/SL	69	1	WVDEP OSR BUFFALO COAL KEMPTON SITE, Lat. 39.218473, Long. -79.491768	WV	Preston	Upper Freeport	NAPP	UGF	Active	Ca(OH)2
raw AMD/sludge	AQ/SL	69		WVDEP OSR BUFFALO COAL KEMPTON SITE, Lat. 39.218473, Long. -79.491768	WV	Preston	Upper Freeport	NAPP	UGF	Active	Ca(OH)2
raw AMD/sludge	AQ/SL	70	1	MARYLAND DOE KEMPTON SITE, Lat. 39.220590, Long. -79.483532	MD	Garrett	Upper Freeport	NAPP	UGF	Active	CaO
raw AMD/sludge	AQ/SL	70	P	MARYLAND DOE KEMPTON SITE, Lat. 39.220590, Long. -79.483532	MD	Garrett	Upper Freeport	NAPP	UGF	Active	CaO
raw AMD/sludge	AQ/SL	70		MARYLAND DOE KEMPTON SITE, Lat. 39.220590, Long. -79.483532	MD	Garrett	Upper Freeport	NAPP	UGF	Active	CaO
raw AMD/sludge	AQ/SL	71		WVDEP AML KEMPTON, Lat. 39.205020, Long. -79.501631	WV	Preston	Upper Freeport	NAPP	SM	Passive	
raw AMD/sludge	AQ/SL	72		MARYLAND DOE MILL RUN SITE, Lat. 39.521140, Long. -79.034960	MD	Allegany	Barton	NAPP	UG	Active	Ca(OH)2
raw AMD/sludge	AQ/SL	73		MARYLAND DOE MCDONALD MINE SITE, Lat. 39.525788, Long. -79.019936	MD	Allegany	Barton	NAPP	UG	Active	Ca(OH)2
raw AMD/sludge	AQ/SL	74	2	MARYLAND DOE BUFFALO 422 SITE, Lat. 39.553777, Long. -78.971345	MD	Allegany	Pittsburgh, Sewickley	NAPP	SM	Active	Ca(OH)2 and NaOH @ low Q
raw AMD/sludge	AQ/SL	74		MARYLAND DOE BUFFALO 422 SITE, Lat. 39.553777, Long. -78.971345	MD	Allegany	Pittsburgh, Sewickley	NAPP	SM	Active	Ca(OH)2 and NaOH @ low Q

									SM	surface mine
									REF	refuse
									UG	underground mine
									f	flooded
type	site code		Field notes, site name and location	state	county	seam	basin	source	treatment	chemical
raw AMD/sludge	AQ/SL	75	MARYLAND DOE HOFFMAN DRAINAGE TUNNEL SITE, Lat. 39.637184, Long. -78.892992	MD	Allegany	Pittsburgh	NAPP	UGf	Untreated	
raw AMD/sludge	AQ/SL	76	WVDEP OSR MARY RUTH, Lat. 39.579643, Long. -79.592737	WV	Preston	Upper Freeport	NAPP	SM	Active	Ca(OH)2
raw AMD/sludge	AQ/SL	77	2 WVDEP OSR VALLEY MINING CHEAT LAKE SITE, Lat. 39.653192, Long. -79.853287	WV	Monongalia	Upper Freeport	NAPP	SM	Active	Ca(OH)2
raw AMD/sludge	AQ/SL	77	WVDEP OSR VALLEY MINING CHEAT LAKE SITE, Lat. 39.653192, Long. -79.853287	WV	Monongalia	Upper Freeport	NAPP	SM	Active	Ca(OH)2
raw AMD/sludge	AQ/SL	78	1 Location restricted under access NDA	PA	Allegheny	Pittsburgh	NAPP	UGf	Passive	0
raw AMD/sludge	AQ/SL	78	Location restricted under access NDA	PA	Allegheny	Pittsburgh	NAPP	UGf	Passive	
raw AMD/sludge	AQ/SL	79	1 Location restricted under access NDA	PA	Allegheny	Pittsburgh	NAPP	UG	Passive	0
raw AMD/sludge	AQ/SL	79	Location restricted under access NDA	PA	Allegheny	Pittsburgh	NAPP	UG	Passive	
raw AMD/sludge	AQ/SL	80	Location restricted under access NDA	WV	McDowell	Refuse - Mostly RED ASH, Lower WAR Eagle, Poca 3	CAPP	ref	Active	CaO, Flocc
raw AMD/sludge	AQ/SL	81	Location restricted under access NDA	WV	McDowell	Refuse - Mostly RED ASH, Lower WAR Eagle, Poca 3	CAPP	ref	Active	CaO, Flocc
raw AMD/sludge	AQ/SL	82	Location restricted under access NDA	WV	Wyoming	Refuse - Mostly Sewell	CAPP	ref	Active	NaOH, Flocc
raw AMD/sludge	AQ/SL	83	Location restricted under access NDA	WV	Wyoming	Refuse - Mostly Sewell	CAPP	ref	Active	NaOH, Flocc

									SM	surface mine
									REF	refuse
									UG	underground mine
									f	flooded
type	site code		Field notes, site name and location	state	county	seam	basin	source	treatment	chemical
raw AMD/sludge	AQ/SL	84	Location restricted under access NDA	WV	Wyoming	Refuse - Mostly Sewell	CAPP	ref	Active	NaOH, Floc
raw AMD/sludge	AQ/SL	85	Location restricted under access NDA	WV	Wyoming	Refuse - Pocahontas #3	CAPP	REF	Active	NaOH, Floc
raw AMD/sludge	AQ/SL	86	Location restricted under access NDA	WV	Wyoming	Refuse - Eagle 5 UG	CAPP	REF and UG(f)	Active	NaOH, Floc
raw AMD/sludge	AQ/SL	87	Location restricted under access NDA	WV	Braxton	Lower Kittanning - (AKA Stockton)	CAPP	UG f	Active	NaOH, Floc. Used Ca(OH)2 8 YRS. AGO
raw AMD/sludge	AQ/SL	88	Location restricted under access NDA	WV	Braxton	Refuse - Lower Kittanning AND SOME Freeport	CAPP	REF and UG(f)	Active	NaOH, Floc
raw AMD/sludge	AQ/SL	89	Location restricted under access NDA	WV	Webster	Clarion	CAPP	UG	Active	NaOH
raw AMD/sludge	AQ/SL	90	Location restricted under access NDA	WV	Webster	Lower Kittanning	CAPP	UG	Active	NaOH, Floc
raw AMD/sludge	AQ/SL	91	Location restricted under access NDA	WV	Nicholas	Unknown	CAPP	SM	Active	NaOH, Floc
raw AMD/sludge	AQ/SL	92	Location restricted under access NDA	WV	Nicholas	Unknown	CAPP	SM	Active	NaOH, Floc
raw AMD/sludge	AQ/SL	93	Location restricted under access NDA	WV	Nicholas	Unknown	CAPP	SM	Active	NaOH, Floc
raw AMD/sludge	AQ/SL	94	Location restricted under access NDA	WV	Nicholas	Coalburg	CAPP	SM & UG(f)	Active	Ca(OH)2, NaOH, Floc
raw AMD/sludge	AQ/SL	95	Location restricted under access NDA	WV	Nicholas		CAPP	UG (f)	Active	NaOH, Floc
raw AMD/sludge	AQ/SL	96	Location restricted under access NDA	WV	Nicholas	Eagle	CAPP	UG (f)	Active	NaOH, Floc
raw AMD/sludge	AQ/SL	97	Location restricted under access NDA	WV	Greenbrier		CAPP	Refuse - Mostly Sewell	Active	Ca(OH)2, NaOH, flocs
raw AMD/sludge	AQ/SL	98	Location restricted under access NDA	WV	Greenbrier		CAPP	UG (f)	Active	NaOH

									SM	surface mine
									REF	refuse
									UG	underground mine
									f	flooded
type	site code		Field notes, site name and location	state	county	seam	basin	source	treatment	chemical
raw AMD/sludge	AQ/SL	99	Location restricted under access NDA	WV	Marion	Middle Kittanning	NAPP	Refuse	Active	H2O2, Floc, NaOH backup
raw AMD/sludge	AQ/SL	100	Location restricted under access NDA	WV	Marion	Middle Kittanning	NAPP	UF(f)	Active	H2O2, Floc
raw AMD/sludge	AQ/SL	101	Location restricted under access NDA	WV	Marion	Middle Kittanning	NAPP	Refuse	Active	H2O2, Floc, NaOH backup
raw AMD/sludge	AQ/SL	102	Location restricted under access NDA	PA	Greene	Pittsburgh	NAPP	UG (F)	Active	Ca(OH)2, Floc
raw AMD/sludge	AQ/SL	103	Location restricted under access NDA	WV	Marshall	Pittsburgh	NAPP	Refuse	Passive	none
raw AMD/sludge	AQ/SL	104	Location restricted under access NDA	WV	Marshall	Pittsburgh	NAPP	Refuse	Passive	none
raw AMD/sludge	AQ/SL	105	Location restricted under access NDA	WV	Marshall	Pittsburgh	NAPP	Refuse	Passive	none
raw AMD/sludge	AQ/SL	106	Location restricted under access NDA	WV	Marshall	Pittsburgh	NAPP	Refuse	Passive	none
raw AMD/sludge	AQ/SL	107	Location restricted under access NDA	WV	Marshall	Pittsburgh	NAPP	Refuse	Passive	none
raw AMD/sludge	AQ/SL	108	Location restricted under access NDA	PA	Westmoreland	Pittsburgh	NAPP	UG(f)	Passive	none
raw AMD/sludge	AQ/SL	109	Location restricted under access NDA	PA	Westmoreland	Pittsburgh	NAPP	UG(f)	Passive	none
raw AMD/sludge	AQ/SL	110	Location restricted under access NDA	PA	Washington	Pittsburgh	NAPP	UG(f)	Active	H2O2
raw AMD/sludge	AQ/SL	111	Location restricted under access NDA	PA	Westmoreland	Pittsburgh	NAPP	UG(f)	Active	H2O2
raw AMD/sludge	AQ/SL	112	Location restricted under access NDA	PA	Westmoreland	Pittsburgh	NAPP	UG(f)	Active	H2O2
raw AMD/sludge	AQ/SL	113	Location restricted under access NDA	PA	Washington	Pittsburgh	NAPP	UG(f)	Active	Ca(OH)2
raw AMD/sludge	AQ/SL	114	Location restricted under access NDA	PA	Washington	Pittsburgh	NAPP	Refuse	Active	NaOH

									SM	surface mine
									REF	refuse
									UG	underground mine
									f	flooded
type	site code		Field notes, site name and location	state	county	seam	basin	source	treatment	chemical
raw AMD/sludge	AQ/SL	115	PADEP FLIGHT 93, Lat. 40.065600, Long. -115.888200	PA	Somerset			SM and UG (f)	Passive	none
raw AMD/sludge	AQ/SL	116	Location restricted under access NDA	PA	Cambria	Pittsburgh		NAPP UG (f)	Active	CaO
raw AMD/sludge	AQ/SL	117	1 Location restricted under access NDA	PA	Cambria	Kittannings, others		NAPP SM	Active	Ca(OH) ₂
raw AMD/sludge	AQ/SL	117	Location restricted under access NDA	PA	Cambria	Kittannings, others		NAPP SM	Active	Ca(OH) ₂
raw AMD/sludge	AQ/SL	118	2 Location restricted under access NDA	PA	Cambria	Kittannings, others		NAPP SM	Active	Ca(OH) ₂
raw AMD/sludge	AQ/SL	119	1 Location restricted under access NDA	PA	Cambria	Kittannings, others		NAPP SM	Active	Ca(OH) ₂
raw AMD/sludge	AQ/SL	120	Location restricted under access NDA	WV	Monongalia	Pittsburgh		NAPP UG (f)	Active	Ca(OH) ₂ , Floc
raw AMD/sludge	AQ/SL	121	Location restricted under access NDA	WV	Monongalia	Pittsburgh		NAPP UG (f)	Active	Ca(OH) ₂ , Floc
raw AMD/sludge	AQ/SL	122	Location restricted under access NDA	WV	Monongalia	Sewickley		NAPP UG (f)	Active	Ca(OH) ₂ , Floc
raw AMD/sludge	AQ/SL	123	Location restricted under access NDA	WV	Monongalia	Pittsburgh		NAPP UG (f)	Active	Ca(OH) ₂ , Floc
raw AMD/sludge	AQ/SL	124	Location restricted under access NDA	WV	Monongalia	Pittsburgh		NAPP UG (f)	Active	Ca(OH) ₂ , Floc
raw AMD/sludge	AQ/SL	125	Location restricted under access NDA	WV	Monongalia	Pittsburgh		NAPP UG (f)	Active	Ca(OH) ₂ , Floc
raw AMD/sludge	AQ/SL	126	Location restricted under access NDA	WV	Monongalia	Pittsburgh		NAPP UG (f)	Active	Ca(OH) ₂ , Floc
raw AMD/sludge	AQ/SL	127	Location restricted under access NDA	WV	Monongalia	Pittsburgh		NAPP UG (f)	Active	Ca(OH) ₂ , Floc
raw AMD/sludge	AQ/SL	128	Location restricted under access NDA	WV	Monongalia	Pittsburgh		NAPP UG (f)	Active	Ca(OH) ₂ , Floc
raw AMD/sludge	AQ/SL	129	Location restricted under access NDA	WV	Monongalia	Pittsburgh		NAPP UG (f)	Active	Ca(OH) ₂ , Floc

									SM	surface mine
									REF	refuse
									UG	underground mine
									f	flooded
type	site code		Field notes, site name and location	state	county	sea m	basin	source	treatment	chemical
raw AMD/sludge	AQ/SL	130	Location restricted under access NDA	WV	Monongalia	Pittsburgh	NAPP	UG (f)	Active	Ca(OH)2, Floc
raw AMD/sludge	AQ/SL	131	Location restricted under access NDA	WV	Monongalia	Pittsburgh	NAPP	UG (f)	Active	Ca(OH)2, Floc
raw AMD/sludge	AQ/SL	132	Location restricted under access NDA	WV	Monongalia	Pittsburgh	NAPP	UG (f)	Active	Ca(OH)2, Floc
raw AMD/sludge	AQ/SL	133	Location restricted under access NDA	WV	Monongalia	Pittsburgh	NAPP	UG (f)	Active	Ca(OH)2, Floc
raw AMD/sludge	AQ/SL	134	Location restricted under access NDA	WV	Monongalia	Pittsburgh	NAPP	UG (f)	Active	Ca(OH)2, Floc
raw AMD/sludge	AQ/SL	135	Location restricted under access NDA	WV	Monongalia	Pittsburgh	NAPP	UG (f)	Active	Ca(OH)2, Floc
raw AMD/sludge	AQ/SL	136	Location restricted under access NDA	WV	Monongalia	Pittsburgh	NAPP	UG (f)	Active	Ca(OH)2, Floc
raw AMD/sludge	AQ/SL	137	Location restricted under access NDA	WV	Monongalia	Pittsburgh	NAPP	UG (f)	Active	Ca(OH)2, Floc
raw AMD/sludge	AQ/SL	138	Location restricted under access NDA	WV	Marion	Pittsburgh	NAPP	UG (f)	Active	MANY, primarily Ca(OH)2
raw AMD/sludge	AQ/SL	139	Location restricted under access NDA	WV	Marion	Pittsburgh	NAPP	UG (f)	Active	MANY, primarily Ca(OH)2
raw AMD/sludge	AQ/SL	140	Location restricted under access NDA	WV	Harrison	Pittsburgh	NAPP	UG (f)	Active	Ca(OH)2
raw AMD/sludge	AQ/SL	141	Location restricted under access NDA	WV	Marion	Pittsburgh	NAPP	UG (f)	Active	Ca(OH)2

Appendix D: Sample Results (from EDX)

- All samples were either raw acid mine drainage (AMD) or AMD treatment solids.
- All samples result from resource production
- All results are reported on a dry mass, elemental basis.
- All samples were taken in either the northern (NAPP) or central (CAPP) Appalachian coal basins.
- All samples were derived from Pennsylvanian rock units
- n/a = no analytical results
- NSS=insufficient sample for analysis

Sample type: Acid Mine Drainage Solids		analytical technique: GC_IMS28V		lanthanides																													
sample type	coal basin	coal seam	state	county	site	Si (ppm)	Sc (ppm)	Y (ppm)	La (ppm)	Ce (ppm)	Pr (ppm)	Nd (ppm)	Sm (ppm)	Eu (ppm)	Gd (ppm)	Tb (ppm)	Dy (ppm)	Ho (ppm)	Er (ppm)	Tm (ppm)	Yb (ppm)	Lu (ppm)	Th (ppm)	U (ppm)	+Y (ppm)	Al (ppm)	Ca (ppm)	Fe (ppm)	Mg (ppm)	Na (ppm)	Cl (ppm)	SO4 (ppm)	
AMD solids	NAPP	Kittanning, others	PA	Cambria	SL-118-2	7.0	13.0	256.0	68.0	185.0	24.7	113.0	31.3	7.8	46.8	7.9	50.0	10.3	28.7	3.9	22.7	3.4	2.5	7.7	603.5	859.5	7.3	4.7	10.2	5.0			
AMD solids	NAPP	Kittanning, others	PA	Cambria	SL-118-2	7.8	17.0	279.0	74.1	200.0	27.1	124.0	34.7	8.5	51.5	8.6	54.0	11.2	31.8	4.4	25.6	3.8	3.1	8.9	659.3	938.3	9.6	2.2	12.6	3.1			
AMD solids	NAPP	Kittanning, others	PA	Cambria	SL-118-2	10.0	16.0	158.0	58.4	141.0	17.9	77.6	20.5	5.0	29.2	4.8	30.6	6.3	17.9	2.4	14.3	2.2	7.5	6.3	428.2	586.2	8.1	5.3	9.3	2.6			
AMD solids	NAPP	Kittanning, others	PA	Cambria	SL-118-2	5.4	13.0	253.0	67.7	180.0	24.6	111.0	30.4	7.7	46.1	7.6	48.5	10.0	28.0	3.8	22.4	3.3	2.3	7.5	591.2	844.2	6.8	2.9	9.6	9.1			
AMD solids	NAPP	Kittanning, others	PA	Cambria	SL-118-2		13.0	149.0	46.3	118.0	16.4	76.0	20.9	5.0	30.8	5.2	33.0	7.0	18.6	2.5	14.5	2.2	3.3	5.8	396.4	545.4							
AMD solids	NAPP	Kittanning, others	PA	Cambria	SL-119-1	18.6	16.0	89.9	49.4	106.0	13.4	56.2	13.4	3.1	17.0	2.9	17.7	3.6	10.5	1.5	9.2	1.4	7.9	5.0	299.3	389.2	7.9	10.4	3.4	0.8			
AMD solids	NAPP	Kittanning, others	PA	Cambria	SL-119-1	12.3	10.0	56.4	27.7	67.1	8.6	37.5	9.1	2.1	11.1	1.8	11.5	2.4	6.8	1.0	6.1	1.0	5.2	3.5	193.8	250.2	5.2	16.5	5.0	0.7			
AMD solids	NAPP	Kittanning, others	PA	Cambria	SL-119-1	9.0	12.0	102.0	37.5	94.7	12.6	54.7	13.7	3.2	18.2	3.0	19.0	4.0	11.2	1.6	9.5	1.5	4.2	4.0	284.5	386.5	5.6	20.8	2.0	1.1			
AMD solids	NAPP	Kittanning, others	PA	Cambria	SL-119-1	6.1	8.0	73.8	26.8	68.4	9.1	39.9	10.0	2.4	13.6	2.3	14.1	2.9	8.3	1.2	6.9	1.1	2.7	3.0	206.9	280.7	4.1	>25	1.4	1.3			
AMD solids	NAPP	Kittanning, others	PA	Cambria	SL-119-1	10.9	16.0	102.0	38.9	103.0	13.2	57.4	14.7	3.4	18.8	3.2	20.0	4.2	12.0	1.7	10.6	1.6	5.8	5.1	302.7	404.7	7.6	16.4	3.1	0.9			
AMD solids	NAPP	Kittanning, others	PA	Cambria	SL-119-1	27.1	18.0	80.1	50.2	118.0	14.7	60.7	13.6	3.0	15.9	2.6	15.9	3.2	9.3	1.4	8.3	1.3	11.1	5.5	318.1	398.2	9.1	0.7	4.5	0.3			
AMD solids	NAPP	Kittanning, others	PA	Cambria	SL-119-1	29.9	12.0	44.4	32.3	71.5	9.1	37.3	8.2	1.8	8.8	1.4	8.9	1.8	5.3	0.8	4.8	0.8	8.0	3.2	192.8	237.2	6.4	0.9	6.2	0.3			
AMD solids	NAPP	Kittanning, others	PA	Cambria	SL-119-1	21.1	23.0	139.0	65.2	150.0	19.1	80.1	19.1	4.5	25.4	4.2	25.4	5.2	14.6	1.9	11.0	1.7	11.3	5.9	427.4	566.4	8.2	2.9	8.3	0.6			
AMD solids	NAPP	Kittanning, others	PA	Cambria	SL-119-1	14.4	9.0	49.0	28.1	66.1	8.5	35.7	8.2	1.8	9.8	1.6	9.9	2.0	5.9	0.8	5.1	0.8	5.9	2.9	184.3	233.3	4.2	13.0	7.6	0.7			
AMD solids	NAPP	Kittanning, others	PA	Cambria	SL-119-1	7.0	35.4	19.1	44.6	5.6	24.0	5.6	1.3	6.7	1.1	7.0	1.5	4.2	0.0	3.4	0.0	3.5	2.3	124.1	159.5								
AMD solids	NAPP	Pittsburgh	WV	Monongalia	SL-120-1	0.0	8.4	2.6	5.1	0.9	4.0	1.1	0.0	1.5	0.0	1.0	0.0	0.0	0.0	0.5	0.0	< 0.6	1.0	16.7	25.1								
AMD solids	NAPP	Pittsburgh	WV	Monongalia	SL-120-5	3.0	20.4	8.1	20.0	2.9	13.0	3.4	0.9	4.5	0.8	4.0	0.9	2.2	0.0	1.6	0.0	1.7	1.2	62.3	82.7								
AMD solids	NAPP	Sewickley AND Pittsburgh	WV	Monongalia	SL-122-1	0.0	3.4	3.8	6.4	0.9	4.0	0.0	0.0	0.0	0.0	0.0	0.0	0.0	0.0	0.0	0.0	0.0	< 0.6	0.8	15.9	19.3							
AMD solids	NAPP	Sewickley AND Pittsburgh	WV	Monongalia	SL-122-2	0.0	2.6	1.7	3.0	0.0	0.0	0.0	0.0	0.0	0.0	0.0	0.0	0.0	0.0	0.0	0.0	0.0	< 0.6	0.5	4.7	7.3							
AMD solids	NAPP	Pittsburgh	WV	Monongalia	SL-124-1	0.0	4.3	1.5	2.8	0.0	0.0	0.0	0.0	0.0	0.0	0.0	0.0	0.0	0.0	0.0	0.0	0.0	< 0.6	0.5	4.9	9.2							
AMD solids	NAPP	Pittsburgh	WV	Monongalia	SL-124-2	0.0	4.0	3.3	6.7	0.8	3.0	0.0	0.0	0.7	0.0	0.0	0.0	0.0	0.0	0.0	0.0	0.0	0.8	0.6	14.5	18.5							
AMD solids	NAPP	Pittsburgh	WV	Monongalia	SL-126-1	<2	1.4	4.6	7.9	<0.6	<2	<0.8	<0.6	<0.6	<0.6	<1	<0.4	<0.8	<0.8	<0.4	<0.6	<0.6	<0.4	12.5	13.9								
AMD solids	NAPP	Pittsburgh	WV	Monongalia	SL-128-1	6.0	30.3	12.8	35.4	5.5	20.0	5.7	1.9	6.8	1.6	6.0	1.8	3.7	1.0	2.9	1.1	4.6	2.0	106.2	136.5								
AMD solids	NAPP	Pittsburgh	WV	Monongalia	SL-129-1	2.0	11.5	1.8	7.2	1.0	5.0	1.4	0.6	2.1	0.6	2.0	0.4	1.2	0.8	0.8	0.6	0.6	0.6	25.5	37.0								
AMD solids	NAPP	Pittsburgh	WV	Monongalia	SL-132-1	2.0	5.4	1.1	3.2	0.6	2.0	0.8	0.6	0.7	0.6	1.0	0.4	0.8	0.8	0.4	0.6	0.6	0.4	13.6	19.0								
AMD solids	NAPP	Pittsburgh	WV	Marion	SL-138-1	2.0	0.2	0.6	0.7	0.6	2.0	0.8	0.6	0.6	0.6	1.0	0.4	0.8	0.8	0.4	0.6	0.6	0.4	10.5	10.7								
AMD solids	NAPP	Pittsburgh	WV	Marion	SL-138-2	2.0	1.5	1.0	1.9	0.6	1.0	0.8	0.6	0.6	0.6	1.0	0.4	0.8	0.8	0.4	0.6	0.6	0.9	11.1	12.6								
AMD solids	NAPP	Pittsburgh	WV	Marion	SL-139-4	8.0	15.8	22.6	49.1	6.0	21.0	4.3	0.8	3.4	0.6	3.0	0.5	1.7	0.8	1.7	0.6	7.1	2.5	116.1	131.9								
AMD solids	NAPP	Pittsburgh	WV	Harrison	SL-140-2	2.0	5.2	3.6	8.0	1.1	4.0	1.0	0.6	1.0	0.6	1.0	0.4	0.8	0.8	0.5	0.6	1.0	0.4	24.0	29.2								

Appendix E: Table of Abbreviations

α	Probability of rejecting a true hypothesis	MDL	Method Detection Limit
AMD	Acid Mine Drainage	MREO	Mixed Rare Earth Oxides
AQ	Aqueous	n	sample size
CAPP	Central Appalachian coal basin	NAPP	Northern Appalachian coal basin
CHP	Chemical Hygiene Plan	NETL	National Energy Technology Laboratory
CI	Confidence Interval	PI	Principal Investigator
CV	Contained Value (value of a given mass of resource)	PPE	Personal Protective Equipment
df	Degrees of Freedom	Q	flow
DO	Dissolved Oxygen	REE	Rare Earth Elements
DW	Dry Weight	SL	Sludge
EC	Electrical Conductivity	SMCRA	Surface Mining Control and Reclamation Act
EDX	Energy Data eXchange	SSQE	Sum of Squares Error
GPS	Global Positioning System	TREE	Total Rare Earth Elements
HREE	Heavy Rare Earth Elements	USDOE	United States Department of Energy
ICP-MS	inductively coupled plasma-mass spectrometry	USEPA	United States Environmental Protection Agency
ICP-OES	inductively coupled plasma optical emission spectrometry	WVU	West Virginia University
L	Liter	XRD	X-ray Diffraction
LREE	Light Rare Earth Elements	XRF	X-ray fluorescence
